Development of sensors for the on-site monitoring of dry-type electrical machines

Doctoral Dissertation
Doctoral Program in Materials Science and Technologies (31st Cycle)

Development of sensors for the on-site monitoring of dry-type electrical machines

Carlo Maria Roggero

Supervisor

Prof. Jean-Marc Tulliani

Doctoral Examination Committee:

Prof. Isabella Natali Sora, Referee,
Prof. Umberto Anselmi Tamburrini, Referee,
Prof. Emma Angelini, Politecnico di Torino,
Prof. Giancarlo Cravotto, University of Torino,
Prof. Carlotta Francia, Politecnico di Torino.

Politecnico di Torino

April 30th, 2019

I hereby declare that, the contents and organisation of this dissertation constitute my own original work and does not compromise in any way the rights of third parties, including those relating to the security of personal data.

Carlo Maria Roggero

Turin, April 30th, 2019

Summary

Electrical transformers can be grouped in two different categories, one that includes liquid insulated machines and another that comprises dry-type equipment. Each category has its own advantages which are strictly connected to the environment where the machines has to installed and the strategy the owner decides to follow. For instance, the first category can have its insulating liquid sampled for diagnosis whereas the second is fire proof and requires a very small amount of maintenance activities. This last characteristic is also a limitation because it originates from the impossibility of sampling any parts of the apparatus for diagnostic purposes. Therefore the need for a tool able to monitor the health conditions of the dry-type transformer (and similar machines like electrical rotating machines) and capable of predicting imminent failures is sought. In dry-type electrical machines the insulation is provided by polymeric material, and mainly by polyesters and epoxy resins. They can be both subjected to electrical and thermal stresses that can start and/or extend degradation phenomena, during which volatile and semi volatile molecules can be released. The detection of said molecules could be correlated to overheating or electrical occurrences.

The purpose of this study was to investigate the thermal degradation of epoxy resin samples provided by a local producer of dry-type transformers, trying to isolate those organic compounds which can be descriptive of incipient or on-going polymer decay. The successive step was, first, to select and then to fabricate solid state sensors, based on metal oxides, able to interact with the compounds of interest and provide an exploitable response.

Contemporarily, a portable and remotely controllable device was realized using commercial sensors and installed on in-service transformers to monitor their correct functioning. The main target was to link faulty behaviors to a possible concomitant release of semi volatile organic molecules.

Finally the aforementioned device was coupled with the sensors developed in the lab to check for the feasibility of an industrial in-field application.

This thesis is made of 6 parts that herewith shortly described.

The **first chapter** is an introduction explaining the need for this kind of research. It describes the state of the art of transformers and of solid state sensors.

The **second chapter** defines the objectives of the research

The **third chapter** describes the experiments and the related results of the thermal degradation of epoxy resins

The **fourth chapter** explains the synthesis of metal oxides, the fabrication of solid state sensors and testing over the target molecules selected after the degradation experiments

The **fifth chapter** describes the construction of the portable device (based on commercial sensors) to be installed on dry-type transformers, its in-field validation and its coupling with a solid state sensor produced in the lab.

Acknowledgment

First I would like to thank my supervisor, Professor Jean Marc Tulliani, for accepting me as his student despite the limited amount of time I could dedicate to the research activities.

I'm grateful to Sea Marconi and especially to Tumiatti Family for the support granted throughout these years and the help provided to pursue the doctorate.

I'm also grateful to Prof. Kapila (University of Missouri) for the long scientific collaboration and for being a source of inspiration.

I express my gratitude to Andrea Marchisio for his useful assistance and the fruitful and witty discussions.

Finally my thanks goes to my family who patiently tolerated the fancies of an old student.

Contents

1 Introduction

Electric machines, such as transformers, electric motors and generators, classified as energy converters, whose functioning is based on electromagnetic forces, are fundamental for the generation, transmission and distribution of electric energy. Motors have moving parts which convert electric power in mechanical force, generators work in the opposite way, transformers are static machines. These devices come under different design and constructive solutions and are manufactured and used in compliance with dedicated international standards (e.g. International Electrotechnical Commission – www.iec.ch). The global market value of electrical transformers is huge and in 2017 was estimated to be around 28.48 billion dollars [1]. Transformers can be classified according to application, power, voltage and insulation type which can be either liquid or dry. However, the design and construction of transformers has not evolved much within the latest years. A transformer is made of several parts that from the mere point of view of functionality do not vary between an oil-insulated and a dry-type model. In the first case the core, which works as a guidance for the magnetic flux, consists in high-magnetic-permeability steel strips or coils, named laminations, which can be either stacked or wound and are separated by a thin coating of electrically insulating material (e.g. craft paper) [2]. In the second case the windings are normally made of aluminum foils whose expansion coefficient is in line with the shrinking or enlargement of the resin used for encapsulating the coils[3]. Even though transformers are generally considered highly efficient machines, transformation of alternating electric power generates heat. The total heat loss is he sum of the no-load core loss and the full-load coil loss (I^2R, where I is the current intensity and R the resistance) [4]. Large power transformers (*100 MVA* and higher), can have more than *99%* efficiency, whereas smaller one may be less than *85%* efficient. For instance heat loss for a 150 kVA (and smaller) transformer is 50 Watts/kVA (aprox. 5%), whereas in the case of a machine larger than 2500 kVA is 15 Watts/kVA (aprox. 1.5%) [5]. The insulating materials inside the transformers (oil, paper, enamel or resin) can withstand a limited amount of heat and temperature and when a given threshold is exceeded their properties start to be compromised [6]. Currently, mineral oil is the preferred material used to fill up liquid-insulated transformers, which account for most of the worldwide fleet [7]. Polyurethane and epoxy resins in particular are used to manufacture dry-type transformers and related equipment (e.g. switchgears) [8]. It's estimated that 4.5 million transformer units are used in Europe, 4% of which is classified as dry type [9]. The

average life span of a dry-type transformer is around 20-30 years (40 years for an oil-insulated machine), with a failure rate ranging from 0.5 to 2.5% according to the application, but in case of dry-type machines the rate can rise up to 5% (for instance in wind-farm setting up where stress factors are significant) [10][11]. The high fire risk associated to liquid-filled transformers, that can lead to catastrophic damages, is one of the reason why dry-type devices can turn into the preferred choice, but if and only if the power needed is not too high (manufactures are currently producing cast-resin transformers up to 50-60 MVA). Another motivation is the absence of maintenance. This characteristic can be seen from the divergent perspectives of an advantage, when a zero-maintenance solution is sought or a disadvantage when having the possibility to identify and treat faults is an assurance of durability [12]. Consequently dry-type transformers find application in the renewable energy and infrastructure (photovoltaic panels installation, wind turbines, etc.) systems, but also anywhere explosion and fire risks, typically associated with oil insulated transformers, become unacceptable (smart grids, large ships, airports, hospitals, etc.). However, the low fire risk does not imply that cast resin transformers are immune from failures [13]. Compared to oil-filled transformers they show some disadvantages, one for all, the impossibility of having their components easily checked for physico-chemical properties. On the contrary, a long history of use has enriched insulating mineral oil of a copious set of technical standards and analytical methods (e.g. those issued by IEC or ASTM (American Society for Testing Materials)) meant to identify thermal faults and functional and environmental issues (polychlorobiphenyl (PCB) contamination). Most of the analytical techniques are carried out in specialized laboratories after a correct sampling of the oil from the transformer. Total acid number (acidity), moisture, dissolved gases and dissipation factor (an index of insulation) are some of the typical properties sought to understand the state of the transformer itself. In addition, a limited number of less sophisticated on site and on-line analytical methods are also available. One of the properties commonly explored through an on-site technique is dissolved gases (DGA – dissolved gas analysis of permanent gases, hydrogen and hydrocarbons derived from oil molecule degradation), whose analysis can provide information about the existence of electrical and thermal stresses. Normally, despite the intrinsic limitations, a good and reliable on-line monitoring must quickly and efficiently identify and classify the symptoms of incipient problems that can lead to faults and failures. However, with regards to cast resin transformers (mainly epoxy resin), the possibility of performing on-site analyses and tests can't be realized, due to the impracticability of sampling parts and components. As a matter of facts in cast resin transformers the windings

are made of stacked layers of either aluminum or copper foils alternated with polyester films as insulators. The derived assemblage is immersed in an almost equally balanced blend of inorganic fillers (silica) and epoxy resins cross-linked with polyfunctional compounds suitable for electric applications [14].

A typical component mixture, which provides a material with optimal chemical resistance and insulating properties, is made by bisphenol A (BPA), epichlorohydrin and an organic anhydrides as curing agent (aromatic, alicyclic, aliphatic – a very common crosslinker is methyl tetrahydrophthalic anhydride) [15]. In figure 1, some of the main commercial epoxies are shown. All the resins based on the epoxies listed in figure 1 find application in the electric and electronic sectors, because of a high glass-transition temperature, high elastic modulus and mechanical strength, good resistance to corrosion and chemicals, good dielectric properties and high creep resistance. Brominated epoxies, at least till some years ago, were used in the production of printed circuit boards due to their ignition resistant feature. Novolac epoxies are used in the fabrication of electrical laminates and encapsulations because of their high chemical resistance. Cycloaliphatic epoxy resins can replace porcelain in insulators thanks to their higher heat-distortion temperatures and lower dielectric constants.

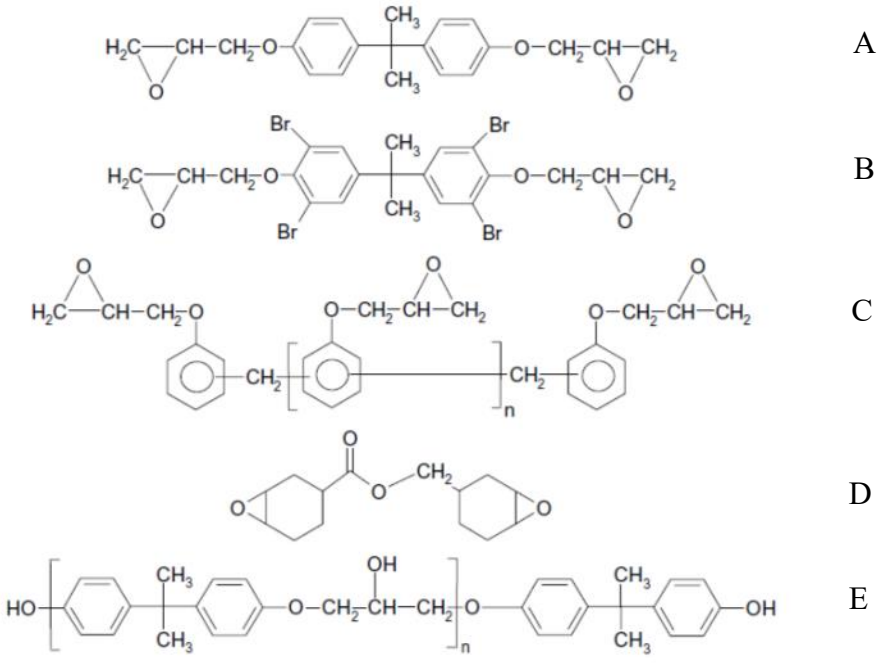

Figure 1: Main commercial epoxies; Diglycidyl ether of Bisphenol A (A), Brominated epoxy resins (B), Epoxy Novolac (C), Cycloaliphatic epoxy resin (D), Phenoxy resin (E).

In order to obtain a usable product, the resin needs to be cured [16]. The process consists in a macromolecule chain formation followed by linear and branched growth, gelation and final vitrification to a crosslinked network. Generally speaking, epoxy resins are typically cured with amines, which however introduce more polar groups into the polymer making it not perfectly suitable for electrical applications [17]. Consequently, other crosslinking compounds are preferred, like anhydrides (figure 2) which can undergo catalyzed or non-catalyzed reactions. Primary and secondary amines are used as curing agents, while tertiary amine as catalysts (see figure 3 for some examples) and accelerators (especially when anhydrides (figure 4) are used as curing agents).

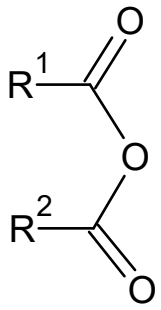

Figure 2. Anhydride functional group

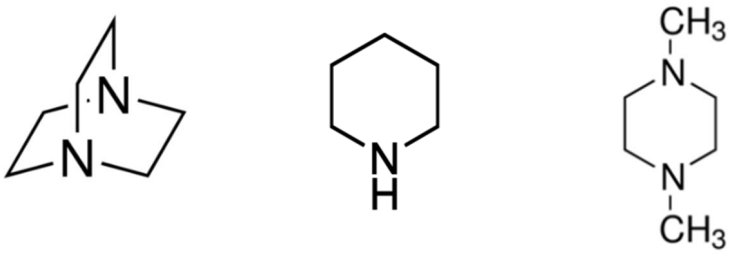

A B C

Figure 3. Some amine compounds. A: Triethylenediamine (tertiary); B: Piperidine (secondary, common curing agent); N,N-dimethylpiperazine (tertiary) [16]

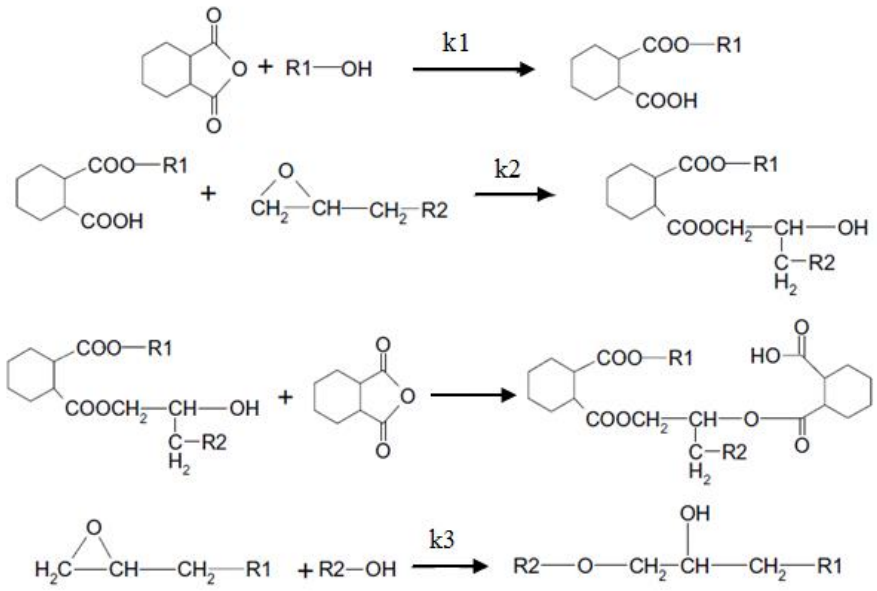

Figure 4. Uncatalyzed anhydride-based curing reactions [15]

In the manufacturing of transformers, the resins are not used in the pure form, but they are mixed with inorganic fillers like quartz sand [18]. Actually, the producers purchase suitable reagent mixtures from the market and pour them onto the windings inside a vacuum-oven for curing. When the hardening phase is over, the machine is completed and tested. In figure 5 an in-service 300 kVA cast-resin transformer is shown. In figure 6 the main components of a transformer are displayed: the core, the low and high voltage (LV and HV), the windings and the casted resin. Across the gap between LV and HV sectors air can circulate either thanks to a stack effect (lower and upper parts have different temperatures) or it can be forced by dedicated air blowers. In the specific case of the transformer displayed in figure 6 the heat is dissipated by a natural air flow. The internal parts of any transformer can be subjected to localized excessive temperature rise, known as hot spots, whose occurrence can be reduced through forced air systems. Whether fans are present or not becomes a manufacturer's choice, according to its own design, even though some common rules are generally followed. In any case the room or compartment where the transformer is placed must have a good air exchange with the outside.

Figure 5. Example of a cast resin transformer (250 kVA)

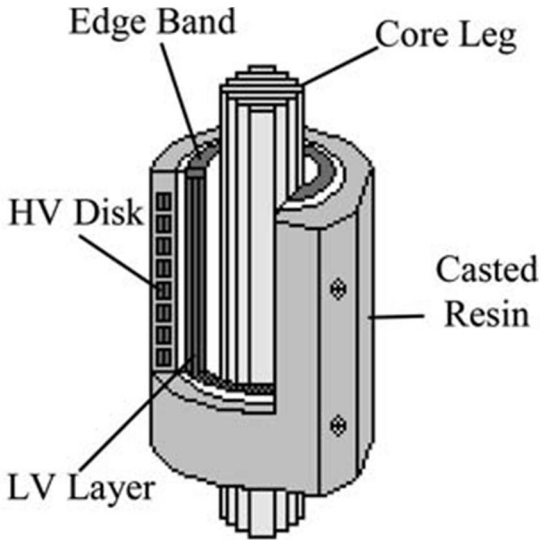

Figure 6. Vertical section of a cast resin transformer [19]

It becomes quite obvious that no part of a cast-resin, in-service machine can be removed without impairing its functioning. In any case, during the energy transformation, harmful electric and thermal phenomena can occur. Even non-experts, dealing with resin-insulated electric devices, know that thermal stresses produce typical profiles of degradation of polymeric materials (detectable by the human nose if in sufficient amount - smell effect). Nevertheless, even in the presence of a strong, typical reek of burnt electronics it's impossible to understand if the machine has been internally affected by thermal degradation

phenomena or electrical discharges, that can impair its correct operative conditions. In fact, partial discharges occur in a limited portion of the transformer and do not necessarily produce an instant failure but can induce or accelerate the decay of the materials. A study on epoxy resin degradation revealed that a prolonged electric field induces a relevant ageing of the resin [20]. Electric properties such as dielectric loss and volume resistivity showed a measureable variation that can be explained by an overall and not isolated structural modification of the material. In fact, scanning electron microscopy (SEM) observations revealed the formation of large dark regions of degradation, which seem to start in the surroundings of inadequate contact points between the resin and the field source [21]. Temperature also has an influence over the chemical structure both of the epoxy resin and the polyester film insulating the aluminum or copper windings. As a matter of fact, heating up a polymeric material causes the macromolecules to break, reduce their chain length and release smaller volatile or semi-volatile compounds. The duration of the heating step and the presence of oxygen have also an impact on the degradation mechanism and by-products formation [21].

At present, two properties are monitored when a transformer is in service: the temperature of the resin (taken in a fixed point by a probe immersed in the bulk) and the current load. Producers carry out lab measurement and factory tests according to international standards. For instance they perform partial discharges test (IEC 600726) [22], temperature rise (IEC 60076-2) [23] and noise (IEC 60076-10:2001) [24].

Even though the makers feather their own nest and assure about the reliability of their products, cast resin transformers are still affected by a higher failure rate compared to liquid-filled equipment. Several factors, which can be either concomitant or independent, can be addressed as responsible for faults. High temperature, insufficient ventilation, dust (especially if conductive), salty air (vicinity to the sea) and inadequacy of design, construction and testing [25]. Cast resin transformers are tested after manufacturing according to several international standards (International Standard Organization (ISO) or ASTM), but unfortunately it becomes quite hard and expensive to check for their correct functioning while they are in service [26]. Comparable disadvantages are also observed when dealing with rotating electrical machines such as motors and generators. At least six causes can be pointed out as responsible for electric motor failures: over-current, low resistance, overheating, dirt, moisture, vibration [27]. Over-current is an unpredictable event which can have a sudden devastating impact on the correct functioning of the motor and is caused by a draw of current exceeding the motor overall capacity. The lowering of a motor's insulation

resistance is an expected behavior accountable for a lot of failures. Overheating is responsible for a quick deterioration of the motor winding insulation. It is reported that, for every ten degrees centigrade rise in temperature, the insulation life is cut in half [27]. Dirt can be an indirect source of overheating since it hinders heat exchange. Moisture is a cause of corrosion and vibrations can bring moving parts to misalign or even come off. Analogously to dry-cast transformers only some electrical properties are monitored constantly through dedicated sensors installed onto the motor (for instance SKF company offers a system which " operates with one voltage measurement per buses and current sensors installed for each motor. It analyzes over 120 electrical parameters and compares the results to user defined limits, alerting the user if these limits are exceeded…"). Many times, but not always, a cast resin transformer is equipped with current (load) and temperature sensors [28]. These sensors are sometimes connected to a centralized monitoring system but most of the times they are simple stand-alone tools. In any case, it seems that the market does not provide any comprehensive system devoted to monitor the effects of physico-chemical properties other than those related to electric power. Personal interviews with some owners of transformers revealed the necessity to find a solution that, through a constant on-line monitoring, can assess the conditions of resin-insulated electric machines, anticipate failures and predict remaining operative lives. As a matter of fact, the individual or combined actions of prolonged heating, overheating, electrical discharges and vibrations can cause a resin to change its chemical and physical structure and start a so-called degradative or decomposing process. During said process the crosslinked macromolecules of the resins start to cleave their bonds, reduce their size and let off smaller semi-volatile molecules that can travel some distance away from the bulk [29]. Literature can offer different explanations of epoxy resin degradation which vary because of dissimilar synthesis methods (e.g. different curing agents) and stress conditions. An interesting study provides information [30] regarding the degradation pattern of insulating anhydride-cured epoxy resins. It seems that all starts in the cleavage of an ester bond. The three principal small by-products released are formaldehyde (CH_2O), carbon dioxide and water (figures 7,8). The aldehyde is the most abundant compounds and derives from the decomposition of epoxy functional groups, whereas CO_2 comes from the carbonyl bond in the anhydride part. The epoxy resins for electrical applications are affected by defects normally induced during the manufacturing process, the transportation and the operation. Such defects (grooves, gas gaps for instance) make the resin vulnerable to partial discharges, which can cause a local temperature increase that ranges from 170°C to 1000°C. The consequence is the increased possibility of breakdown caused by

the development of an electric tree [31]. The degradation forms also water that can rise the surface conductivity of the resin.

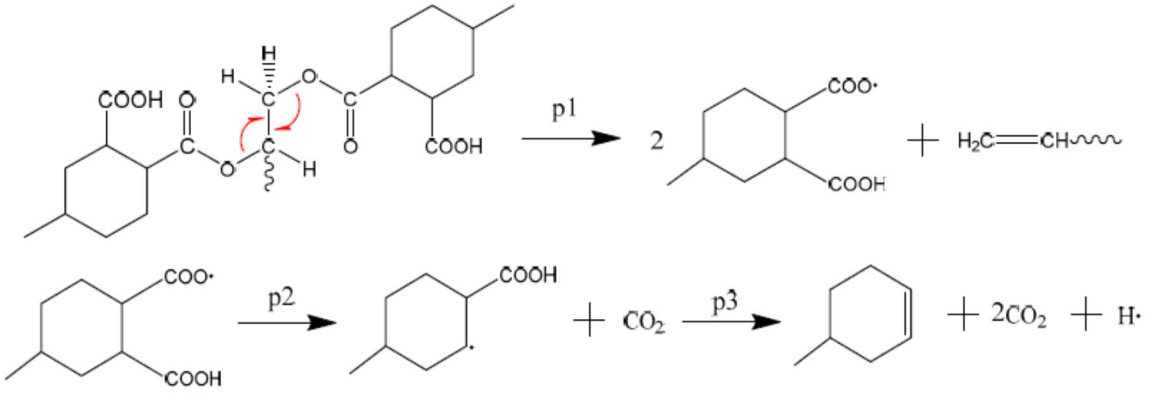

Figure 7. Example of mechanism of CO_2 formation [30]

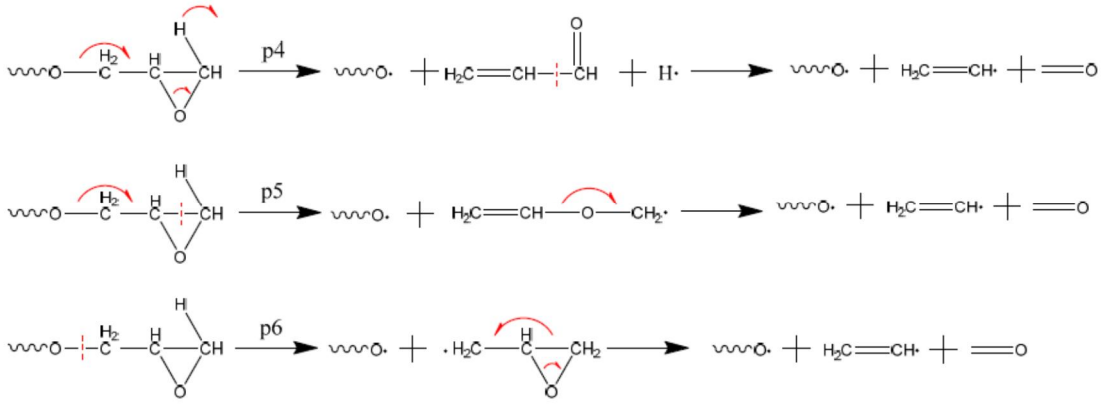

Figure 8. Example of mechanism of CH_2O formation [30]

The importance of monitoring the conditions of the machines is directly linked to the application. In fact, the price of a dry cast transformer is normally not very high (for instance a Class N 1 MVA transformer price is around 14,000 €) [31], but the losses derived from lost production can become exceedingly relevant. If, in case of fire, the combustion of polymeric materials lasts for sufficient time (resin tend to be self-extinguishing materials), a wide-ranging amount of gaseous, volatile and most of the time toxic fumes is generated. In particular when the electrical machine is coated with epoxy resin, the risk of phenolic compound release is quite high. One common compound is bisphenol A, which may cause an

allergic skin reaction, causes serious eye damage, may cause respiratory irritation, suspected of damaging fertility and is toxic to aquatic life with long lasting effects [32]. So any emissions of fumes from these resins, linked to a thermal fault and starting from consequent electrical failure of the transformer, constitutes a health and environmental pollution risk This adds to the consequences of any transformer outage, i.e. stops in electricity distribution, which in turns means loss of revenues for the owner of the power generation infrastructure and loss of production or service for the industrial or civil users immediately downstream.

On the basis of what stated so far, it should go without saying that an on-line and on-site monitoring of an electric machine must be extremely important especially in those sectors where forecasting failures can reduce downtime, direct costs and indirect losses. However, what are the properties that should be monitored to achieve a comprehensive understanding of the conditions of the machine? Are cast resin transformers and rotating electrical machines characterized only through physics or is there any space for chemistry as well? Physical properties like current and temperature are already monitored continuously through probes connected directly to the machine, whereas partial discharges are typically measured in an off-line mode, mainly during the initial tests. Nonetheless it's quite evident that dry-type transformers and motors have some chemistry hidden within. A question that arises spontaneously is if it could be possible to analyze and quantify some organic vapors (likewise DGA in liquid-insulated transformers) which can be directly linked to thermal and electric problems and incipient faults. There have been studies attempting to find a correlation [33] between the degradation of the polymeric materials and the decay of insulating properties and thus the increment of fault probabilities. Said studies have demonstrated that a lot of small volatile molecules, like aromatic, heteroaromatic (phenolic) and aliphatic compounds, can be released after overheating, prolonged heating, electric stress. A few sensors already exist, which can detect the presence of said molecules. Some of them work on optical properties and the capacity of certain molecules to absorb energy in specific regions of the electromagnetic spectrum (e.g. phenolic compounds absorb both in the UV and in the infrared region), and others are built using semiconductors (normally metal oxides) which are characterized by a lower degree of selectivity [34]. Sensors can be either specific or aspecific towards a wide range of molecules and vary according to the environment and the materials they are intended for. Those meant to be used in liquids should have different characteristics than those developed for gas-phase applications, which are the inevitable choice when

electrical machines are put under investigation. Gas sensors based on metal oxide semiconductors are quite inexpensive, fast responding and have a good sensitivity [35]. Since the early sixties of the former century it was discovered the conductivity of a metal oxide could be varied by adsorbing and desorbing a gas from its surface. The first reliable and effective sensor was built using zinc oxide. This type of sensor, like all the others that were developed successively, works on the principle that there is a certain energy gap (0.5 -5.0 eV) between the valence and conduction bands. But if sufficient energy is provided to the system (above the Fermi level) electrons can flow between the two bands and increase conductivity [36]. In metal oxide gas sensor, the surface normally adsorbs oxygen and changes its charge carrier concentration, thus its conductivity. Sensors can be divided into the categories of n-type and p-type semiconductors. In the former case an oxidizing gas decreases conductivity whereas a reducing gas increases it. In the latter the behavior is reverse.
The mechanism can be summarized in the following table.

Classification	**Oxidizing gases**	**Reducing gases**
n-type	Resistance increase	Resistance decrease
p-type	Resistance decrease	Resistance increase

Table 1. Conductivity change for n- or p-type semiconductors in the presence of a gas

The adsorption of oxygen on the sensor surface is governed by the following equilibrium 1.1:

$$\frac{1}{2} O_2 = O^{2-} + 2\, p^{+} \qquad 1.1$$

Where O^{2-} is the superoxide anion and p^{+} is a proton

And the ratio between the resistance before (baseline resistance in clean dry air) and after exposure is given by the following formula:

$$R / R_0 = 1 + A[C] \qquad 1.2$$

Where A is constant dependent on the temperature and [C] is the concentration of the selected compound C.

A model of molecule adsorption was proposed, whose schematic is shown in fig. 9.

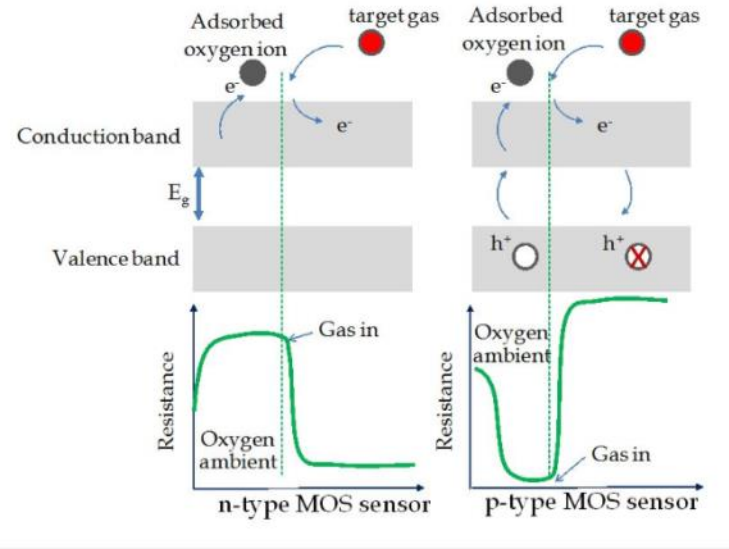

Figure 9. Effect of a reducing gas on the signal provided by an n-type or p-type sensors [37]

In figure 9, it is possible to see the difference between the behaviors of a n-type and p-type sensor. The former decreases its resistance when a reducing gas is adsorbed on the surface, while the latter shows the opposite behavior.

Several sensors based on metal oxides are already used on an industrial scale and many others, old and new, are under investigation, like the aforementioned zinc oxide, but also copper, tin, titanium and aluminum oxides, taken as pure compounds or doped with other metals. Sintered tin oxide (SnO), for instance, is used by a Japanese company (Figaro Engineering Inc.) as the sensitive element for its hydrogen sensors (TGS 821) [38]. Despite the fact of being a well-established market product, it's still undeniably affected by a non-negligible responsiveness to other common gases, like carbon monoxide and methanol, which represents a limitation to potential uses (figure 10). Other commercial sensors which are based on zinc oxide and titanium oxide are those produced by Synkera and Nissha Fis. By looking at their technical data sheets it's evident that these kind of sensors must be intended to determine the presence of a class of compounds (e.g. flammable gases) more than single molecule types. To evade from this kind of flaws, possible countermeasures can be found in noble-metal addition, transition- metal doping, temperature variation, sensor array assembly and nanostructure development [39, 40]. For instance, Zeolite Imidazolate Frameworks (ZIF) can be used to improve the selectivity of TIO_2-base sensors towards hydrogen [39]. Another example is tin oxide which is a n-type semiconductor that can be turned into a p-type by the addition of iron (doping).

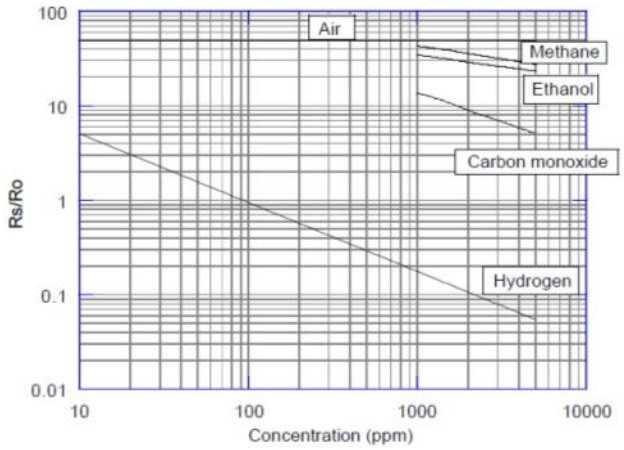

Figure 10. Response of Figaro hydrogen sensor TGS821; the vertical axis is the resistance ratio (R_s/R_o) where R_s is the sensor resistance at different concentrations and R_o is the sensor resistance at 100 mg kg^{-1} of hydrogen [38].

Tin oxide and zinc oxide are the most common material used for gas detection [41]. ZnO, equally to SnO, is an n-type semiconductor available in single large crystal. However, its n-type conductivity is unintentional and can be deeply influenced by small concentrations of native point defects and impurities. This electrical property seems to be related the accidental incorporation of impurities such as hydrogen which gets included during crystal growth and processing. The band gap of ZnO is 3.77 eV at room temperatures and it can be modulated by adding Mg and /or Cd. The mechanism of how the conductivity is deeply influenced by the exposure to various gases is scarcely understood. Cupric oxide is another compound which could be used to fabricate solid state sensors. In contrast with ZnO, it is a natural p-type semiconductor with a bandgap energy of 2.1 eV, allegedly patented long before the starting of the Ge and Si era (1926). This compound, far from being an important subject of study, has recently won renewed interest with respect to solar-cell-applications. The p-type nature of CuO is determined by vacant copper ion lattice sites. It is reported that anhydride-cured-epoxies (in the adhesive sector) can have a certain affinity towards copper oxide. The carbic anhydride crosslinker can react with cuprous oxide on the copper surface of a transformer winding (for instance) oxidizing cuprous ions to cupric and forming carboxylates. It seems that an analogous behavior can be observed in the case of zinc oxide [42].

Copper is often used as a dopant of other metal oxides. For instance, it has been used in conjunction with tin or aluminum [43]. In the latter case, by varying the deposition and annealing procedures either an n-type or a p-type sensor could be fabricated, with a superior

sensitivity of the second towards ozone. Additionally, by keeping the operating temperature at 300°C, the interference from other volatile compounds like acetone, ethanol and carbon monoxide could be reduced.

From what stated so far, it is evident that sensitivity and selectivity are the two main properties a sensor should have. The type of volatile compound or gas which needs to be detected and the place where the sensor has to be used are intimately connected. As a matter of fact, ambient temperature, humidity and the presence of molecules different from the target (interferences) can deeply and negatively influence the response. Hence, the preferred research route could be to start from a general purpose sensor and then to refine the path tuning a sensor tailored to fit a complex industrial situation. Actually dry-type transformers are used in different types of environments and can be positioned in rooms, cabinets or metal cases. They can be subjected to varying workloads in agreement with the machine or service they have to feed. Consequently a sensor suitable for the detection of molecules deriving from the thermal and electrical degradation of the polymeric materials should be sensitive, selective and reliable. A lot of compounds can be used to assemble gas sensors, even though only a few are actually exploited commercially, being the rest still a topic for research. Said compounds are normally inorganic oxides even if some organic polymers (e.g. molecular imprinted polymer [44]) have been tested, at least on a lab scale. However the on-line monitoring of dry-type transformers is a brand new application where molecules not normally investigated (at least in the gas phase) are the targets. Consequently a more cautious approach should be preferred, like the one based on metal oxides. Among the possible choices, which could be tested as detectors for target molecules, copper and zinc oxides sounds like a good starting point. The former is a p-type detector not sensitive to humidity (which is an ubiquitous interfering molecule in industrial environment), the latter is n-type detector which shows a good interaction with a broad spectrum of molecules. Furthermore it has been already and widely adopted to fabricate sensors for environmental monitoring, showing satisfactory degrees of versatility and durability. Finally these metal oxides shows good affinities with acidic compounds and heteroaromatic molecules. Thus, by creating a sensor array based on both sensors and by regulating the working temperatures it is expected to realize a system able to reveal the presence of molecules like those deriving from an overheated dry-type transformer, with a minimum interference from other compounds, normally pervading industrial facilities.

1.1 References

[1]Market Growth Led By T&D Infrastructure Investments In Developing Regions And Replacement Demand In Developed Regions; Global Transformer Market, Frost & Sullivan, 5th August 2016

[2] Electrical Engineering Portal, Transformers, Power Transformer Construction – The Core; 23rd August 2012; https://electrical-engineering-portal.com/power-transformer-construction-core; (accessed 15th April 2019)

[3] Sirmet Costruzioni Elettromeccaniche; https://www.sirmet.it/images/trasformatori/catalogo_new.pdf; (accessed 31st March 2019)

[4] Scheider Electric Group; https://www.schneider-electric.us/en/faqs/FA101863/; (accessed 31st March 2019)

[5] Engineering ToolBox - Resources, Tools and Basic Information for Engineering and Design of Technical Applications; https://www.engineeringtoolbox.com/heat-gain-equipment-d_1668.html; (accessed 25th March 2019)

[6] Transformer Ageing: Monitoring and Estimation Techniques, First Edition; Tapan Kumar Saha and Prithwiraj Purkait; JohnWiley & Sons Singapore, 2017

[7]CWIEME world's largest event dedicated to coil winding; https://www.coilwindingexpo.com/berlin/knowledge-hub/global-transformer-market-trends; (accessed 26th March 2019)

[8] CEM, manufacturer of cast resin insulators; http://www.cemcastresin.com/cast-resin.html; (accessed 5th April 2019)

[9] Digital Journal, Global Power Transformer Market Projected to Reach USD 34.6 Billion by 2024; http://www.digitaljournal.com/pr/3864346; (accessed 26th March 2019)

[10] RBaker, Electrical and mechanical services; https://www.rbaker.co.uk/transformer-life-expectancy/; (accessed 25th March 2019)

[11] Power Transformer, Part 3: Life management and extension; Carlos Gamez; Transformers magazine, Volume 1, Issue 3, pages 162-163, 2014

[12] Electrical and Engineering Portal, Do dry type transformers cost less than oil-filled?; https://electrical-engineering-portal.com/dry-type-transformers-costs; (accessed 23rd March 2019)

[13] Transformers – Surroundings; Axa insurance company; GAPS Guidelines 5.9.0.2, 2015

[14] Ecodesign Transformer Brochure; TESAR – Transformer Manufacturer; 2019

[15] The curing of epoxy resins as studied by various methods; M.Younes, S.Wartewig et al.; Polymer, Volume 35, Issue 24, November 1994

[16] Curing Agents for Epoxy Resin; Three Bond Technical News; Three Bond International company (adhesives and coating producer), Bulletin N. 32, December 20, 1990

[17] The curing mechanism of epoxy resin; W. Fisch, W. Hofman et. Al; Journal of Applied Chemistry, Volume 6, Issue 10, October 2007

[18] Ztelec Group, Electrical Equipment producer; https://www.ztaero.com/ ; (accessed 12th April 2019)

[19]. Analysis of Temperature Distribution in Cast-resin Dry-type Transformers; Ebrahim Rahimpour, Davood Azizian; Electrical Engineering, Volume 89, Issue 4, March 2007

[20] The effect of electrical ageing on a cast epoxy insulation; Y.Li, J.Unswort, et al.; Electrical Electronics Insulation Conference and Electrical Manufacturing & Coil Winding Conference, 4-6 October 1993

[21] 7 - Thermal Degradation of Polymer and Polymer Composites; Sudip Ray, Ralph P.Cooney; Handbook of Environmental Degradation of Materials (Second Edition); Elsevier, 2012.

[22] IEC 60076-11:2004, Power transformers - Part 11: Dry-type transformers, Pub date 2004-05-27

[23] IEC 60076-2:2011 Power transformers - Part 2: Temperature rise for liquid-immersed transformers, Pub. Date 2011-02-23

[24] IEC 60076-10:2001 Power transformers - Part 10: Determination of sound levels, Pub date 2001-05-22

[25] Machine Design, division of Informa (international research center); https://www.machinedesign.com/mechanical/top-3-reasons-transformer-failures; (accessed 31st March 2019)
[26] Bright Hub Engineering; https://www.brighthubengineering.com/commercial-electrical-applications/78579-determining-causes-for-electric-motor-failure/; (accessed 30th March 2019)
[27] Efficient Plant Magazine; https://www.efficientplantmag.com/2003/04/overheating-electric-motors-a-major-cause-of-failure/ EP Editorial Staff | April 1, 2003; (accessed 30th March 2019)
[28] Sea, Transformer Manufacturer (It); https://www.seatrasformatori.it/en/accessories-dry-type-transformers.html; (accessed 21st March 2019)
[29]Theoretical Study on Decomposition Mechanism of Insulating Epoxy Resin Cured by Anhydride; Xiaoxing Zhang, Yunjian Wu, et al. ; Polymers, Volume 9, Issue , August 2017
[30] Photooxidation of Anhydride-Cured Epoxies: FT-IR Study of the Modifications of the Chemical Structure; V. Ollier-Dureault, B. Gosse; Journal of Applied Polymer Science, Vol. 70, Issue 6, November 1998
[31] Cast Resin Transformers brochure; Legrand -Electrical infrastructure Specialist; https://www.legrand.nl/; (accessed 15th March 2019)
[32]SigmaAldrich, Chemicals Supplier; Material Safety Data Sheet https://www.sigmaaldrich.com/MSDS/MSDS/DisplayMSDSPage.do?country=IT&language=it&productNumber=239658&brand=ALDRICH&PageToGoToURL=https%3A%2F%2Fwww.sigmaaldrich.com%2Fcatalog%2Fsearch%3Fterm%3Dbisphenol%2520A%2520MSDS%26interface%3DAll%26N%3D0%26mode%3Dpartialmax%26lang%3Dit%26region%3DIT%26focus%3Dproduct%26F%3DPR%26ST%3DRS%26N3%3Dmode%2520matchpartialmax%26N5%3DAll; (accessed 12th March 2019)
[33] The effect of voltage and material age on the electrical tree growth and breakdown characteristics of epoxy resins; J V Champion and S J Dodd; Journal of Physics, Volume 28, Number 2, 1998.
[34] Optical Chemical Sensors; Colette Mc Donagh, conor S. Burke et. al.; Chemical Reviews, ACS Pub., Volume 108, Issue 2, 2008
[35]Metal Oxide Semi-Conductor Gas Sensors in Environmental Monitoring; George F. Fine, Leon M. Cavanagh et el.; Sensors, Volume 10, Issue 6, 2010
[36] Metal Oxide Gas Sensors: Sensitivity and Influencing Factors; Chengxiang Wang, L. Yin et al. ; Sensors, Volume 10, Issue 3, 2010
[37]Metal-Oxide Nanowires for Gas Sensors; Supab Choopun, Niyom Hongsith and et al.; IntechOpen, December 19th 2012; https://www.intechopen.com/books/nanowires-recent-advances/metal-oxide-nanowires-for-gas-sensors; (accessed 25th March 2019)
[38] Special Sensor for Hydrogen Gas - Figaro TGS 821. Technical Data Sheet. Figaro; http://www.figarosensor.com/; (accessed 15th March 2019)
[39] Resistive-type hydrogen gas sensor based on TiO2: A review; Zhong Li, Zheng Jun Yao, et al.; International journal of hydrogen energy, 43, Issue 45, 2018
[40] Methods of selectivity improvements of semiconductor gas sensors; Grzegorz Halek , Miroslaw Malewicz ; 2009 International Students and Young Scientists Workshop "Photonics and Microsystems, 25-27 June 2009
[41] Facile Preparation of a ZnO/SnO2-Based Gas Sensor Array by Inkjet Printing for Gas Analysis with BPNN; Mingyue Peng, Dawu et.al.; Journal of electronic materials, Vol. 48, No. 4, 2019
[42]Vibrational spectroscopy of the gas-solid interaction between anhydride molecules and oxide-covered polycrystalline zinc substrate; C. Szumilo, P. Dubot et al.; Journal of Adhesion Science and Technology 11, issue 4, January 1997
[43] P-Type copper aluminum oxide thin films for gas-sensing applications; Camilla Baratto, Raj Kumar, et al.; Sensors and Actuators B Chemical, Volume 209, March 2015
[44] Molecularly-imprinted polymer sensors: realising their potential; Biosensors and Bioelectronics; Lokman Uzun, Anthony P.F. Turner; Biosensors and Bioelectronics, Volume 76, February 2016

2 Research Objectives

The research to be presented starts with a study on the thermal degradation of epoxy resins samples delivered by a local manufacturer. The work serves, on one hand, to confirm the results found in literature and on the other hand to provide a more complete explanation of thermal degradation phenomena, especially on a real industrial sample. The study was performed with the support of different analytical techniques like thermogravimetry, mass spectrometry and infrared spectrophotometry. A certain degradation pattern was established and several volatile compounds were isolated.

Additionally, an air-sampling device, to be installed near an in-service transformer, was assembled in order to trap molecules which can be possibly released from a dry-type transformer in real operative conditions.

After collecting plentiful chemical and analytical data, the topic of the research was redirected towards the development of solid-state sensors for the on-site detection of degradation markers of epoxy resins. Two different metal oxides were tested, copper and zinc oxides. First of all, they were synthesized and then deposited on a circuitized alumina substrate, by a screen printing technique. The resulting sensors were tested with different compounds at different temperatures and under different humidity conditions. Interference from common molecules were also investigated.

Finally, a prototype device equipped with several sensors was engineered and installed in the cabinet accommodating a dry-type transformer.

3 Epoxy resin degradation study

3.1 Instrumentation

Herewith a list of the main equipment used to perform the degradation experiments on epoxy resin is given.

1. The thermogravimetric analyses were carried out with a TA thermogravimetric analyzer Q50. The analyzer was operated under the following conditions:

Sample pans:	platinum
Amount weighed:	5 – 15 mg
Gas flow rate:	40 mL/min
Form of the samples:	chunks, powder
Purge gas:	nitrogen or air.
Heating:	different ramps and isothermal

2. The gas chromatographic (GC)/mass spectrometry (MS) analyses were performed using an Agilent 6890 GC coupled with a 5973 Network MS and a Thermo Scientific Trace 1300 GC coupled with a TSQ8000EVO MS.

   Conditions used for GC analyses were as follows:

   I) Agilent 6890

Amount Injected:	1µL
Initial temperature:	80°C
Initial hold:	2 min
Temperature program:	20°C/min up to 240°C then 30°C/min up to 300°C, hold 5 min
Carrier gas:	Helium

Column:	Capillary, DB-5/ms, (5%-Phenyl)-methylpolysiloxane, 50 m
Flow:	1mL/min
Linear Velocity:	27 cm/s

II) Thermo Scientific Trace 1300

Amount Injected:	1µL
Initial temperature:	80°C
Initial hold:	5 min
Temperature program:	3°C/min up to 200°C then 10°C/min up to 300°C,
Carrier gas:	Helium
Column:	Capillary, TG-17 sil, (50%-Phenyl)-methylpolysiloxane, 30 m
Flow:	1.2 mL/min

Conditions employed for MS analyses were as follows:

III) HP 5973 Network

Ionization. Electron Impact
Energy: 70 eV
Filter: Quadrupole
Source temperature: 150°C
Filter temperature: 150°C

IV) Thermo TSQ8000EVO triple quadrupole

Ionization. Electron Impact
Energy: 70 eV
Filter: Quadrupole (Triple Quadrupole)
Source temperature: 150°C
Filter temperature: 150°C
Second ionization gas: Argon

Energy of second ionization gas: 5-10 eV

This mass spectrometer (figure 1) can be used in two ways. As a simple single quadrupole either in full scan acquisition mode or Selected Ion Monitoring (SIM) mode or as a triple quadruple in the selected reaction monitoring (SRM). In the latter configuration the noise caused by the matrix and the unwanted interfering molecules can be eliminated by selecting a parent ion of the molecule of interest and inducing a dissociation through the collision with Argon molecules.

Figure 1. Thermo Scientific Trace 1300 and TSQ8000EVO triple quadrupole

3. The thermal degradation of the resin was carried out in a ventilated oven Memmert Universal Oven U:

   Heating ramp: 10°C/min
   Target temperatures: 100, 150, 200, 250, 300°C

4. The surface analyses of heated resin samples were carried out with a Fourier -Transform Infrared Spectrophotometer Perkin Elmer 2000 and Perkin Elmer Spectrum Two.

Wavenumber range:	500-4000 cm^{-1}
Resolution:	4 cm^{-1}
Accessories:	ATR - diamond crystal and ATR SeZn crystal (trapezoid)

3.2 Experimental Study

The experiments regarding the thermal degradation of epoxy resin were carried out on a section taken from a brand new transformer which failed during the commissioning, in an area not involved in the failure, like the one shown in figure 2. In this specific case, the manufacturer assembled the windings using copper, even though aluminum is normally the preferred metal, thanks to the comparable dilation coefficients between the epoxy and this latter metal. The casted resin and the alternate stacking of copper sheets and polyester films, forming the windings, can be easily observed.

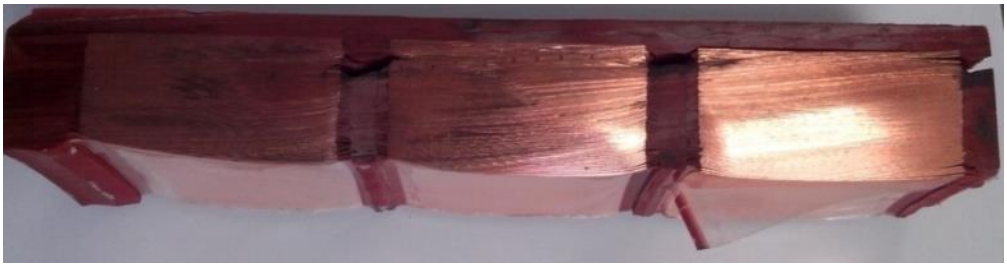

Figure 2. Cast resin transformer assembly. Epoxy resin (red part) and polyester polymer (transparent film) are clearly visible. The multilayer structure (copper-polyester alternate stacking) is evident.

The thermal degradation was first studied through several thermogravimetric analyses both under inert atmosphere and air and with the epoxy resin samples in the powder and solid forms. Powder samples were prepared using an electronic grinder (IKA A11 Basic).
Successively, from the transformer portion described above, several small samples were cut out to perform thermal degradation experiments under different heating conditions. The resulting lumps of resin, both in their bare state and together with the copper sheets and the polyester films, were introduced into a 300 mL glassware apparatus (Figure 3), which was then placed into a ventilated oven and tested at different target temperatures (100, 150, 200, 250, 300°C). The upper part of the apparatus was equipped with a silicon septum to enable the sampling of the evolved gasses, which were then dissolved into a weighed amount of acetone or isopropanol (0.500 mL of gas slowly bubbled with a 10 µL micro-syringe into 1 mL of isopropanol). Acetone is preferred if a fast evaporation of the solvent is necessary (e.g. in the case of deposition on a KBr crystal for infrared analysis). The resulting solutions were

analyzed both through GC-MS/MS and FT-IR techniques. At the end of each test the inner parts of the apparatus were also rinsed with 25 mL of 2-propanol, and the solution analyzed again with the MS-coupled GC.

Pieces of resin were also placed in the ventilated oven without being inserted in any closed vessel, thus being subjected to a stronger action

The surface of the various resin samples, heated and not heated, were analyzed with a FT-IR instrument in the attenuated total reflectance mode (ATR)

Polyester films were heated at the same temperature as the resin, under nitrogen. Furthermore, they were also exposed to organic anhydride fumes at around 80°C for 30 minutes. Superficial FT-IR/ATR spectra were performed on said samples.

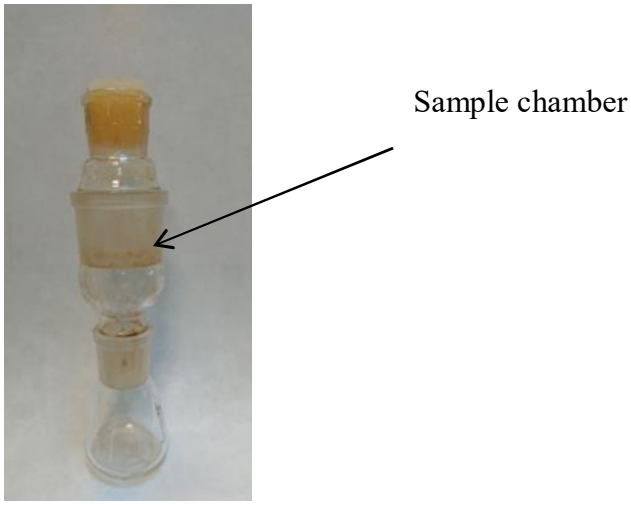

Figure 3. Glassware apparatus used to carry out thermal degradation experiments

After evaluating the results of the infrared analyses some samples of epoxy resins underwent a reaction with bromine in a closed vessel. As a matter of fact, the appearance of the samples and the IR profiles after the thermal treatments, induced to believe that either double bonds had formed or residual epoxy groups were present. To that end, treated and untreated samples were kept in a closed Pyrex bottle in the presence of few drops of bromine at ambient temperature for 30 minutes. Afterwards ATR-FT-IR analyses were performed to assess the effect of the halogen vapors on the surface of the polymer.

Finally, in order to accelerate the degradation phenomena, samples of pulverized resin were exposed to various temperature gradients in a stream of air (0.5 mL/min). The outcoming gases and vapors were immobilized in a trap filled with silanized wool (Figure 4), which was

successively rinsed with methanol for compound recovery. Finally, the resulting solutions were analyzed with a GC-MS technique. The sample was pulverized using an electronic grinder (IKA A11 Basic).

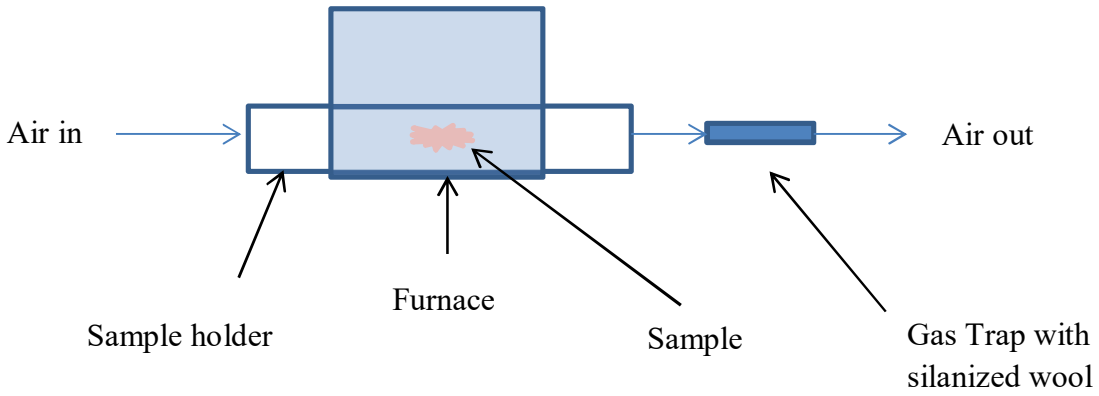

Figure 4. Schematic of the apparatus used to investigated the accelerated degradation of the epoxy in the powder form.

3.3 Results and Discussion

3.3.1 Thermogravimetric analyses

The heating experiments and the thermogravimetric analyses on the epoxy resins described above were conducted to determine the decomposition temperatures and the nature of the molecules produced by a rise in temperature, in the attempt to simulate the thermal phenomena that might occur in a cast resin transformer. As already stated, the temperature growth varies in relation to the presence or absence of a forced-air cooling system, sure that a mere air convection determines higher temperature increments. It seems that in a forced ventilation arrangement, the highest hot spots are observed in the upper part of the high-voltage coil (an observed value is, for instance, 140°C), in contrast with natural cooling where more intense hot spots locates in the upper part of the low –voltage coil (it can be as high as 166°C). Amount, intensity and duration of hot spots (presumably even higher than 166°C) is a direct consequence of environmental conditions, load and design of the transformer. In fact, producers specify the ambient settings under which a transformer has to operate, on pain of forfeiture of the warranty. For instance, ABB, one of the biggest global transformer producers, declares that the temperature of service of one of its cast resin transformers has to be comprised between -10 and +40°C.

Thermogravimetric analyses were the first experiments performed to understand whether literature results match those obtained from a "real" sample taken from an in-service transformer. In figures 5-8, four different thermogravimetric patterns can be observed.

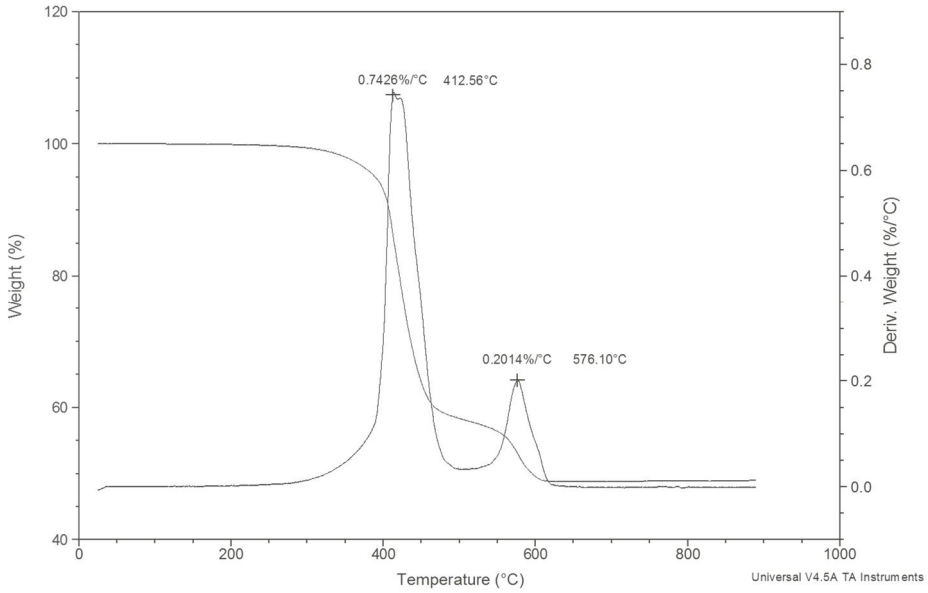

Figure 5. 30°C/min thermogravimetry of a 15 mg piece of epoxy resin in air

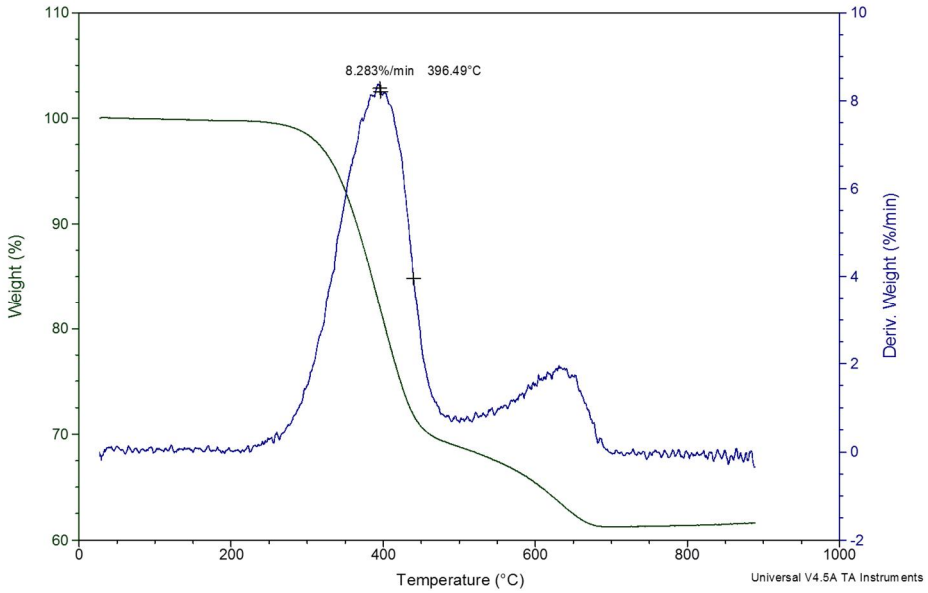

Figure 6. 30°C/min thermogravimetry of a 5 mg piece of epoxy resin under nitrogen

The thermogravimetry shown in figure 5 reveals that only 50 % of the industrial artefact is produced with epoxy resin (in agreement with what declared by the manufacturer). The remaining part is made of inert materials (allegedly quartz sand, an inexpensive optimal

insulator).The thermal degradation starts around 300°C and then shows two peaks. The first and sharper aroud 400°C, the second between 550°C and 600°C. Other thermogravimetry analyses, found in literature, show similar results when air is used as reagent gas, whereas the behavior changes when nitrogen is used, showing a three steps decomposition pattern with the first decomposition event between 300 and 350°C.[1]

The graphs in figures 5 and 6 show a 16°C difference in the temperature at which the decomposition rate is maximum. Even though the thermogravimetry relative to figure 6 was carried out under nitrogen, the first decomposition peak occurs at a lower temperature, in contrast to an expected shift of the degradation temperature to higher values. Apparently, the reason could be ascribed to the lower weight of the sample (3 times less than in the experiment of figure 5, 5 mg instead of 15 mg). However studies have demonstrated that the sample mass doesn't seem to affect the decomposition significantly [2]. Among heating rate, sample mass and gas flow, the first parameter has the strongest influence over the rate of disruption of the polymeric matrix. Consequently it might be inferred that the resin has sufficiently disomogeneous structure and composition that may lead to results with limited repeatibility and in apparent contradiction with previsions, thus requiring a high number of repetitions. Nevertheless the aim of the thermogravimetric analyses was not to assess the exact temperatures at which the resins show heat-induced modifications, but to understand their general behavior, partly because industrial products can have different compositions and follow proprietary production methods, that could only lead to a broad miscellany of different behaviors.

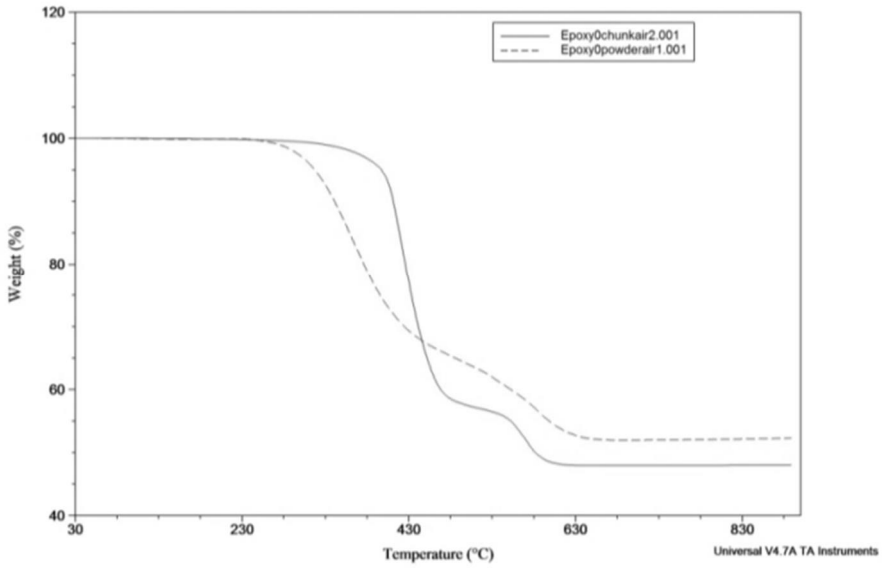

Figure 7. Comparison between thermogravimetry of epoxy resin samples in powder (dotted line and lumpy form (solid line)

In figure 7, a comparison between gravimetric curves of epoxies in powder and solid forms is shown. A finely divided state seems to determine a lowering in the temperatures at which the degradation starts and accelerates as a consequence of a higher surface area which can prompt multiple decomposition onset points.

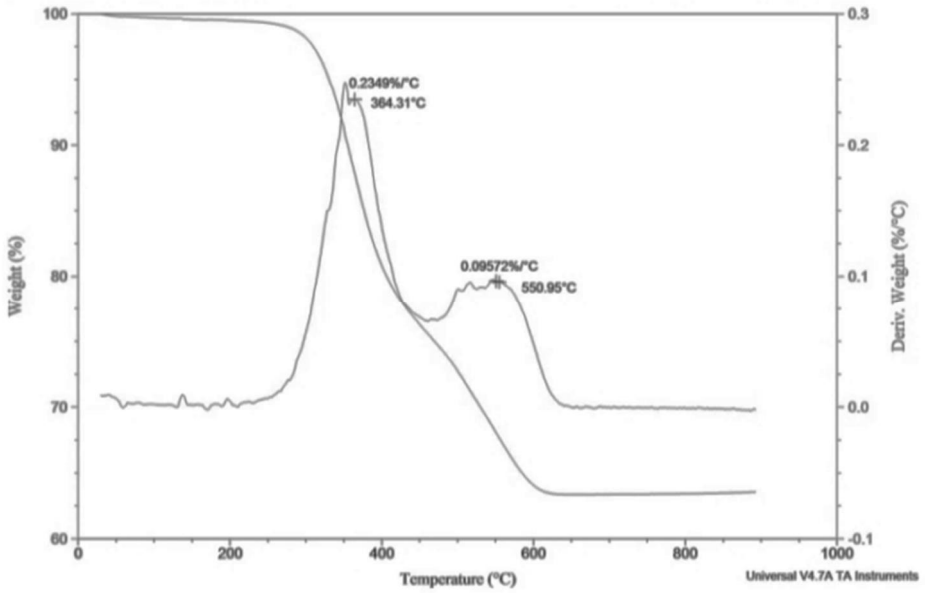

Figure 8. Thermogravimetry of an epoxy resin sample which underwent a previous thermal treatment at 200°C for 6 hours.

Thermogravimetric studies were also performed on resin samples which were pre-exposed to heat. In the specific case shown in figure 8, the resin was kept at 200°C for 6 hours. After that, the polymer started having a blackish appearance, indicating an incipient degradation. In the subsequent thermogravimetric analysis, the weight loss started at a much lower temperature (364°C against 396°C). Besides, the initial part of the curve doesn't appear as flat as in the curves previously shown (figures 5-7) suggesting the presence of a diffused number of vulnerable points, which determine a start of the weight loss as low as 120°C.

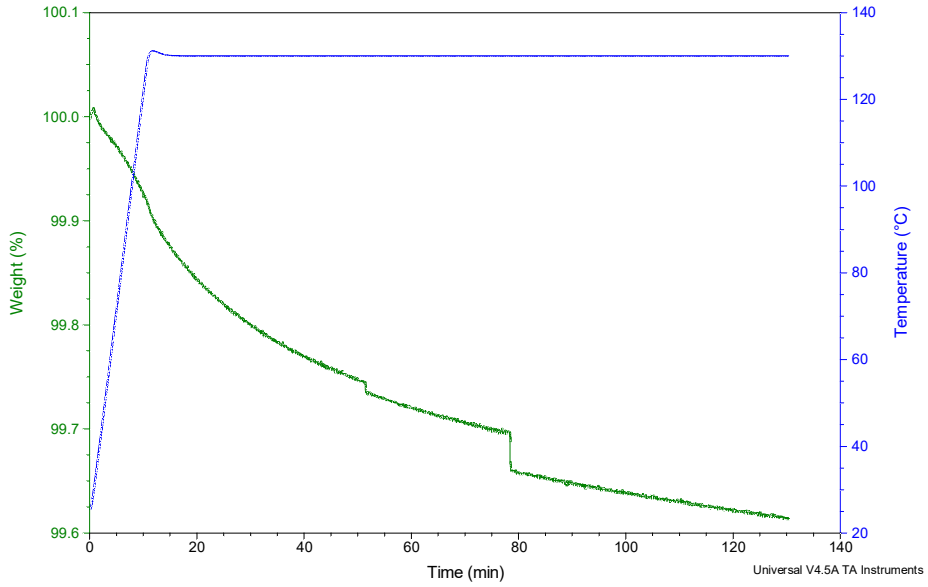

Figure 9. Thermogravimetry under isothermal condition (130°C). The oblique curve indicates the weight loss.

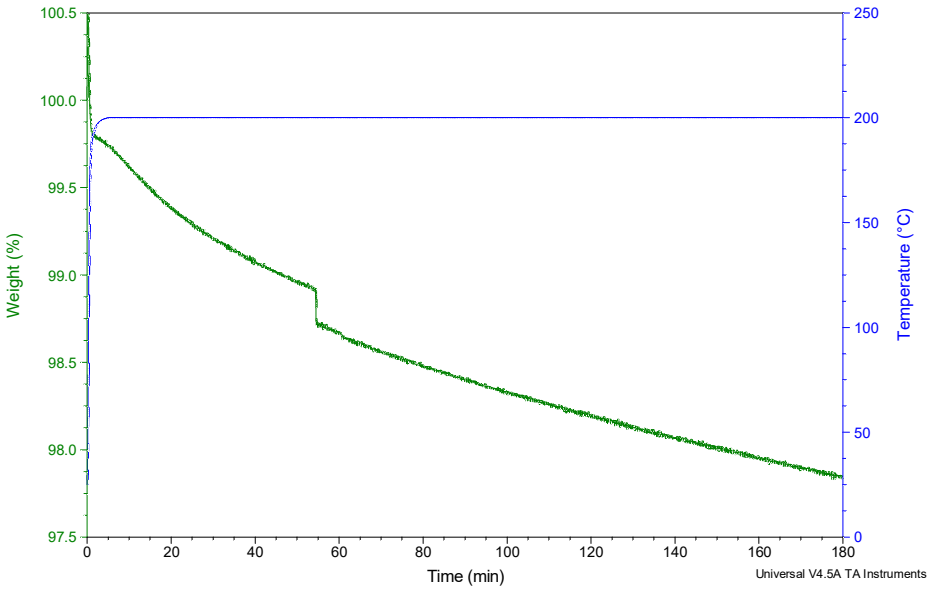

Figure 10. Thermogravimetry under isothermal condition (200°C). The oblique curve indicates the weight loss.

Untreated samples of resin were also kept under isothermal conditions at 130°C and 200°C for 130 and 180 min (see figures 9 and 10). In the former case a minimum weight loss can be

observed (0.35%), in the latter the decrease is obviously higher (2.5%). Such a decrease could be explained through the release of small molecules.

It can be concluded that the thermogravimetric results are fairly consistent with those found in literature with minor differences attributable to experimental conditions, sample composition and degree of homogeneity. Therefore, epoxy resins from at least a macroscopic perspective are stable polymer even above 300°C, showing similar behaviors regardless the fact they are heated in air or nitrogen. However, in the case they have to endure thermal stresses for sufficient time, even at temperature around 200°C, a reduction in the value at which the decomposition starts becomes observable. Structural changes can also be caused by electrical phenomena, as revealed by a measurement of the dielectric loss and volume resistivity, which are a reflection of the general condition of the polymeric network. A deterioration of the aforementioned properties can only be explained by a diffused bond cleavage along the macromolecular grid [3].

What is also important to point out is that a more accurate observation reveals a noteworthy weight reduction in the range between 120°C and 200°C, which finds its justification in the results described further down.

3.3.2 Heating experiments

The results of the heating experiments performed with the apparatus of figure 2 are described herewith. In figure 11, a picture of the resin samples exposed to different temperatures is shown. The obvious result is that an increasing temperature and a prolonged heating time (in the specific case three different temperatures are compared: 100°C, 150°C, 200°C for 48, 24 and 6 hours respectively) cause a superficial deepening of the colour. There is no apparent change between a new resin and a sample kept at 100°C for 2 days, but when the temperature rises to 150°C the red colour starts getting darker just after one day. However, in the apparatus, the samples are exposed to the sole amount of oxygen trapped at the beginning of the experiments. Considering the volume of the apparatus, 300 mL, and the fact that 24.2 L of a gas contain one mole of gas, at ambient temperature, there is 0.0123 mole of oxygen in the apparatus. The superficial area of the sample kept at 150°C, for instance, is approximately 36 cm^2. The limited amount of oxygen compared with the surface of the samples cannot be held responsible for oxygen-induced oxidative phenomena. Consequently, the darkening of the resin should be ascribed to other reasons, for instance the genesis of insaturations. To prove

that, the surface of the samples was analyzed through an ATR equipped FT-IR spectrophotometer. A sample of resin was also kept at 250°C for 6 hours in the oven under the continuous influence of air (oxygen) (figure 12). Since its color has turned from red to almost black, an additional ATR-IR analysis was performed

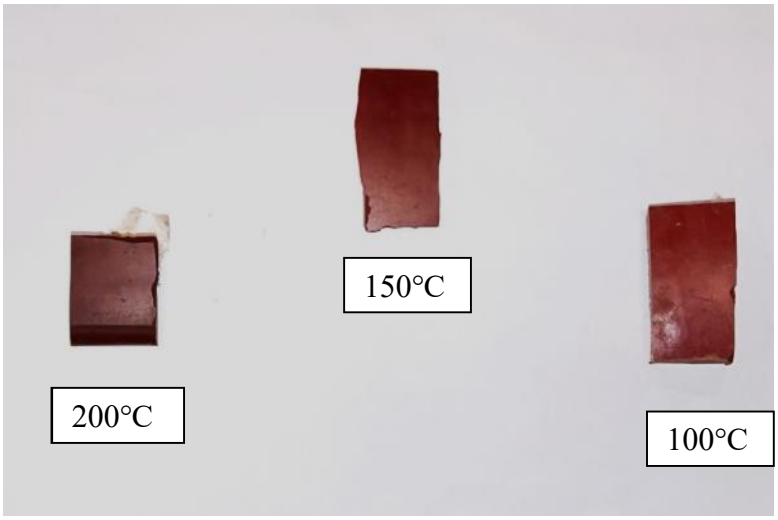

Figure 11. Blocks of resin kept under different temperatures for several hours. No difference in color is noted between an untreated sample and one kept at 100°C for 48 hours. The blackening seems to start around 150°C (24 hours). The left-hand sample was kept at 200°C for 6 hours

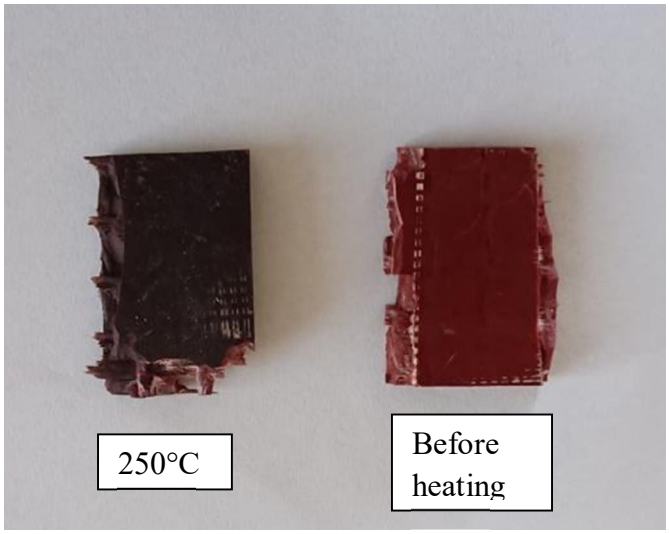

Figure 12. Blocks of resin kept at 250°C in a ventilated oven for 6 hours. In contrast with Figure 11, the sample was not inserted in any vessel.

In figures 13 to 17 infrared spectra of epoxy samples exposed to heat are shown.

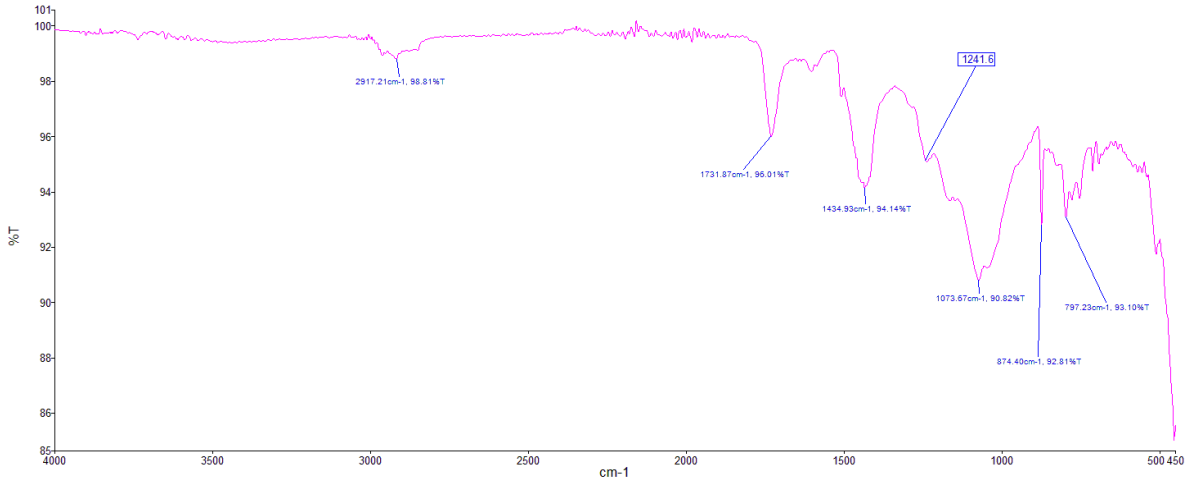

Figure 13. ATR-FT-IR spectrum of a resin sample not exposed to heat

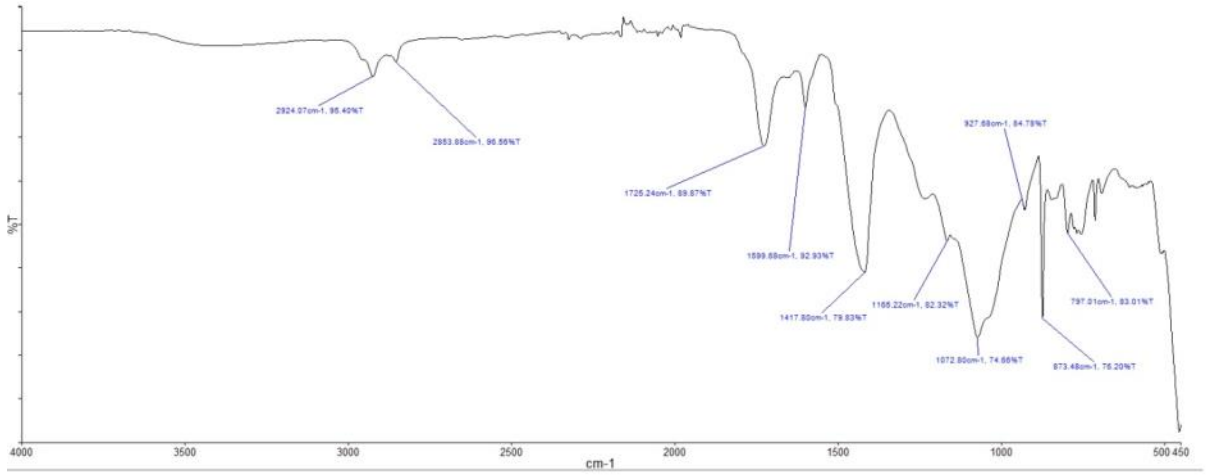

Figure 14. ATR-FT-IR spectrum of a resin sample kept at 200°C for 6 hours.

The IR spectra shown in figure 13 is obtained from a resin sample not exposed to heat and the one visible in figure 14 is relative to a sample kept at 200°C for 6 hours in a vessel placed in a ventilated oven. The spectrum of the sample kept in the same oven at 250°C for 6 hours out of the vessel has a practically identical spectrum (not shown here). In table 1, the assignments of the main absorption bands are listed.

Functional group	Wavenumber (cm^{-1})
p-Phenylene	874
Phenylene	1600
Aromatic ether	1241
Aliphatic ether	1073
Phenyl – $C(CH_3)_2$ – phenyl	1184
Ester	1731

Table 1. Infrared band assignment relative to spectra of figure 13

In figure 14 some changes can be observed in comparison with the spectrum of figure 13:

- the formation of a new small band at 937 cm^{-1},
- the shift of the carbonyl stretching from 1731 to 1724 cm^{-1} (see figure 13)
- the increase in absorption near 1800 cm^{-1}.

From the spectra it is evident that no oxygen has entered into the macromolecular structure even though the resin has started getting darker. A band between 900 and 950 cm^{-1} could be attributed to double bonds, which can also be responsible for a change in the color tone.

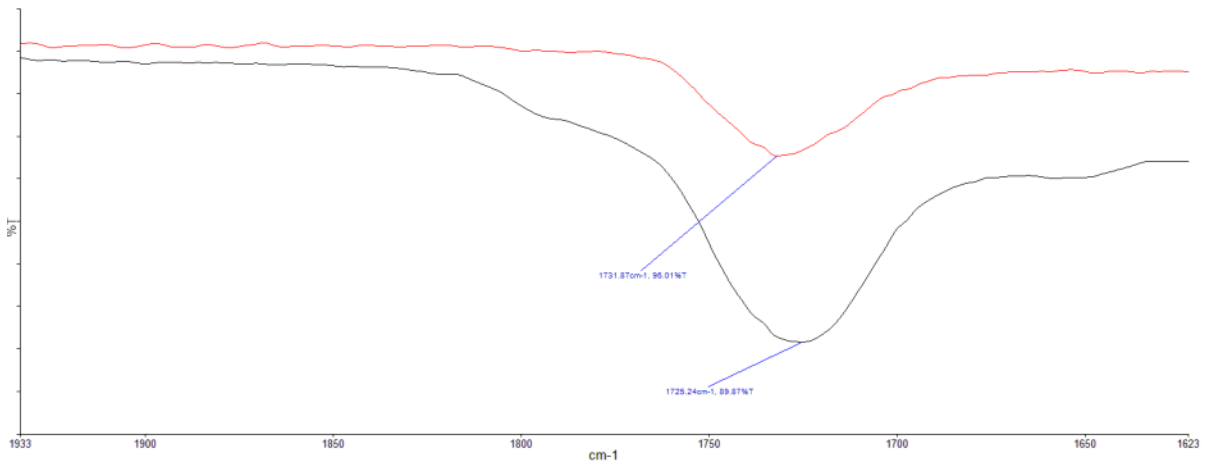

Figure 15. Exploded view of the carbonyl absorption peak above 1700 cm^{-1} between a non-heated sample (red line) and one heated at 200°C for 6 hours (black line)

In figure 16 the IR spectra of the samples displayed in figure 11 are compared. Through a merely visual analysis it is not possible to evaluate the absorption difference of the 937 cm^{-1} band but a difference exists and it is summarized in table 2. Here the absorption areas of the band of interest, of the band at 874 cm^{-1} used as reference for normalization and of the ratio between the two values are listed. It turns out that the higher the temperature the higher the band assigned to insaturations becomes.

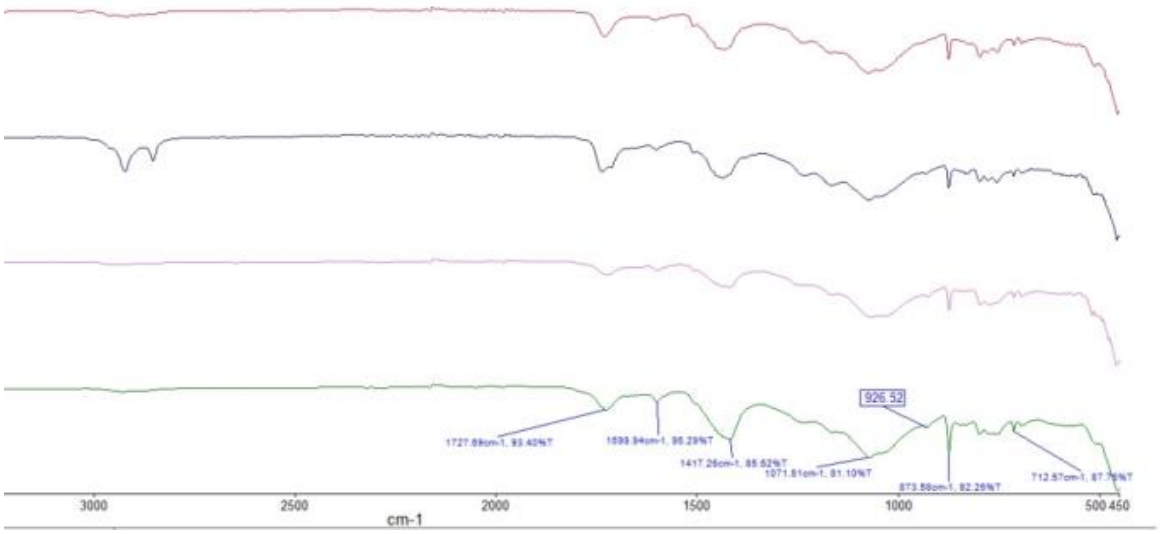

Figure 16. Comparison between the ATR-FT-IR spectra obtained analyzing the resin block shown in picture 11

Sample	**927 cm-1 band height**	**874 cm^{-1} band height (Ref)**	**Ratio**
No exposure	<0.0001	32	-
100 °C 48 h	0.8	29	2.8
150 °C 24 h	1.1	26	4.2
200 °C 6 h	2.8	45	6.2

Table 2. Relative abundance of the band at 927 cm^{-1} associable to double bonds and band at 874 cm^{-1} cm used as reference

The FT-IR superficial analysis was also carried out on a different instrument (perking Elmer 2000) using a trapezoid ATR SeZn crystal. The aim was to see if the typical carbonyl stretching bidentate band of an organic cyclic anhydride could be visualized.

As a matter of fact, such a band shows up even though at lower frequencies than expected, 1769 cm^{-1} instead of 1860-1850 cm^{-1} (weaker) and 1705 cm^{-1} instead of 1780 – 1760 cm^{-1} (stronger), when a sample is kept at 130°C for 4 hours. The bands are very weak because of the still low temperature and brief exposure time, but the absorbance ratio is somehow respected (see figure 14). The association of the spectra of figure 14 and 17 leads to suppose that the anhydride used to cure the resin emerges from the bulk diffusing out and spreads in the surroundings. It's likely to be unreacted anhydride.

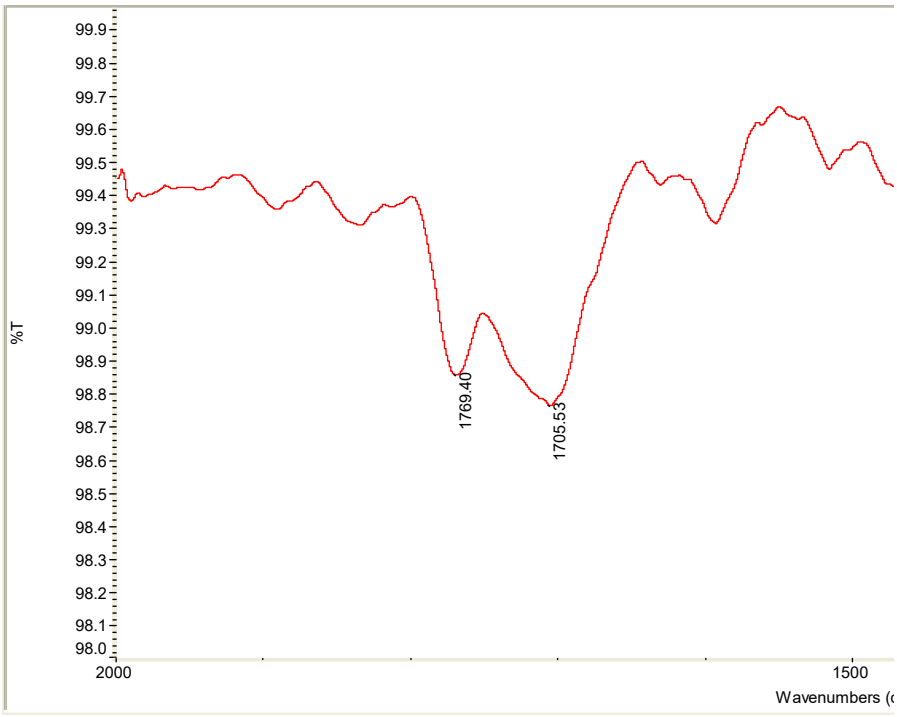

Figure 17. ATR-FT-IR spectrum of the surface of the epoxy resin sample kept at 130°C for 4 hours. The two absorption bands fall at 1769 cm^{-1} and 1705 cm^{-1}

A transmission FT-IR spectrum of the acetone solution obtained from the rinsing of the reacting vessel is shown in figure 18. The sample was kept at 300°C for 1 hour. The bands at 1843 and 1773 cm^{-1} can be unmistakable assigned to an anhydride.

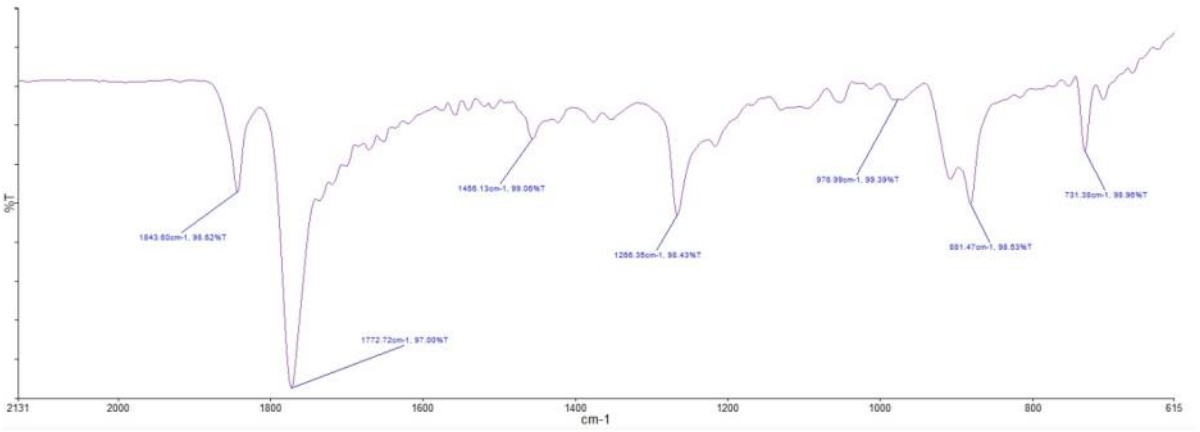

Figure 18. A transmission FT-IR spectrum of the acetone solution obtained from the rinsing of the reacting vessel The sample was kept at 300°C for 1 hour. The acetone was evaporated from the KBr crystal.

Consequently, the spectrum shown in figure 14 and the results collected in table 2 demonstrate that the exposure to moderately high temperature, even for short times, promote the outbound diffusion of anhydride, which should be responsible for the darkening of the resin surface. To confirm the validity of such a supposition, the samples which underwent heat treatments, were also exposed to bromine vapors, in order to accomplish the following reaction:

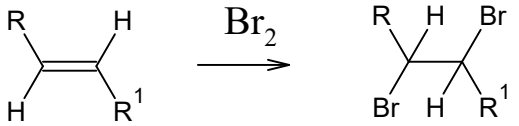

3.1

However the exposure of the samples to the bromine vapors doesn't favor reaction 3.1 only but it promotes also the side reactions with the residual epoxy groups, which leads to the formation of hydroxyl groups (reaction 2).

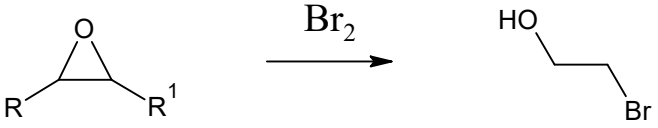

3.2

In figure 19 the comparison among spectra of samples kept at different temperature is shown. The band at 927 cm^{-1} which is not present in the untreated samples shows up in the heated samples but not in those that were subsequently treated with bromine.

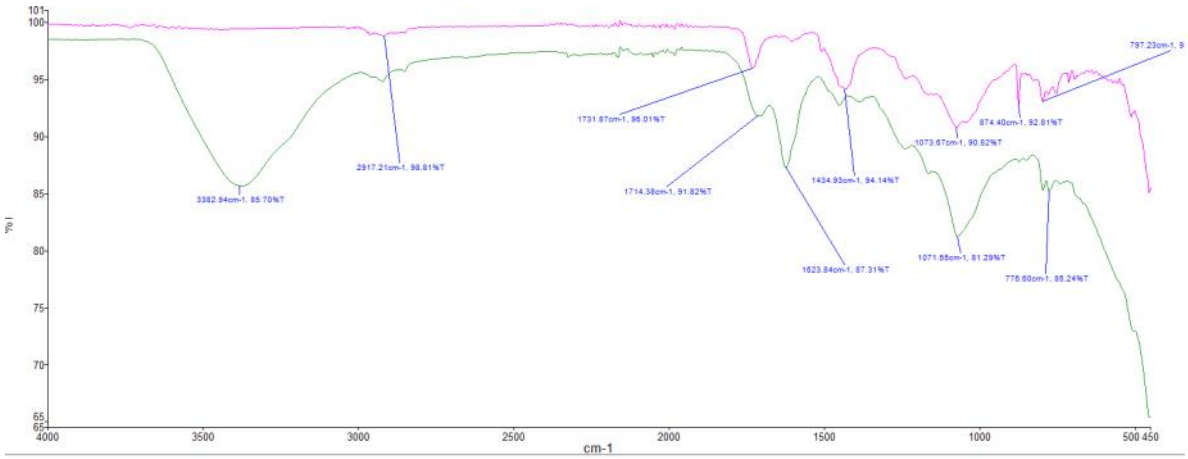

Figure 19. ATR-FT-IR spectra of the resin sample exposed to bromine fumes (green line) compared with the unexposed one (pink line).

The formation of a broad band at 3380 cm^{-1} can be explained through the second reaction detailed above showing the opening of the epoxy ring due to the action of bromine. The band at 874 cm^{-1} is in fact caused by a nearly degenerate half ring vibration of the residual epoxy rings, which disappears after the bromine reaction. The absorption band of a bromide group should fall between 500 and 900 cm^{-1}. In the figure 19, the widening of the absorption in said interval could be attributed to the presence of carbon-bromine bonds.

If the resin is heated for few hours at a temperature between 100°C and 150°C a different behavior is noted. In such conditions the release of methyl tetrahydrophthalic anhydride occurs and its presence is detected on the surface of the samples and of the vessel used to carry out the trial.

3.3.3 Gas chromatographic analyses

The apparatus of figure 3 was equipped with a septum for gas sampling and consequent analyses. The internal walls of the equipment were also rinsed with 2-propanol and the resulting solution analyzed. The results of the various analyses performed with GC-MS/MS are collected and commented in the figures 20-28. The chromatograms relative to the solutions obtained by dissolving the decomposition vapors in isopropanol or by rinsing the walls of the reaction vessels are actually identical, with the exclusion of intensities. In figure 20, the chromatogram of the solution deriving from the treatment of the epoxy resin at 200°C is shown. The first peak (9.93 min) can be associated to an amine compound and the others to isomers of an organic anhydride. The amine compound, which mass spectrum in scan mode is shown in figure 21, resulted to be dimethyl piperidine (supposedly in position 2 and 6), having a nominal mass of 113 amu. As a matter of fact, a compound containing an odd number of nitrogen groups has always an odd mass. The transition from 113 amu to 98 amu is produced by the loss of methyl groups (15 amu). If we apply the equation 3 to calculate the amount of ring and double bonds (RDB) we obtain:

$$RDB = X - 0.5 * Y + 0.5 * Z + 1 = 7 - (15/2) + 0.5 + 1 = 1 \qquad 3.3$$

Where X is the number of tetravalent atoms, Y of the monovalent atoms and Z of the trivalent atoms.

When the result is a whole number the ion is an odd electron ion. The result is 1 so the molecule has a ring, is an odd electron ion and thus contains a nitrogen atom.
The percentage ratio between the signals at 114 and 113 amu (relative abundance) is 7.8 %. Considering that the environmental abundance of C^{13} is 1.1 %, the value of the 114 amu signal account for 7 carbon atoms (the contribution to the M+1 signal is negligible for nitrogen and hydrogen).

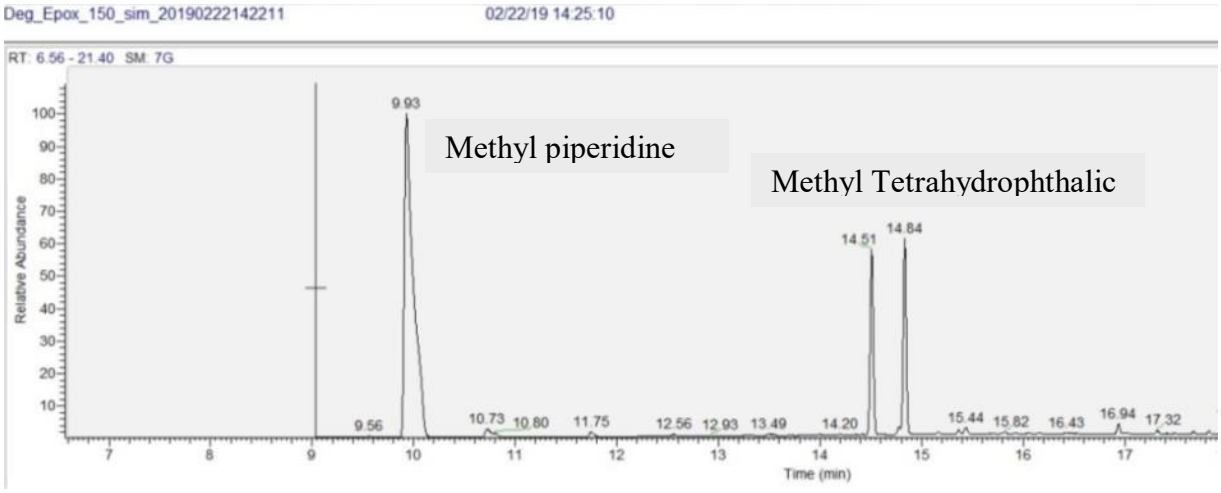

Figure 20. GC-MS/MS chromatogram of a solution deriving from the treatment of the epoxy resin at 200°C for 6 hours.

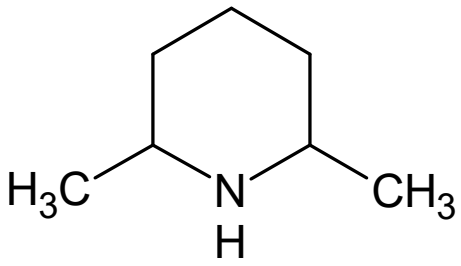

Figure 21. Chemical structure of 2,6-dimethyl piperidine (MW 113.2)

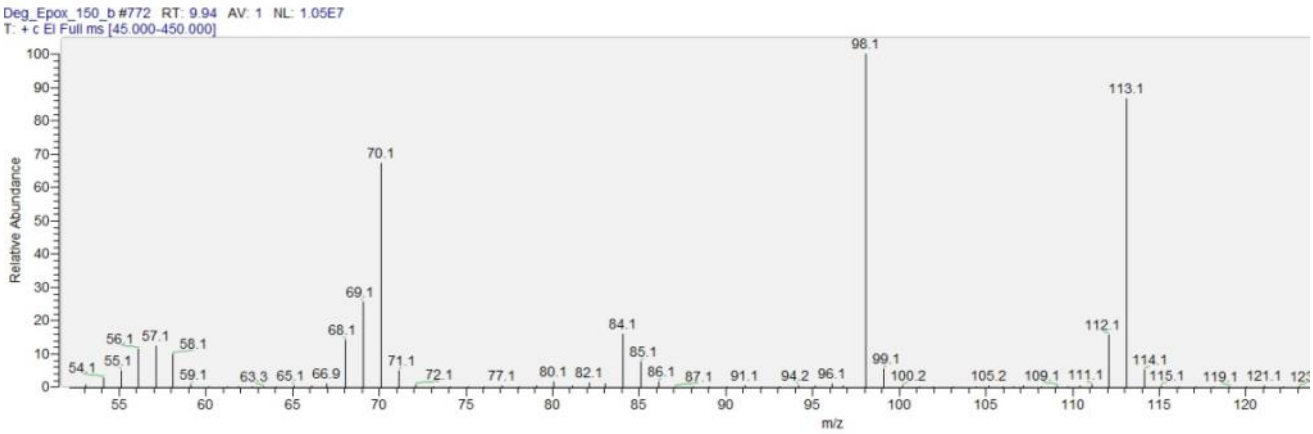

Figure 22. Mass spectrum in SCAN mode of 2,6-dimethyl piperidine.

The other two peaks in the chromatogram at 14.5 and 14.8 minutes can be assigned to isomers of methyl tetrahydrophtalic anhydride which molecular weight is 166 amu.

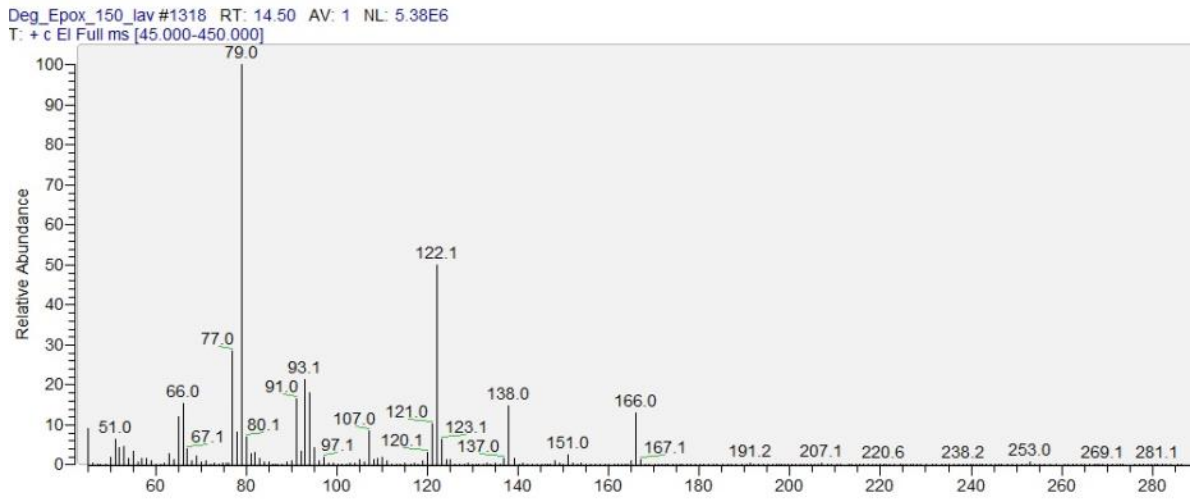

Figure 23. Mass spectrum in SCAN mode of tetrohydrophthalic anhydride

In order to remove the interfering ions, the gas chromatographic analyses were also conducted using the SRM mode (triple quadruple) thus isolating a target ion and a parent ion. The consequential mass spectra of piperidine and anhydride are displayed in figure 24 and 25 respectively

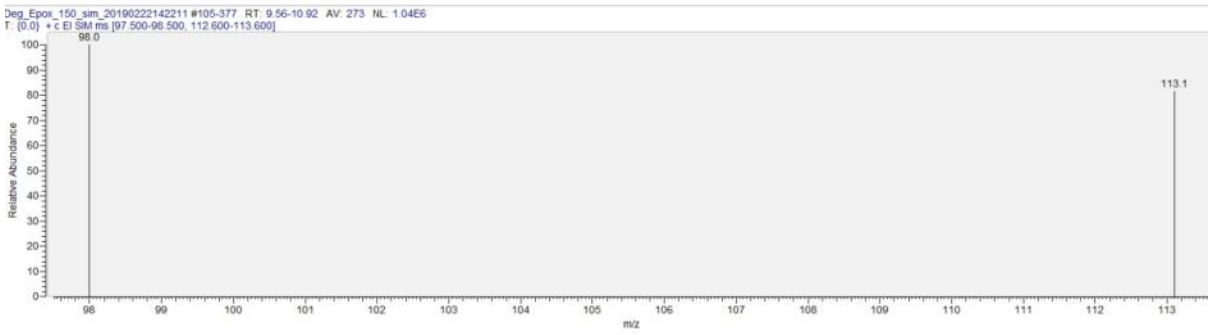

Figure 24. Mass spectrum in SRM mode (MS/MS) of 2,6-dimethyl piperidine. Target ion 113 amu, parent ion 98 amu

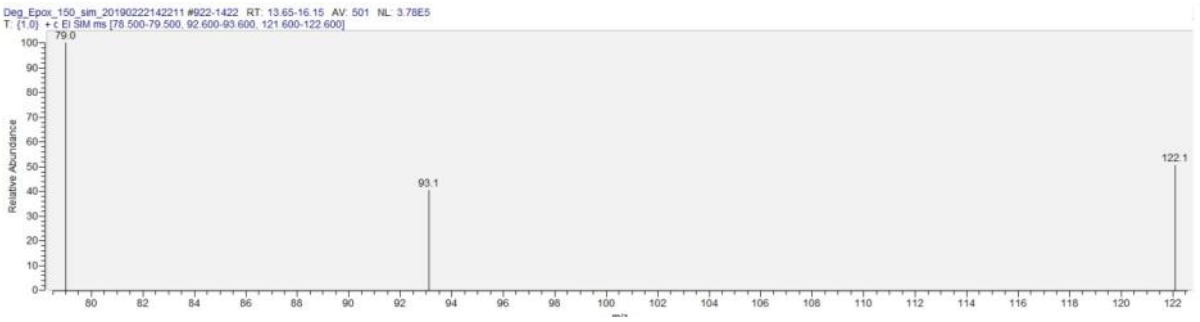

Figure 25. Mass spectrum in SRM mode (MS/MS) of methyl tetrahydrophthalic anhydride. Target ion 122 amu, parent ions 93 amu and 73 amu

Finally, a more accelerated degradation was accomplished by grinding the samples to fine powder, which was then placed in a furnace and heated up according to a certain temperature gradient. Clear evidence of decomposition was obtained from GC-MS data for the methanol rinse of the trap used to collect the thermal decomposition products between 150 - 300°C. The results of said experiments are exemplified in the next figures, 26 and 27. The chromatogram contained peaks that were also observed in the chromatogram of the ”blank” trap extract. However, trace quantities of toluene, phenol, cresols and bisphenol A were observed in the rinse. The other peaks resulted from the polysiloxane column bleed. The presence of bisphenol A clearly indicates that decomposition of epoxy insulating material had started at 150°C. Furthermore, a white cloud was then observed when the reactor tube temperature climbed above 225°C indicating decomposition of the epoxy insulating material.

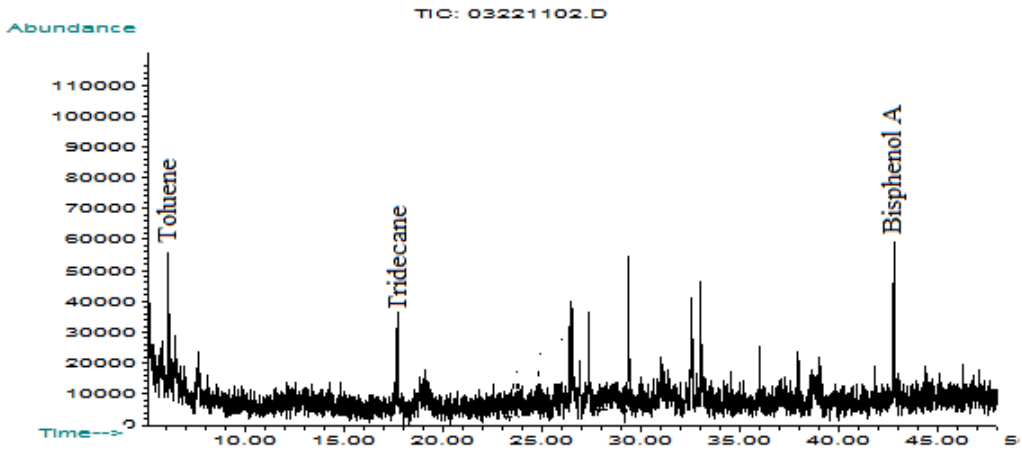

Figure 26. Mass spectrum in SCAN mode of methanol rinse after decomposition at 150°C

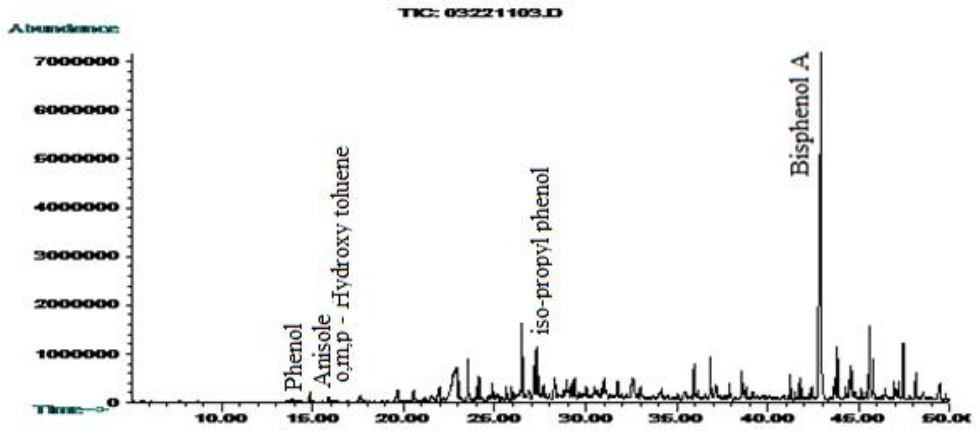

Figure 27. Mass spectrum in SCAN mode of methanol rinse after decomposition at 300°C

3.3.4 Polyester film analysis

The polyester film which works as insulator among the copper coils have been subjected to heat treatments. Normally said films are not exposed to air (unless some bubbles get trapped during manufacturing). Notwithstanding this some samples underwent the same treatments as the epoxy resins. In figure 28 the two ATR-FT-IR spectra before treatment and after a 12-hour exposure to 200°C are shown. No apparent difference can be noted, confirming the stability of the polymer, despite the presence of air.

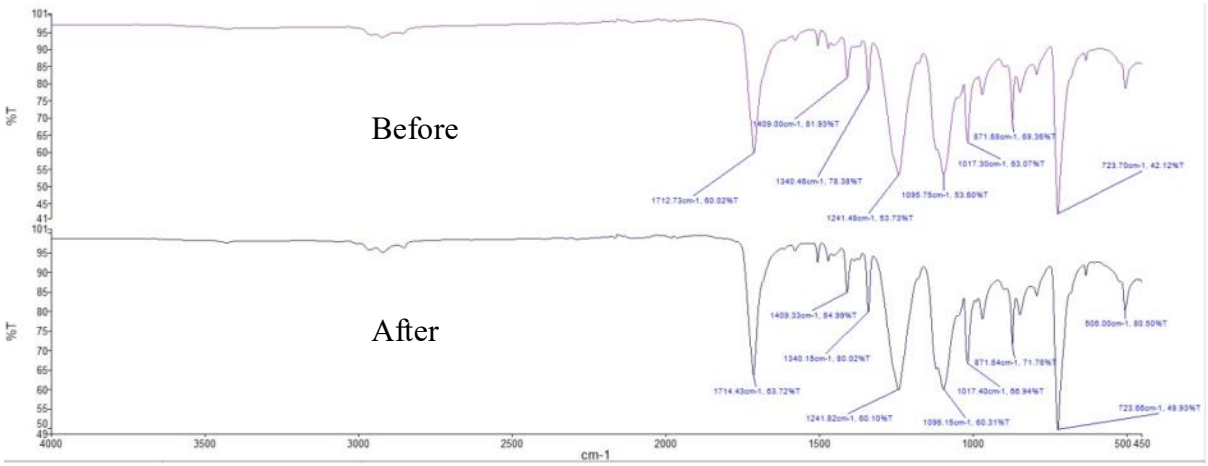

Figure 28. Polyester film ATR-FT-IR analysis before and after exposure to 200°C for 12 hours

3.4 Conclusions

The results of the experiments described so far seems to match those available in the literature even though some differences have been noted. The epoxy resins for electrical applications, which are normally cured with anhydrides, are thermally stable materials up to 300°C, with the first peak of decomposition between 350°C and 400°C. However some hints of incipient degradation have been observed at a temperature as low as 150°C with the deliverance of small molecules and traces of bisphenol A. The temperature of bisphenol A release seems to be in agreement with literature data when the resin sample is handled as a bulk, but it lowers to 150°C when the specimens are reduced to powder. This behavior can prompt the supposition that either some unreacted bisphenol A is present in the body of the resin or mechanical stress can create latent degradation-onset areas [4], which evolve in a molecular disruption when heat is applied. As a matter of fact, the analyses confirm that unreacted epoxy groups and curing molecules are available inside the resin. The crosslinking agent, which, in the specific case, is methyltetrahydrophthalic anhydride, starts to diffuse out of the bulk at a moderately high temperature (130°C), causing a darkening of the color of the resin. It is reported in the literature [5], that heating up a resin, which has not completed its crosslinking phase should restart the curing process leading to a harder product. However it looks as if the unreacted epoxy groups are incapable of combining with the residual anhydride, which in contrast follows a different route and emerges from the surface. Other studies assess that, along with hydrocarbons, bisphenol A, anhydrides and amines additional small volatile molecules (for instance formaldehyde) can be freed as a result of the thermal degradation of the epoxy [6]. Traces of amines confirm the need manufacturers have in order to ease and accelerate the crosslinking processes.

The fact that different molecules can depart from the bulk of a resin exposed to heat could be used to set up a diagnostic tool able to provide a correlation between the thermal stresses and the properties of the materials composing a dry-type transformer. The first step to accomplish that is to build and test sensors which can detect and possibly provide a rough quantitative estimation of the evolved molecules. This step will be the main topic of the next chapter.

3.5 References

[1] Thermal behavior of the epoxy and polyester powder coatings using thermogravimetry/differential thermal analysis coupled gas chromatography/mass spectrometry (TG/DTA-GC/MS) technique: Identification of the degradation products; D.F. Parra, Lucildes P. Mercuriet al.; Thermochimica Acta Volume 386, Issue 2, April 2002

[2] Effects of Variation in Heating Rate, Sample Mass and Nitrogen Flow on Chemical Kinetics for Pyrolysis, Centre for Environmental Safety and Risk Engineering, 18th Australasian Fluid Mechanics Conference Launceston, Australia 3-7 December 2012 Victoria University, Victoria 8001, Australia

[3]The effect of electrical ageing on a cast epoxy insulation; Y.Li, J. Unsworth et al.; Proceedings of Electrical/Electronics Insulation Conference; 4-7 Oct. 1993

[4] Evolution of peroxide-induced thermomechanical degradation of polypropylene along the extruder; A. V. Machado, J. M. Maia et al.; Journal of applied polymer science, Volume 91, Issue 4, December 2003

[5] Influence of post-curing and temperature effects on bulk density, glass transition and stress-strain behaviour of imidazole-cured epoxy network; Ching-Shiun Wu; Journal of material Science;, Volume 27, Issue 11, June 1992

[6] Theoretical Study on Decomposition Mechanism of Insulating Epoxy Resin Cured by Anhydride; X. Zhang, Y. Wu et.al.; Polymers, Volume 9, Issue 8, August 2017

4 Development and testing of solid state sensors

The experiments described in chapter 4 have demonstrated that epoxy resins for electrical application can release several organic molecules when heat is applied. It seems that this kind of polymers, which are normally cured with organic anhydrides and are considered thermally stable, start to let off volatile compounds at temperatures even lower than 150°C. These compounds can be related to different phenomena such as an incomplete curing of the resin or an incipient molecular disruption or even an ongoing degradation. Within the case of the samples under investigation, some distinctive markers were detected: methyltetrahydrophthalic anhydride, the dimethylpiperidine, phenol, bisphenol A. Hereafter, two molecules were selected to be used as model compounds in the development of solid state sensors: Carbic Anhydride and Phenol. The former is an unsaturated organic anhydride commonly used as a curing agent and the latter can be treated as a functional model. The presence of heteroatoms as well as of aromatic structures may lead to believe there could be a kind of interaction with metals or metal compounds. As a matter of fact, the aforementioned molecules could combine with atoms like zinc, copper and aluminum [1, 2] .

Said metals, and zinc in particular, are those commonly chosen to realize metal-oxide-based sensors, especially in the gas-detection application. Consequently the activities and experiments related to the construction and testing of ZnO and CuO based sensor are detailed herewith.

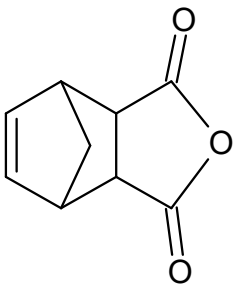

Figure 1. Structure of Carbic anhydride

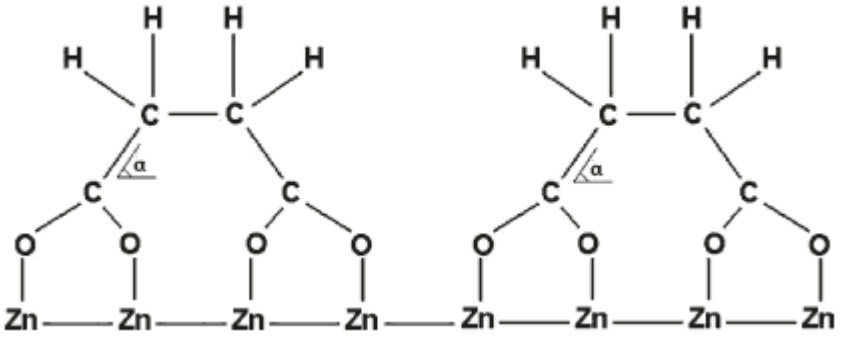

Figure 2. Absorption of decomposed organic anhydride on Zinc [3]

4.1 Instrumentation

Herewith a list of the main equipment used to perform the degradation experiments on epoxy resin is given.

1. The metal-based inks were printed onto the alumina substrates by means of a screen printer manufactured by Officine Baccini S.p.A., equipped with a 0.45 μm printing mesh.

2. The sensors were fired in a Furnace, Carbolite CWF 12/23.

   The heating conditions were:

   a) 5°/min up to the maximum point
   b) Isothermal conditions for 1 hour
   c) 5°/min cool down phase to ambient temperature

3. The impedance of the sensor was measured through an LCR meter, Hioki 3533-01, Nagano, Japan. The meter was set at an AC tension of 1 V, 1 kHz.

4. The air flow was dosed and measured with a flowmeter Teledyne Hastings (Instruments HFM 300 controller and flow meters HFC 302, Hampton, VA, USA).

5. The metal oxides were characterized with x-ray diffraction technology using a XRD Pananalytical X'Pert Pro

6. The metal oxides underwent also electronic microscopy investigation with a FESEM Zeiss Supra 40

7. The metal granulometry of the metal oxides was measured either with a manual sieve Geotech Hand Shaker or with a laser diffraction particle size analyzer Mastersizer 3000 (Malvern Panalytical)

4.2 Experimental

4.2.1 Synthesis of CuO

The copper oxide-based ink was prepared according to the herewith detailed procedure [4, 5, 6].

The synthesis of CuO was obtained starting from copper chloride (MW 170.48, Sigma Aldrich, 99.9%, powder) and sodium hydroxide (Sigma Aldrich, 97% pellet), used without any further purification. A 0.1 M $CuCl_2$ solution was prepared by dissolving 3.4 g (0.020 mole) of $CuCl_2 \cdot 2H_2O$ in 0.200 L of deionized water. The solution was poured in a flask and kept under stirring at 22°C for 15'; then 5 g of NaOH (0.12 mole) in powder form were rapidly added producing a black precipitate (equation 4.1). The solution was maintained at 22°C for 2 hours under stirring then heated at 100°C and maintained at this temperature for other 2 hours, again under stirring (4.2). After centrifugation the precipitate was isolated and rinsed several times with ethanol and water. Then it was placed in a ventilated oven at 200°C for desiccation, until no weight loss was observed. Finally, the resulting black powder was manually milled directly in a mortar. Crystal structure identification was obtained through X-ray diffraction (XRD).

$$CuCl_2 \cdot 2H_2O + 2\,NaOH \longrightarrow Cu(OH)_2 + 2\,NaCl + 2H_20 \qquad 4.1$$

$$Cu(OH)_2 \xrightarrow{\Delta} CuO + H_20 \qquad 4.2$$

4.2.2 Synthesis of ZnO

The zinc oxide-based ink was prepared according to the herewith detailed procedure [6, 7, 8]. Two different solutions were prepared starting from zinc nitrate hexahydrate ($Zn(NO_3)_2 \cdot 6H_2O$, Sigma Aldrich, 99.9%) and soluble potato starch ($(C_6H_{10}O_5)_n$, Sigma Aldrich), used without any further purification. The first solution was obtained dissolving 0.040 mole of $Zn(NO_3)_2 \cdot 6H_2O$ in 100 mL of deionized water, the second adding 0.45 mole of potato starch in the same amount of deionized water. To ensure a proper starch dissolution the latter was kept at 75-80°C for 1 hour under vigorous magnetic stirring. Next, the two solutions were maintained under stirring for 15 additional minutes and then mixed together directly in an alumina crucible producing a cloudy mixture as a consequence of a partial starch gelling. Eventually, the crucible was placed in a water bath set at 90-95°C and kept under continuous agitation for roughly 5 hours to allow water evaporation and viscosity increase. The resulting product was a dense white-yellowish gel.

After that the crucible was transferred in an electric furnace and heated at 10°C/min up to 300°C and there maintained for 30 minutes to remove residual water and promote the ignition of reagents, which had 1 minute duration. The outcome looked like a soft, porous brown mixture, that the TGA analysis revealed to be zinc oxide, partially unreacted reagents and carbon. Finally, said product was manually milled directly in the crucible and treated in an electric furnace at the temperature of 500°C (10°C/min heating ramp) for 2 h producing a bright white fine powder of zinc oxide that was stored for characterization (XRD, FESEM, TGA)

4.2.3 Making of the sensors

The sensors were prepared by spreading the metal oxide (ZnO and CuO) onto α-alumina substrates by means of a screen-printing machine. The ceramic plates, with a purity of 96%, were provided by Coorstek (Golden, CO, USA, ADS-96) and had a size of 16 x 8 mm (figure 3). The electrodes were printed on the surface of the substrate using a platinum-based ink (5545-LS, ESL, King of Prussia, PA, USA), which was then fired at 980°C for 18 minutes with a heating/cooling ramp of 2°C per minute. Hence the electrical conductivity and the adhesion onto the ceramic substrate could be ensured. The electrodes have a thickness of 400 µm and a clearance of 450 µm between each other. In figure 4, the solid black lines are the

platinum interdigitated electrodes, the dark grey area represent the active sensing material and the remaining white part is the α-alumina substrate.

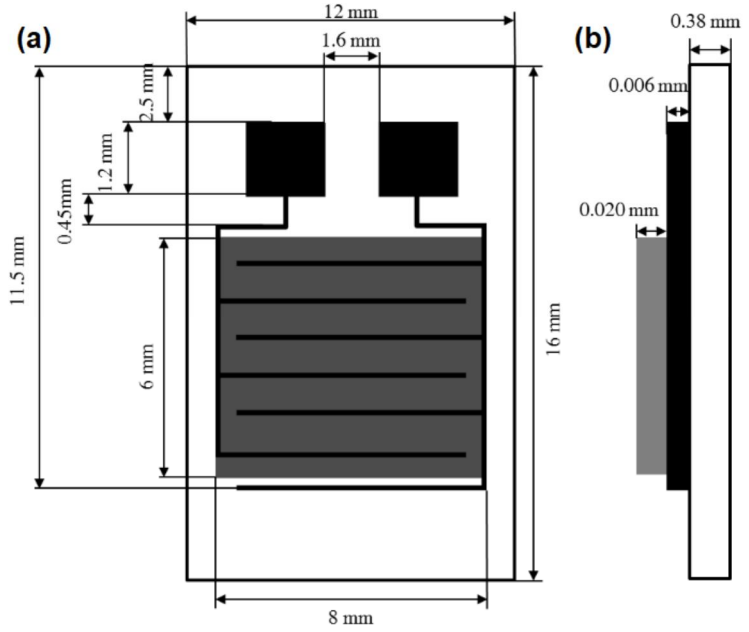

Figure 3. Scheme of the sensor prepared by screen-printing technique: (a) front view, (b) side view. The drawing has an arbitrary scale even though the associated dimensions are correct.

After completion, the sensors were tested with the selected compounds.

4.2.4 CuO and ZnO sensors

The ink was prepared by mixing the metal oxide powder (both the one synthesized as described above and a commercial product) with an organic medium (ethyleneglycol monobutyral ether, Emflow, Emca Remex, USA), as a viscosity adjuster, and polyvinyl butyral (PVB, Sigma Aldrich, Milan, Italy) as a temporary film binder before firing.
Before screen printing the ink on the circuitized alumina substrates some adhesion experiments were performed, in order to find the optimal temperature at which the ink could stick as strongly as possible to the alumina surface. First the deposition was carried out on bare alumina substrates which, after an overnight drying stage, were then exposed to different temperatures (from 400°C to 800°C, 100°C increments) in a furnace. The adhesion test

consisted in evaluating the amount of metal oxide which could be removed by the action of a short segment of adhesive tape (3M magic tape 810) attached to the surface of the substrate. The tape employed in the tests could provide an adhesion strength, referred to steel, of 2.5 N/cm (Scotch® Magic™ tape 810 product information sheet). Finally, the substrates were screen printed with a 0.45 μm steel mask and fired at the selected temperature, to remove all the organic residues and to ensure the correct adhesion of the ink to the ceramic substrate

4.2.4.1 Response of the sensors

The response of the sensor (R) was calculated according to 4.3 in the case of reducing gases:

$$R = Zg/Z_0 \qquad 4.3$$

and according to 4.4 if oxidizing gases are considered:

$$R = Z_0/Zg \qquad 4.4$$

Where Zg is the impedance value of the sensor exposed to the target gas and Z_0 is the impedance value of the sensor in equilibrium with a dry air flow.

Response time and recovery time were both evaluated. The time a sensor needs to reach 90% of the total impedance change after gas adsorption is called the response time while the time required to reach 90% of the total impedance change when the gas is desorbed is defined as the recovery time.

The sensors were exposed to the target molecules in a way that could reproduce as accurately as possible the conditions that might be encountered in the room or cabinet where a dry-type transformer is kept. Normally it's a place that can become saturated with organic molecules since extremely variable degree of ventilation can be found, ranging from a no-ventilation condition to a forced-air setting. The former is the most dangerous condition because it can lead to an overheating situation. Thus, the experiments where conducted according to the following procedure:

1. Wait for signal and temperature equilibration under a flow of dry air
2. Start the recording of the signal

3. Close the dry air flow (e.g. after 300 seconds from the start)
4. Introduce the sample (e.g. after 400 seconds from the beginning)
5. Keep on recording the signal with the inlet valve closed (e.g. till 800 seconds from the beginning)
6. Open the valve after a certain time to force out the target compound
7. Stop the recording (e.g. after 1300 seconds after the beginning)

The sequence detailed above has the purpose to recreate the situation where the transformer, due to an increase in temperature, start releasing organic molecules that fill up the space around and can be only extracted by a slow limited ventilation.

4.3 Material Characterization

The CuO and ZnO samples underwent some characterization analyses, such as particle size dimension and distribution, X-ray diffraction (XRD) and field-mission scanning electron microscopy (FESEM), finalized to determine their structure. Both compounds were fisrst hand milled in a porcelain mortar and then analyzed.

In the case of copper oxide the particle size distribution was performed using a multistage handheld sieve.

The XRD characterizations were performed according to the hereafter instrument configuration:

Source of X-Rays: Cu Kα, 1.54 Å. (wave length), Mo Kα, 0.71 Å (Wavelength)
Detector: CCD

Sample stage:	Fixed.
Measurement range:	5º to 70º
Working condition:	40 kV & 40 mA

The FESEM configuration was as follows:

Resolution	1.3 nm @ 15 kV
	2.1 nm @ 1 kV
	5.0 nm @ 0.2 kV
Magnification	12 - 900,000x

Emitter	Thermal field emission type
Acceleration Voltage	0.1 - 30 kV
Probe Current	4 pA - 10 nA

4.4 Sensor testing apparatus

To test the sensors an apparatus (Figure 4), made of the hereafter listed parts, was realized:

1. Sensor and sensor-heater holder (Figure 5)
2. Three-neck round bottom flask (Figure 6)
3. Heater
4. Oil bath
5. Air cylinder

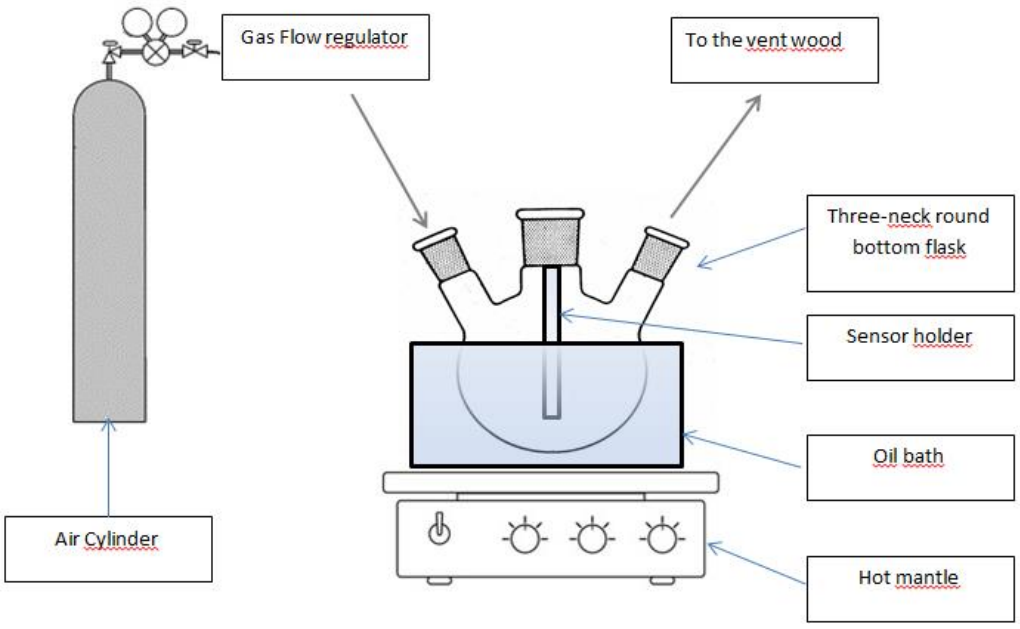

Figure 4. Apparatus used to test the sensors

Figure 5. Support for the sensor and heater

Figure 6. Three-neck flask where sensor and sample are arranged

The support was connected to the middle neck of the flask. The samples could be introduced through one of the other neck. Dry air was circulated across the flask from the cylinder through the flow regulator. The flask could be kept warm by means of a silicon oil bath, positioned on a hot mantle.

The sensors were heated through a Ni-Cr wire placed under the sensor and powered by a DC supply (Peak Tech, Nanjing, Jiangsu, China). To measure the temperature, a PT100 probe was used (RS Pro, London, UK) .

4.5 Sensor Testing

4.5.1 CuO

The copper oxide sensors were the first to be tested and organic anhydrides were chosen as target molecules. Maleic anhydride was used to carry out a preliminary screening due to a presumably higher reactive strength, carbic anhydride was tested later and humidity as last. The sensors used in these experiments were produced starting from the copper oxide synthesized in the lab. The optimal firing temperature was found to be 700°C (see Figure 7).

Figure 7. Adhesion test of Synthesized CuO the alumina substrate; 700°C seems to be the best compromise (red circle).

The tests were conducted following the procedure detailed previously, using a 500 mL 3-neck round bottom flask, keeping a 125 mL/min air flow rate and trying different sensor temperatures. In the case of maleic anhydride and humidity the oil-bath temperature was set at 70°C, but it was increased up to 170°C when carbic anhydride was used.

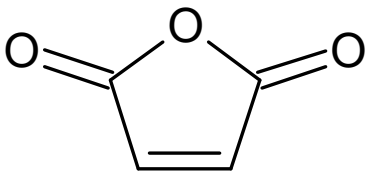

Figure 8. Maleic anhydride structure

4.5.2 ZnO

Contrarily to copper, zinc oxide appears as a white powder. An example of screen printed ZnO flower-like sensors is displayed in Figure 9. The one on the left hand side is unused while the other two, on which a superficial yellowing has become visible, were exposed to different compounds

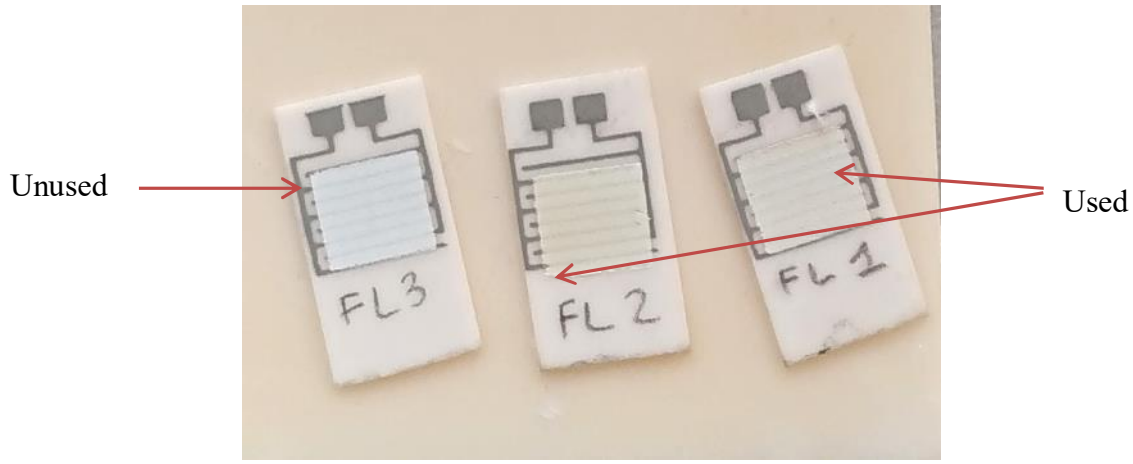

Figure 9. ZnO based sensor (flower-like type, unused and used)

Zinc oxide sensors were tested at different temperatures ranging from 150 to 400°C and against several different functional groups and water:

1. Anhydride
2. Phenol
3. Alcohol
4. Acid
5. Unsaturation

The sensors used in all the experiments were produced using the commercial product and the one synthesized in the lab (flower-like type). The optimal firing temperature was found to be 700°C, again.

4.6 Results

4.6.1 Characterization results

4.6.1.1 CuO

After hand milling, the copper oxide appeared as a black fine powder with a certain size distribution which measured with a handheld sieve is detailed in table 2.

Size range (µm)	Percentage
< 66	2%
66-76	25%
125-89	20 %
210-150	38 %
422-251	15%

Table 1. Particle size distribution of synthesized copper oxide

The copper oxide sample synthesized in the lab was investigated with a Field Emission Scanning Microscope (Fesem) the relative images are shown in figure 10 and 11. The synthesized copper oxide seems to be formed by irregularly shaped agglomerates which a bigger magnification (50kX) reveals to be clusters of berry-like particles. The microstructure shows a diffused micro-porosity and seems to be made by particles much below 200 nm which mainly has a spherical morphology.

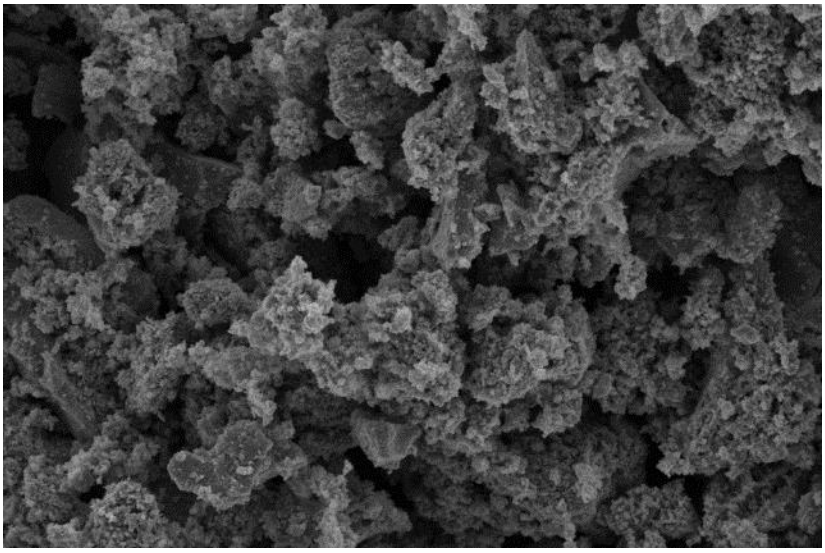

Figure 10. 10 kX magnification of synthesized CuO sample

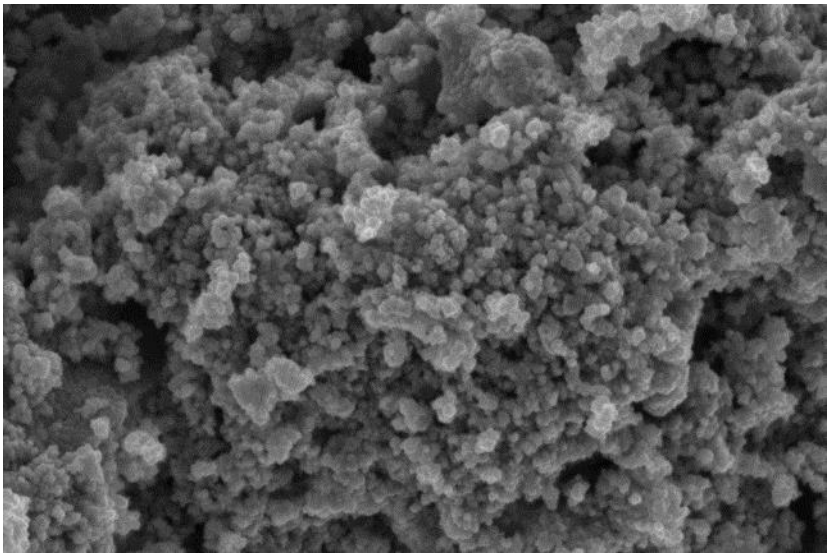

Figure 11. 50 kX magnification of synthesized CuO sample

The copper oxide synthesized according to the procedure detailed above underwent an X-ray diffraction analysis, whose pattern is shown in figure 12. At 35 degrees position, a sharp strong peak is observed, indicating a high crystalline monoclinic structure [10]. In figure 13 the pattern of commercial CuO sample, taken from the literature [11], can be seen as benchmark. The correspondence of these patterns with those of the synthesized sample is evident.

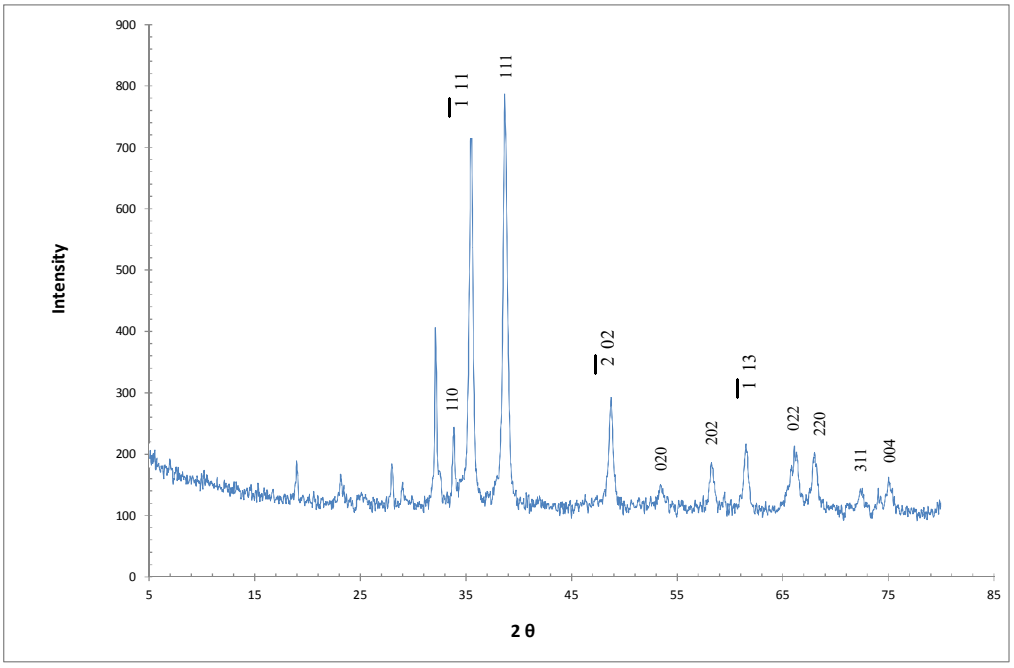

Figure 12. XRD pattern of synthesized CuO sample

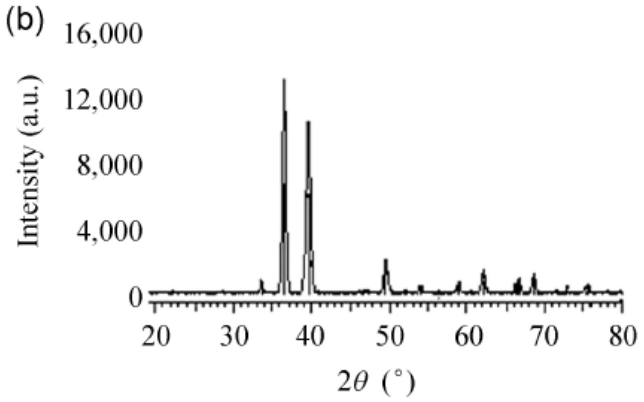

Figure 13. XRD pattern of a sample of commercial CuO (b) [11]

4.6.1.2 ZnO

The particle distribution of flower like and commercial ZnO was measure with Mastersizer 3000 and is shown in table 2. The tests were carried out using water as dispersing agent (1000 rpm stirring speed) andblue and red lasers as electromagnetic sources. The scattering was measured using the Mie solution. Both commercial and flower-like ZnO show the same distribution, with an average apparent diameter equal to 61.0 µm (equivalent to the volume of the sample, D [4;3] in the table).

Size	Commercial	Flower-like
D [4;3]	6.91 µm	42.05 µm
Dx (10)	0.0875 µm	0.697 µm
Dx (50)	0.169 µm	1.25 µm
Dx (90)	0.685 µm	2.15 µm

Table 2. Particle size distribution of synthesized (flower like) and commercial zinc oxide, measured with Mastersizer 3000.

The zinc oxide samples, both the commercial and the one synthesized in the lab, were investigated with a Field Emission Scanning Microscope (Fesem). In figure 14 and 15 the images relative to commercial-type ZnO are shown, whereas in figure 16 and 17 those concerning the lab sample can be observed. The commercial metal oxide seems to be formed by irregular shape particles while the samples obtained in the lab have a flower like structure. In the former case the microstructure seems to have a certain degree of porosity and to be

made of particles with elongated morphology. In the latter one particles have a planar morphology and appear to be formed by stacked and intertwined flakes.

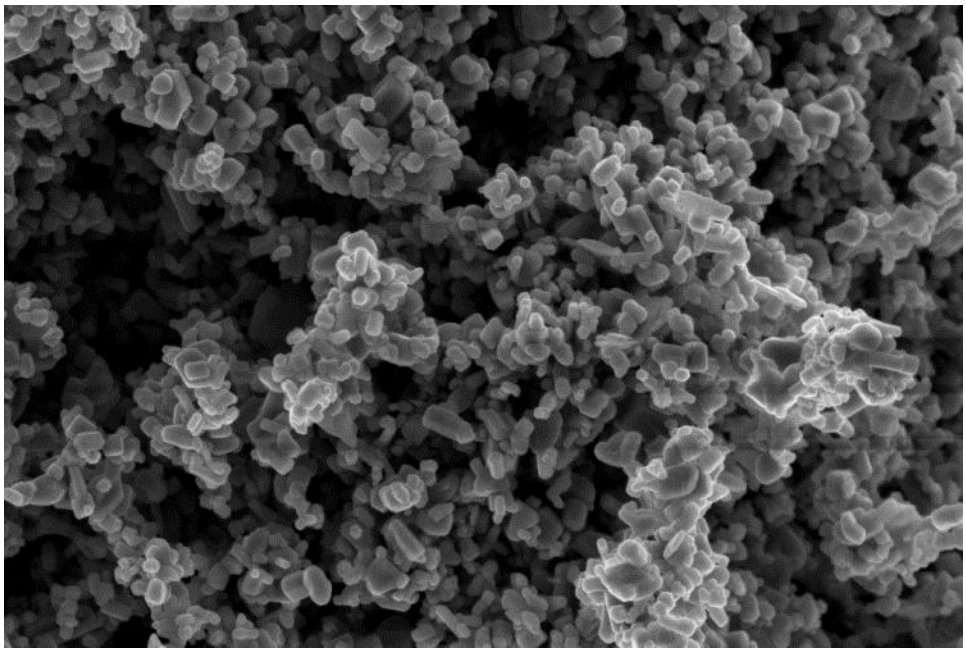

Figure 14. 50 kX magnification of commercial ZnO sample

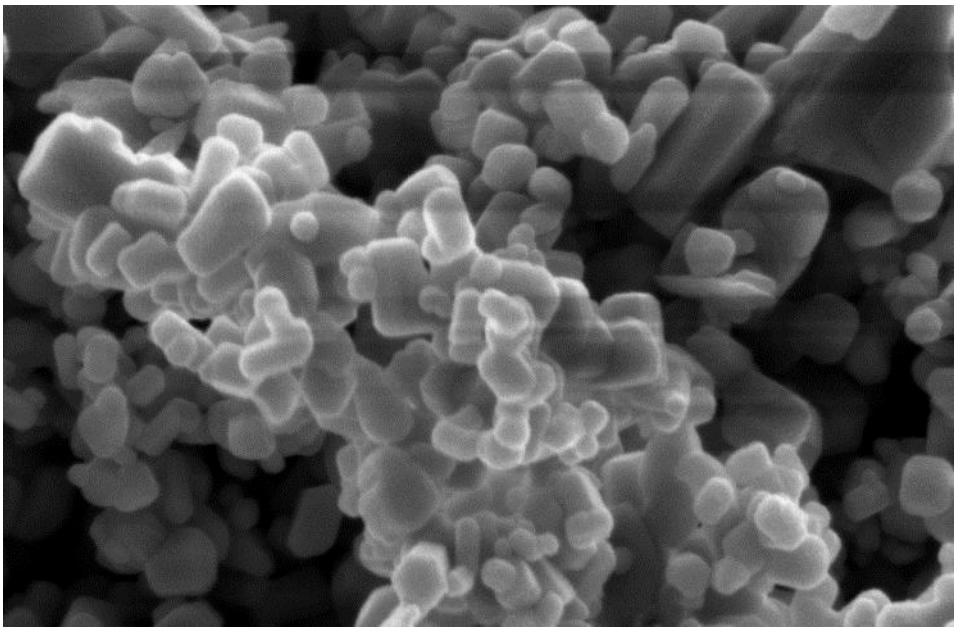

Figure 15. 150 kX magnification of commercial ZnO sample

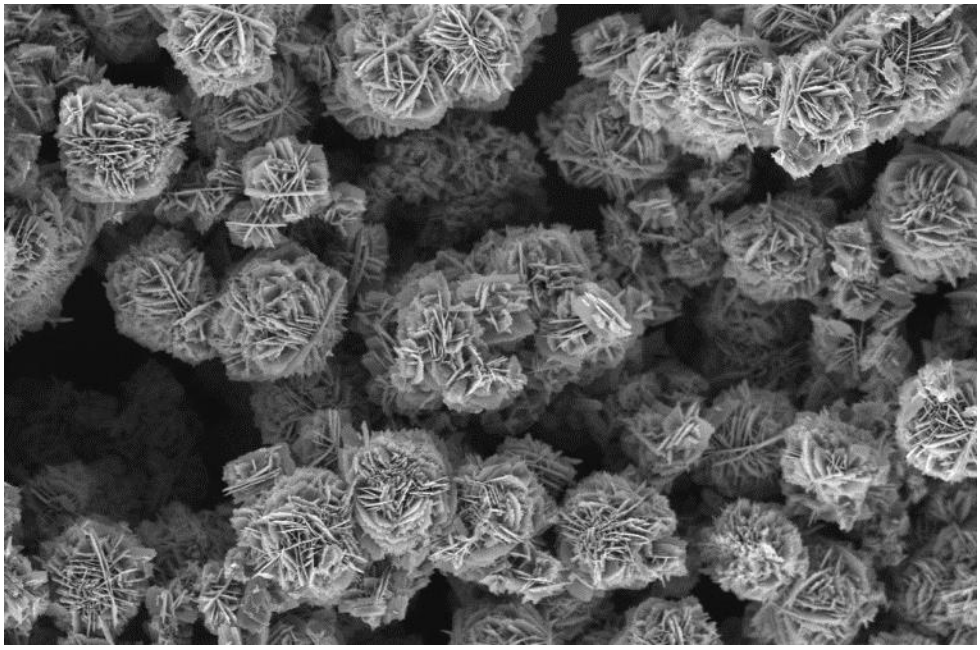

Figure 16. 20 kX magnification of synthesized ZnO

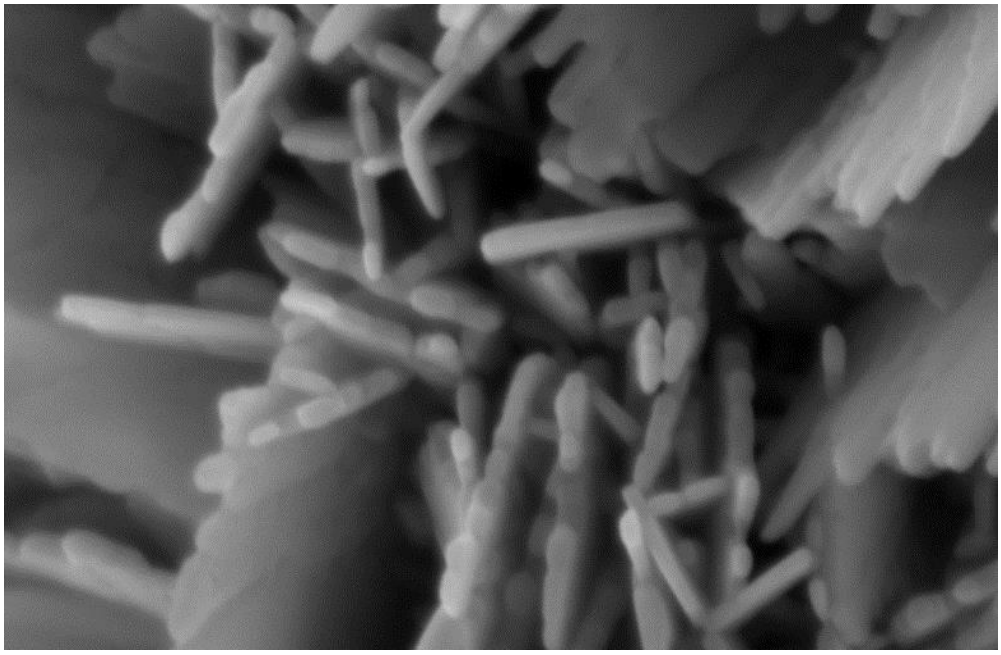

Figure 17. 500 kX magnification of synthesized ZnO

Zinc oxide, also, was investigated through X-ray diffraction analysis. In figure 18 the pattern of commercial ZnO sample, taken from the literature [11], can be seen as benchmark. In figures 19 and 20 the patterns of commercial ZnO and synthesized ZnO (flower-like type) are respectively shown. Both patterns are equal in the number and position of the peaks (thus

confirming that the synthesized sample is really ZnO) but differ in their relative intensities. The peaks at 31.7°, 34.4°, 36.2° and 47.5° are relative to the diffraction planes (100), (002), (101) and (102), respectively (12).

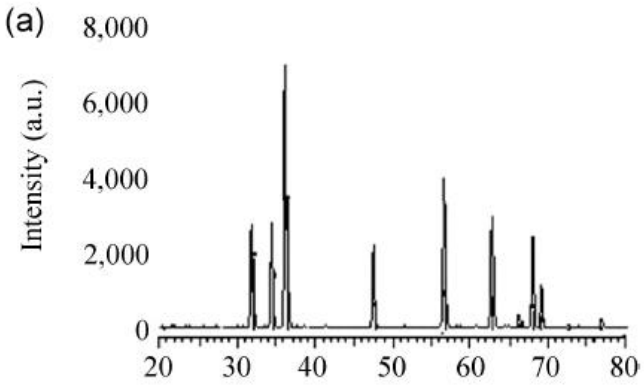

Figure 18. XRD pattern of a sample of commercial CuO (b) [11]

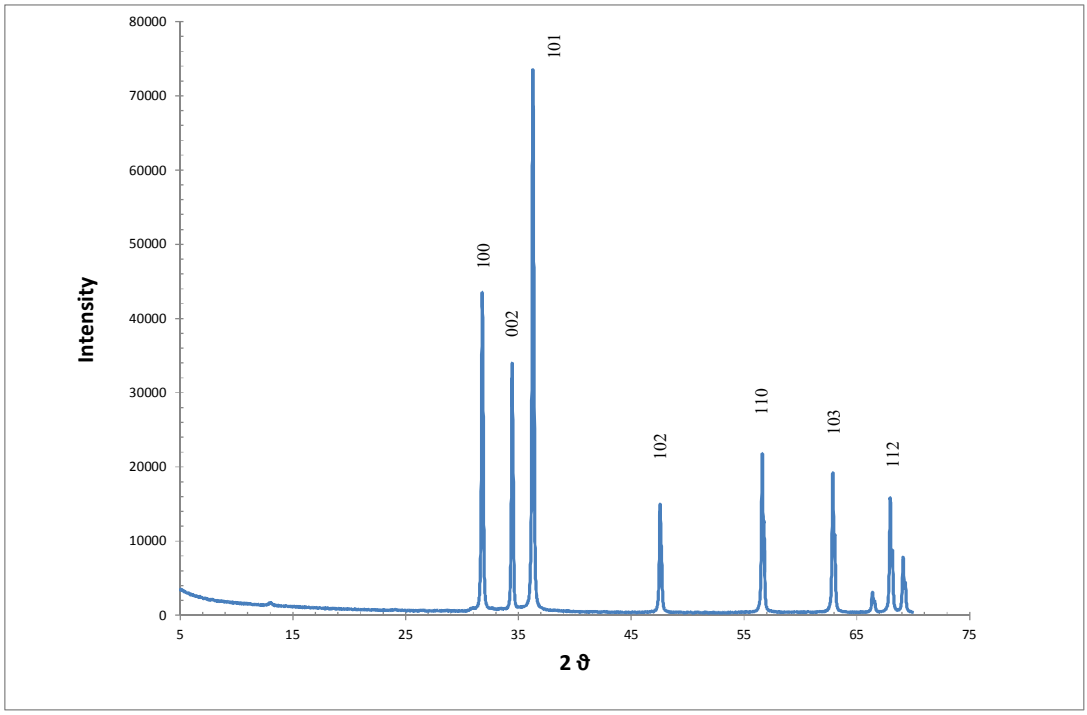

Figure 19. XRD pattern of commercial-type ZnO sample

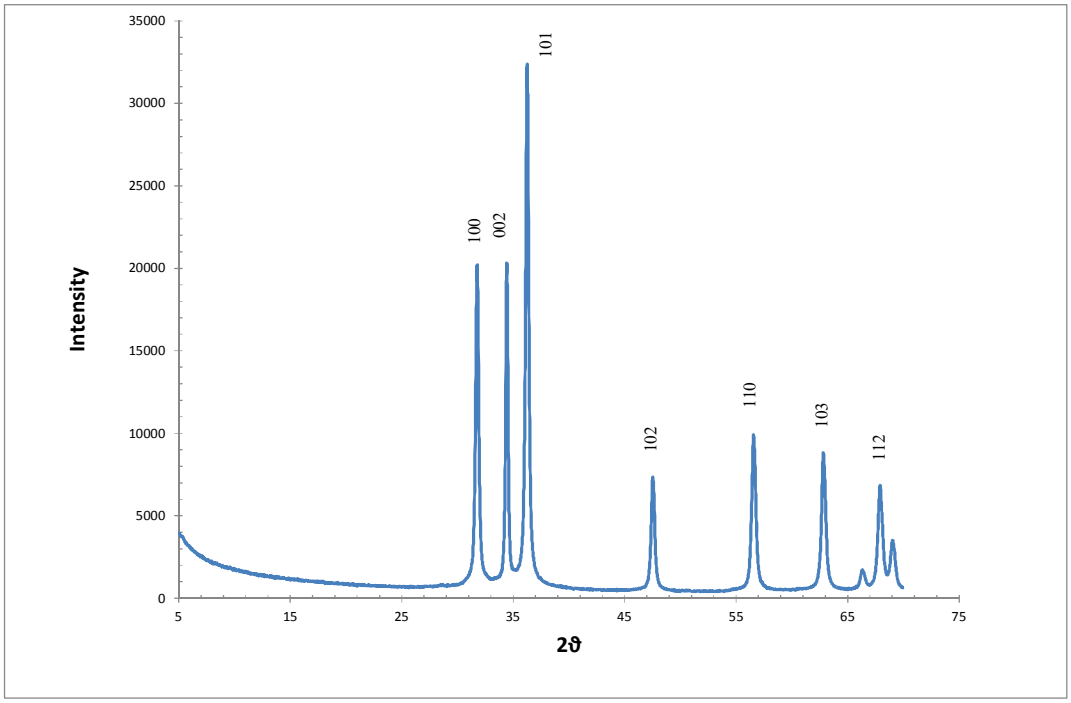

Figure 20. XRD pattern of flower-like-type ZnO sample

4.6.2 Sensor Testing results

4.6.2.1 CuO

A copper oxide sample synthesized in the lab is shown in figure 21. The smallest particles had a size comprised between 66 and 76 µm and were isolated using a manual sieve (used also to measure the size) to realize the sensors.

Figure 21. Copper oxide powder synthesized in the lab

The effect of maleic anhydride on the copper-oxide sensor was first evaluated by introducing 0.0050 g of sample.

In the following table (table 3) the main changes of the sensor's response are detailed. It is evident that the exposure to maleic anhydride determines a not very significant variation in the impedance value (12.5% decrease). After forcing the anhydride out of the flask the signal rose back to the initial value.

Time (min)	Z (Mohm)
0-3	3.2 ±0.1
3-22 (Minimum recorded value)	2.8 ± 0.1
22	3.4 ± 0.1

Table 3. Variation of copper-oxide sensor signals during exposure to maleic anhydride

In figure 22 the trend of the impedance of the sensor was monitored in the presence of carbic anhydride which was mixed with sand (20% anhydride 80% sand). The mixture was introduced in the flask (0.1005 g). The influence of sand alone was recorded as well. It seems that no response is induced by this anhydride on the sensor, since the trend of the sand and of the mixture sand/compound is equivalent. The observed response is probably due to humidity adsorbed on sand.

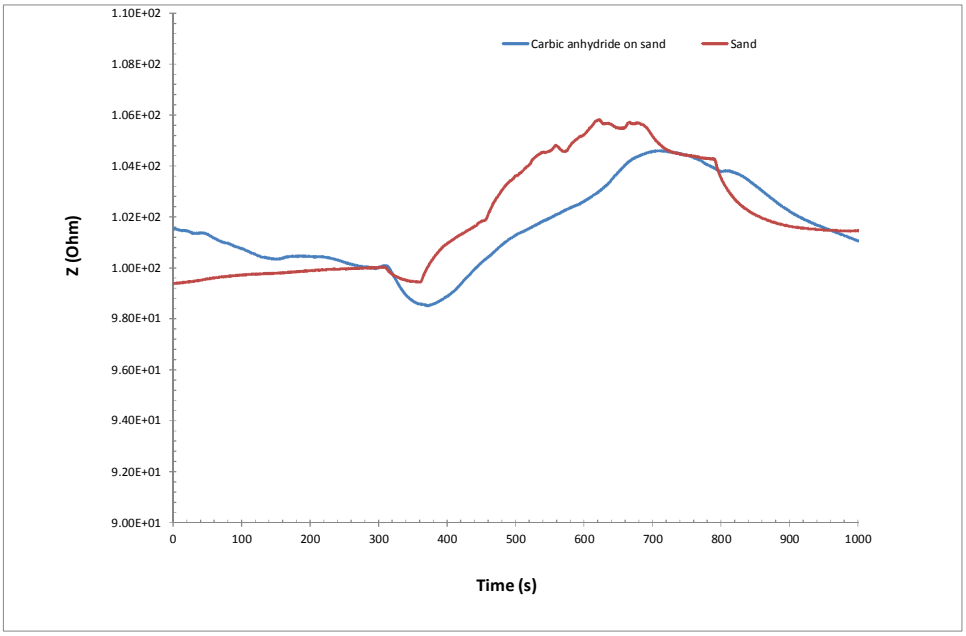

Figure 22. CuO sensor signals. Comparison between pure sand and carbic anhydride adsorbed onto sand. Air flow rate 125 mL/min

The affinity between the sensor and humidity was evaluated by including in the circuit (see figure 4) a gas bubbler filled with water (heated at 40°C) which could be stripped out into the flask. In order to know the right amount of relative humidity present in the flask, a commercial humidity sensor was also installed. In figure 23 the curves produced by the copper-oxide sensor and the humidity sensor are compared. It turns out that, despite the increase in the water (from 5% to 55% of RH) content the sensor didn't provide any significant impedance variation. Differently from the other tests, this one was carried out in a totally continuous mode.

From these preliminary tests it can be concluded that the copper oxide sensor, obtained from the compound synthesized in the lab, does not seem to respond to carbic anhydride and humidity, but only to maleic anhydride and with limited intensity. Experiments found in the literature confirm that p-type sensors do not show any particular interaction with water. However, this type of sensor should show an increase in resistance in the presence of reducing agents. The anhydride is supposed to lose neutral molecules like CO and CO_2 (13) thus causing the carbon atom to change its oxidation state from +3, in the organic form, to +4 in the inorganic one, exhibiting a reducing action.

$$C_4O_3H_2 \longrightarrow CO_2 + CO + C_2H_2 \qquad 4.5$$

$$CO + \tfrac{1}{2}\, O_2 \longrightarrow CO_2 \qquad 4.6$$

The apparent opposite behavior of the CuO sensor which seems to slightly decrease its impedance value in the presence of maleic anhydride can be explained through a no-interaction occurrence between said molecule and the sensor. A further duplicate experiment confirmed said supposition.

Consequently, the research was diverted to a different sensor based on zinc oxide.

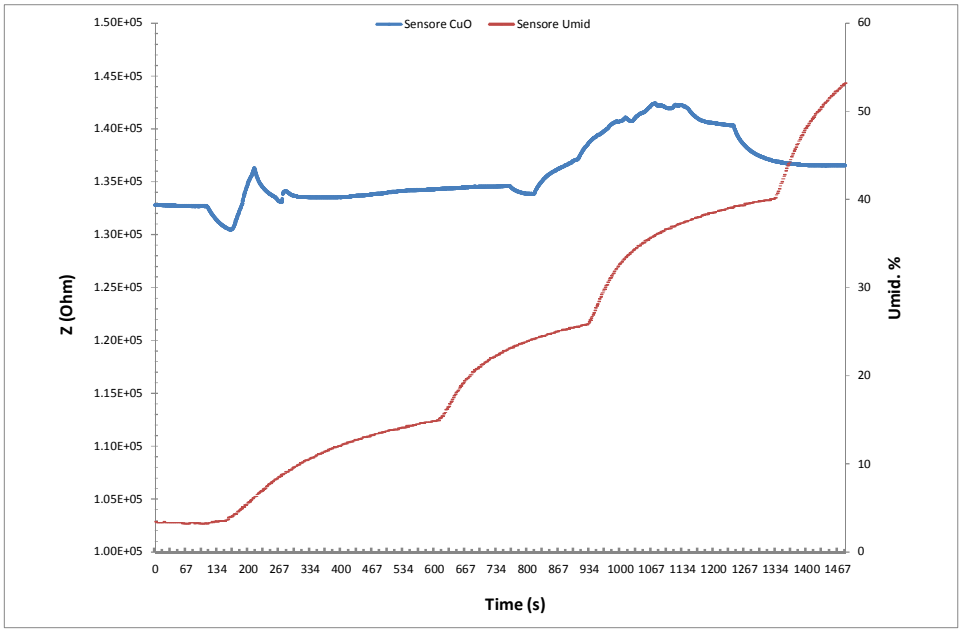

Figure 23. Comparison of signals provided by the CuO sensor and a commercial humidity sensor placed in the same flask.

4.6.2.2 ZnO

4.6.2.2.1 Carbic Anhydride

The effect of the working temperature on the response of sensors based on commercial ZnO and exposed to the same amount of carbic anhydride (0.0050 g) can be observed in figure 24. Four different temperatures were selected: 150, 200, 300, 400°C. After exposure, the impedance signals, which have been normalized for the sake of comparison (% impedance on vertical axis versus time in seconds), decreased as expected. The shape of the curves, in terms of response and sharpness, indicates a compromise between 300 and 400°C, value at which the peak should appear deeper and narrower, as the more effective temperature. However, because prolonged and repeated experiments at that temperature would damage the materials used to fabricate the sensor holder, most of the tests were carried out at 280°C.

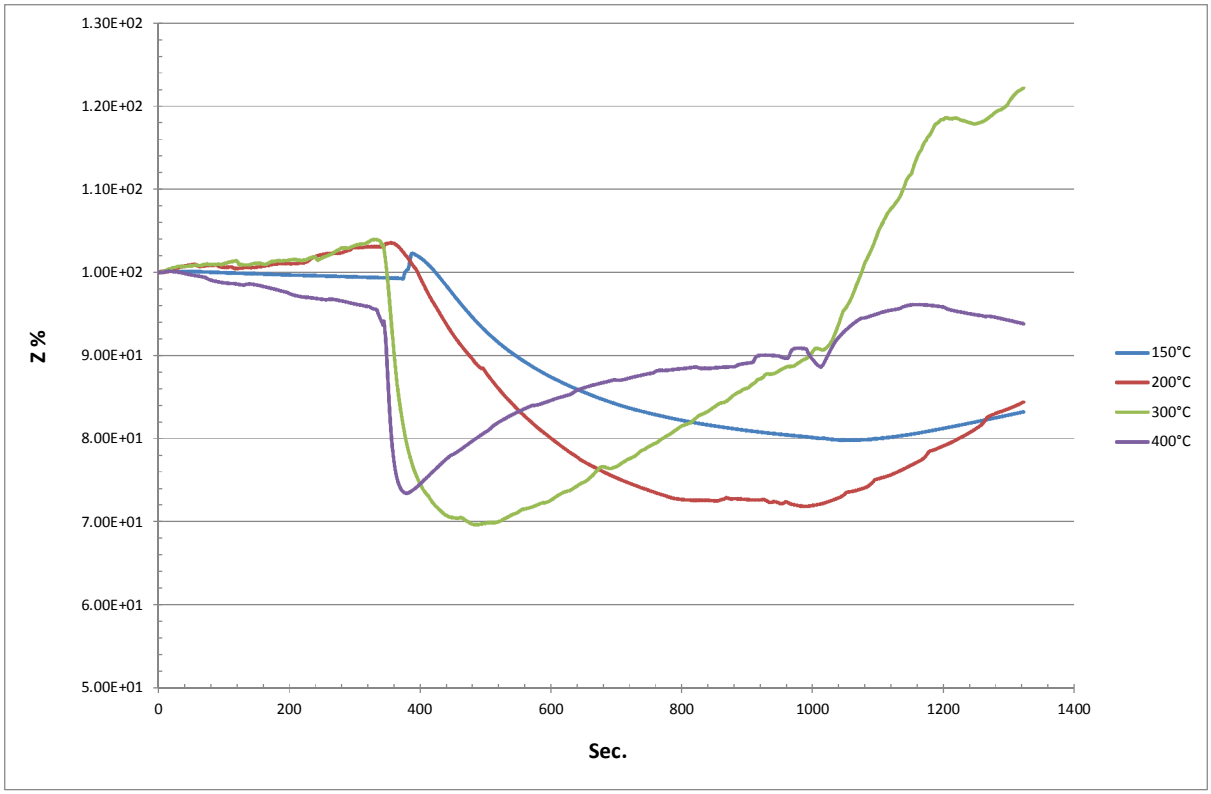

Figure 24. ZnO sensor's response exposed to carbic anhydride and set at different temperatures.

The effects of water (0.025 g) and of different amounts of carbic anhydride inserted in the flask in the powder form, and bare air (blank in the graph) are shown in figure 25 (flower-like ZnO based sensor). The flask was kept at 180°C causing a transition of the samples to the gas phase. It is evident that different weights of anhydride cause very similar reductions in the impedance values (reported as percentage), as if the sensor got saturated even by the smallest amount (0.0040 g). Even 0.0040 g are excessive. Another concomitant event, which could partially explain the behavior, is the partial condensation of the anhydride on the coolest part of the apparatus (especially the upper wall of the flask). Water also, in contrast with the CuO sensor, determines an impedance reduction. ZnO is a n-type sensor that lowers its impedance when exposed to reducing compounds. The carbic anhydride, similarly to maleic anhydride (see equations 5 and 6), should eliminate CO_2 and form a unsaturated cyclic compound.

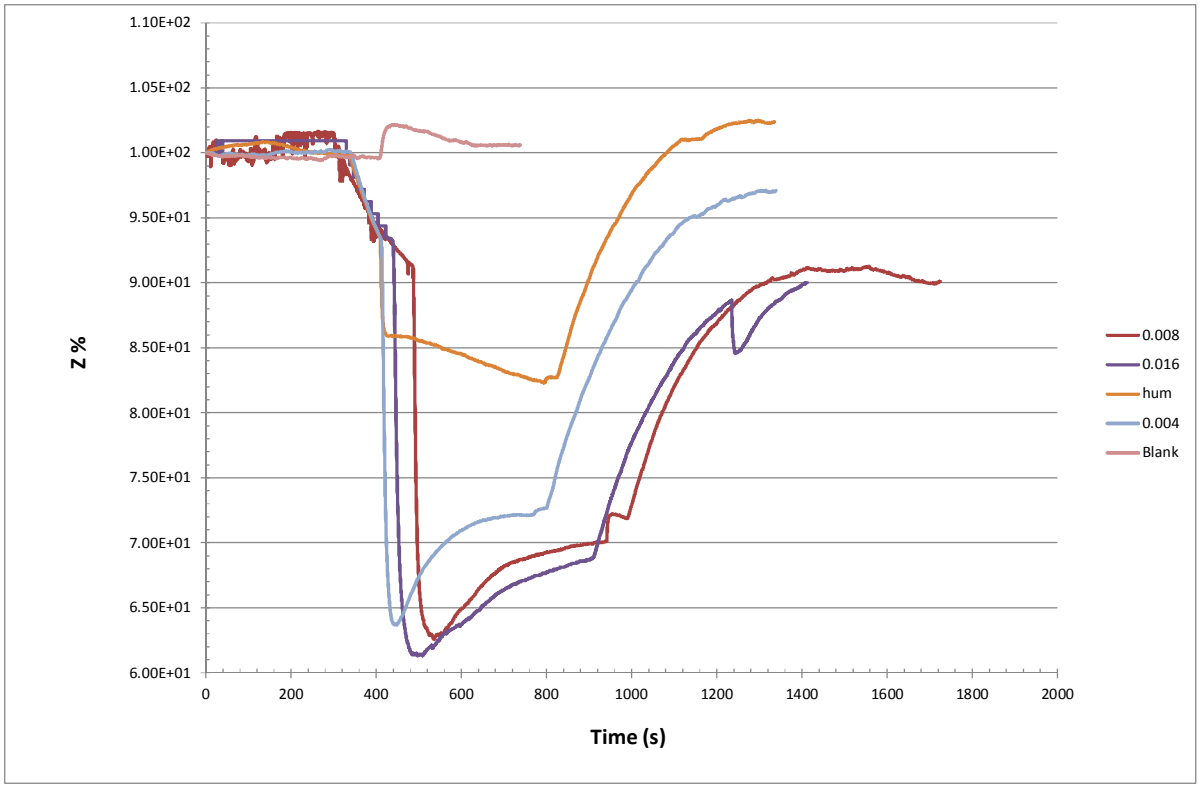

Figure 25. Comparison among different concentrations of carbic anhydride, humidity and blank at 280°C. A flower-like-ZnO- based sensor was used. RH at ambient temperature was 37 %

In figure 26 a different representation of the graph of figure 25 is visible. Here, the amplitudes (arrows) of the impedance values (as a percentage) are shown and can give support to the explanation provided above. The green points on the graph represent the average values of the impedance decrease and the end of the arrows are the minima and maxima recorded in each set of experiments. It is evident how the three different, and evidently excessive, amounts of carbic anhydride can provide partially overlapping signals.

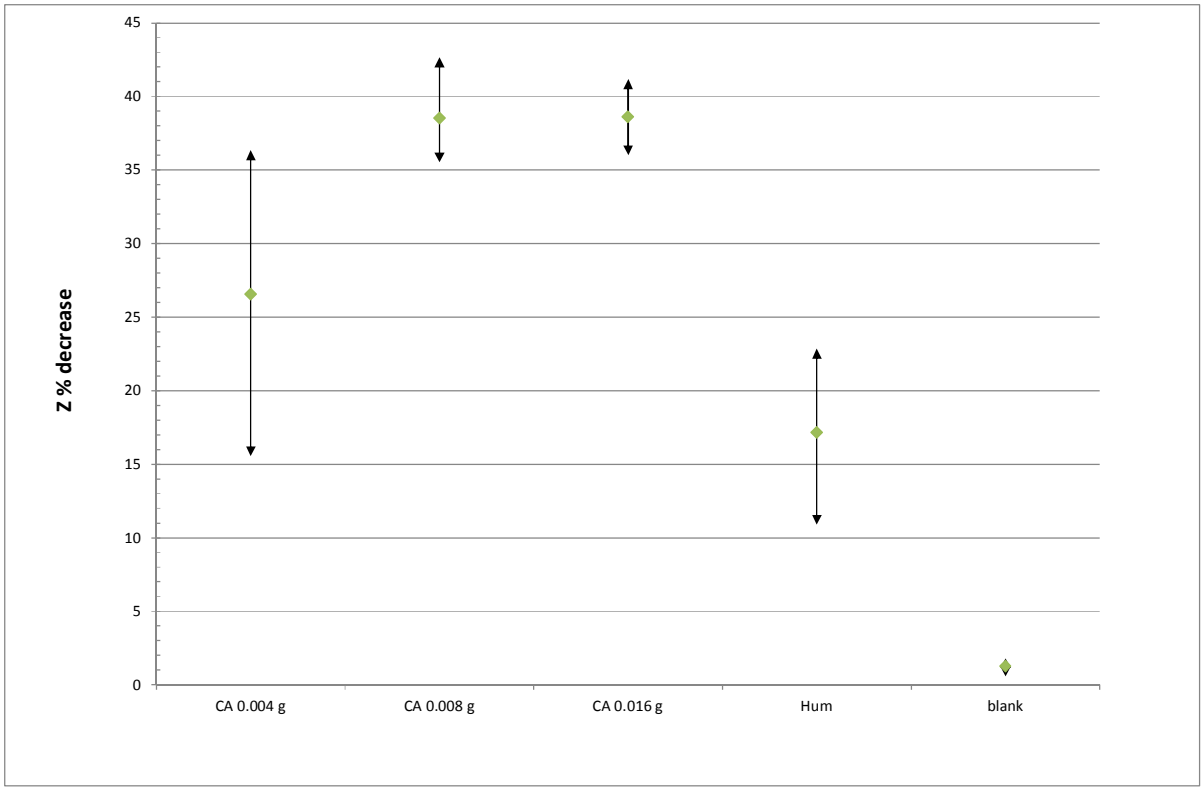

Figure 26 Z% decrease. Comparison among different concentrations of carbic anhydride, humidity and blank at 280°C.

In figure 27, the comparison between a flower-like ZnO sensor and one realized with the commercial ZnO powder is displayed. Both sensors were exposed to the same amount of carbic anhydride (16 mg). The signal after equilibration starts from different values, that in this specific case is lower for the flower-like type (1100 Ω against 5050 Ω). However, the response is very similar. Being the anhydride a reducing gas the response R for the two sensors is the following:

R_{com} = 3.07 E03 / 5.5 E03 = 0.59

R_{Fl} = 0.68 E03 / 1.08E03 = 0.63

The response of the sensor based on the commercial powder is higher respect to the one made with the powder prepared in the lab.

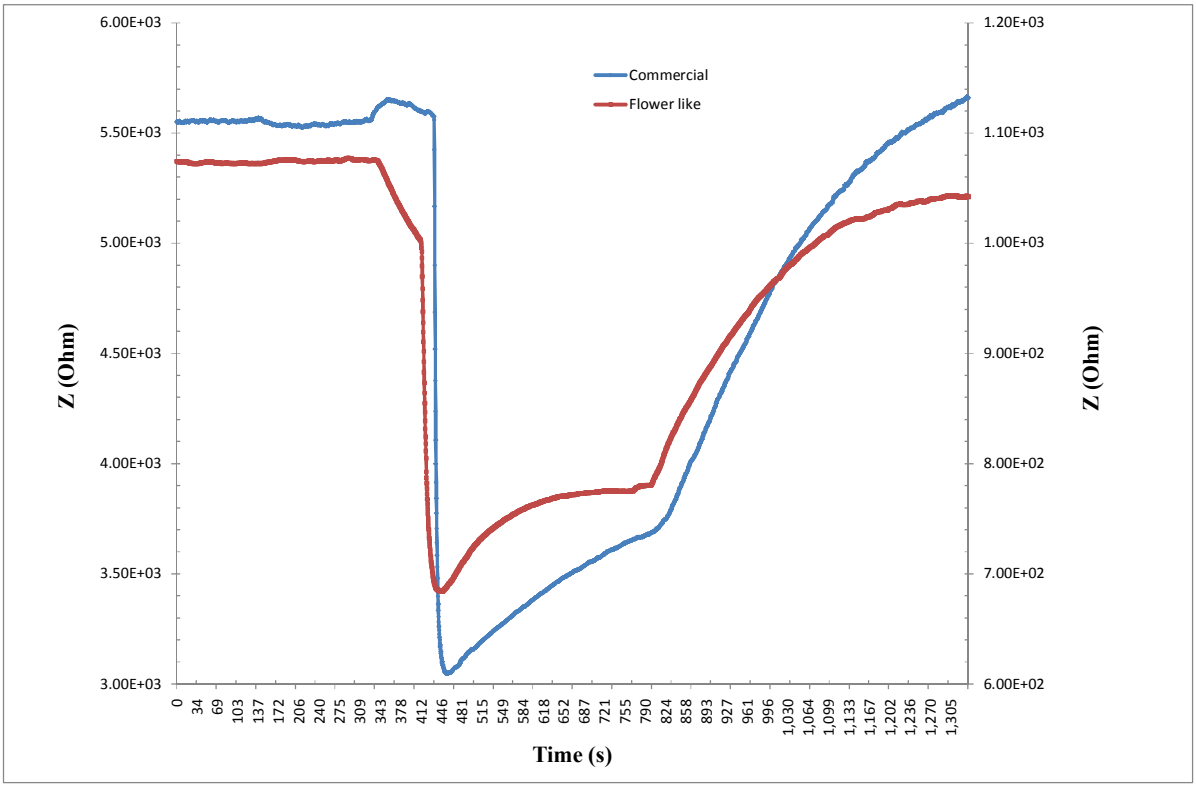

Figure 27. Comparison of the responses provided by ZnO sensors made with flower-like oxide and a commercial product. The scale on the right ordinate axis pertains to the flower-like ZnO sensor; the one on the left ordinate axis is the scale of the commercial sensor.

To overcome the problem of saturation, a 1000 µg/g solution of carbic anhydride in isopropanol was prepared and weighed amounts of it were deposited on glass slides. Thus, after the evaporation of the solvent, a much lower quantity of carbic anhydride (up to 350 µg), compared to the situation described above, could be introduced in the heated flask. In figure 28 the impedance values recorded versus the µg of anhydride employed in the different tests is shown. Surprisingly a linear correlation could be found, demonstrating that smaller, but still meaningful quantities of the compound can be quantitatively determined with the sensor. Besides, the condensation of the anhydride is negligible being the ratio between the amount introduced and the volume of the flask small enough to ensure a stable concentration in the gas phase.

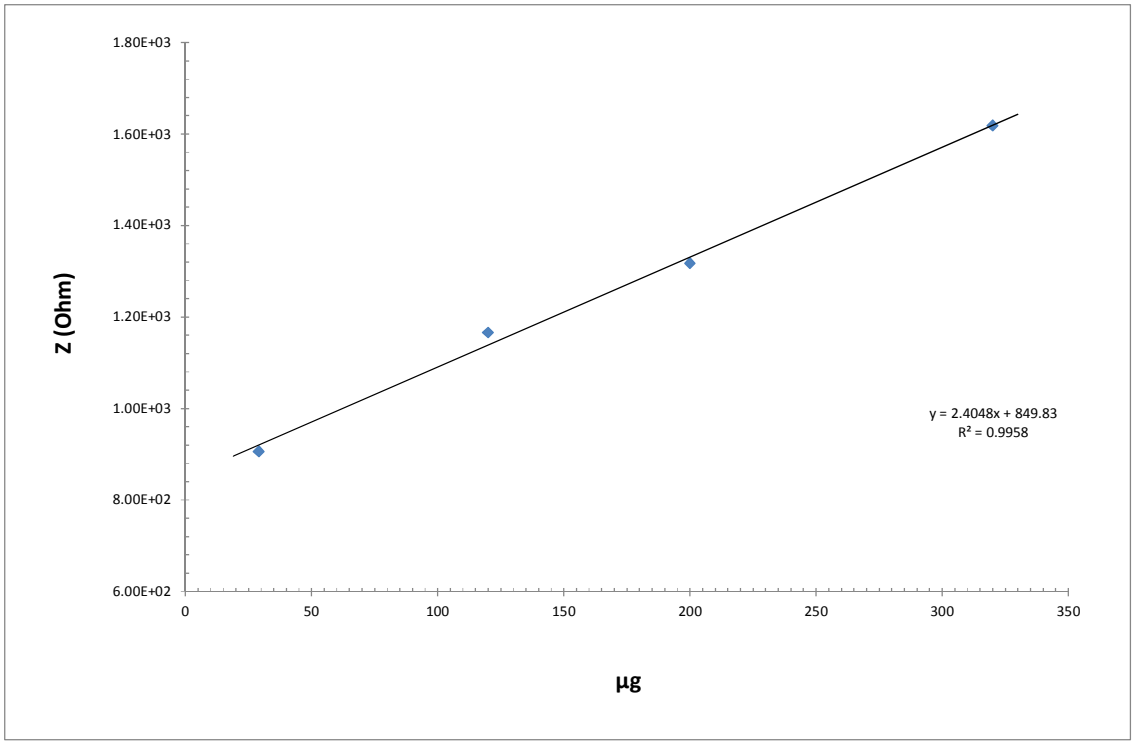

Figure 28. Calibration curve of ZnO sensor (commercial type) at 280°C exposed to different concentrations of carbic anhydride (deposited on glass support).

4.6.2.2.2 Phenol

Along with carbic anhydride the response of the ZnO sensor to pure phenol in the gas phase was also evaluated. The flask was kept at a slightly lower temperature (140-150°C), being phenol more volatile.

As in the case of carbic anhydride the sensor was tested at different temperatures (see figure 29). Here the best compromise seems to be a temperature close to 250°C, which should offer narrower but still high peaks. Two hundred degrees, maybe, would produce a too broad response

In figure 30 a graph showing two different responses is shown. The first behavior that leaps out is the increment of the impedance value, which is quite unexpected, being the ZnO sensor a n-type sensor. As a matter of fact an oxidation of phenol to quinone is what one would expect to occur. In the tests pertaining to the figure the air flow rates, after opening the inlet valve (step 6 of the procedure detailed above) were kept at two different values, 625 and 125 mL/min, in order to recreate two possible real scenarios. The one where the transformer is

kept in a forced-air environment and the other where the air circulation is small. Obviously, the sensor response returns faster to the starting value when the flow rate is higher, due to a more effiecient cleansing of the environment .

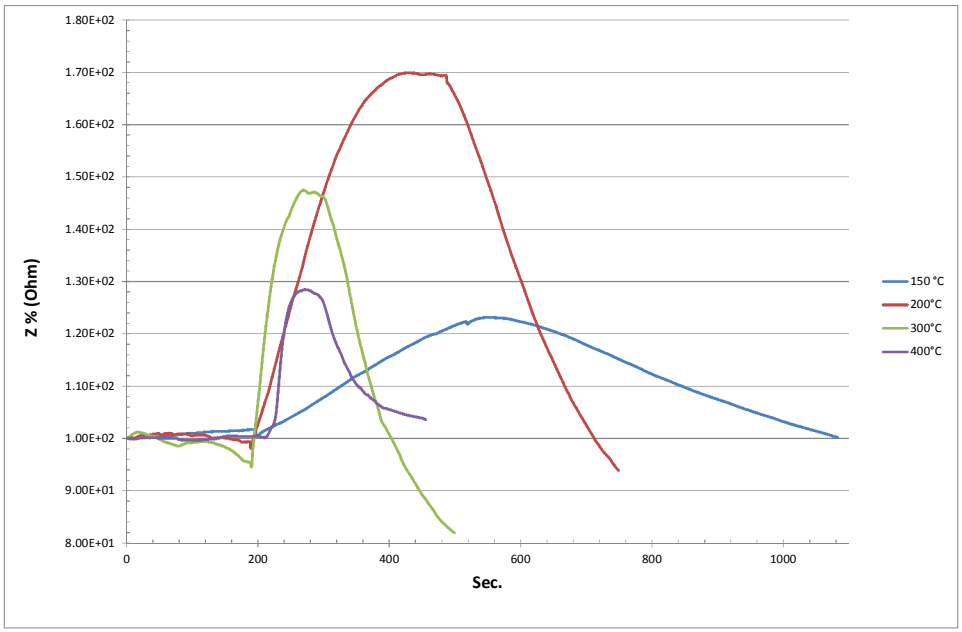

Figure 29. Comparison of the ZnO sensor's response exposed to phenol and set at different temperatures.

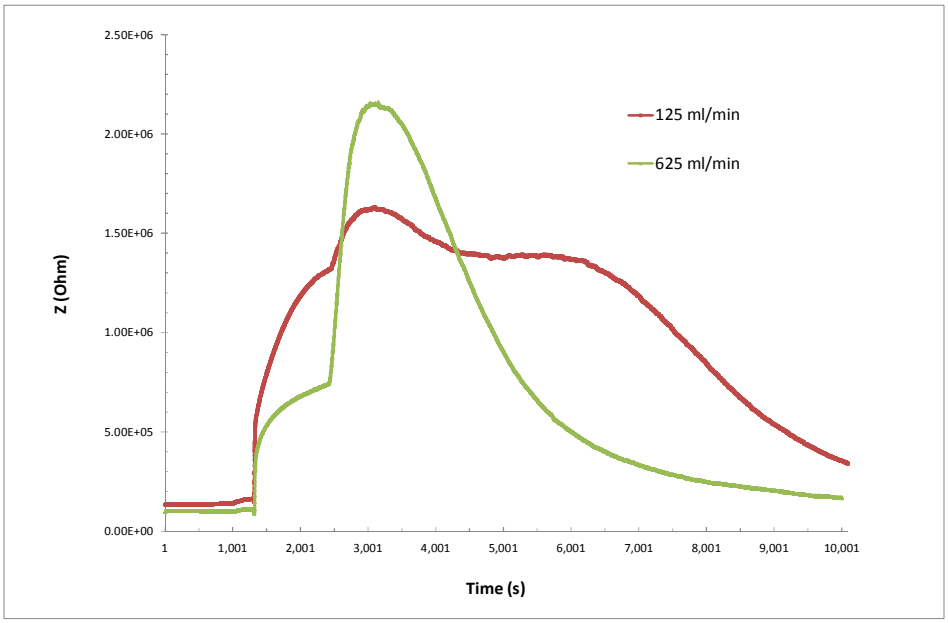

Figure 30. Detection of phenol using ZnO sensor. Comparison between different flow rates, 125 mL/min red line and 625 mL/min green line. 0.0025 g of phenol. The temperature of the sensor was set at 250°C

In figure 31 the response of the sensor to two different amounts of phenol (11 and 25 mg) is shown. The response is very high, but contrarily to the anhydride case, there is a direct even though not linear correlation between the amount and the sensor's response and no saturation is observed, at least when 11 mg are introduced in the flask.

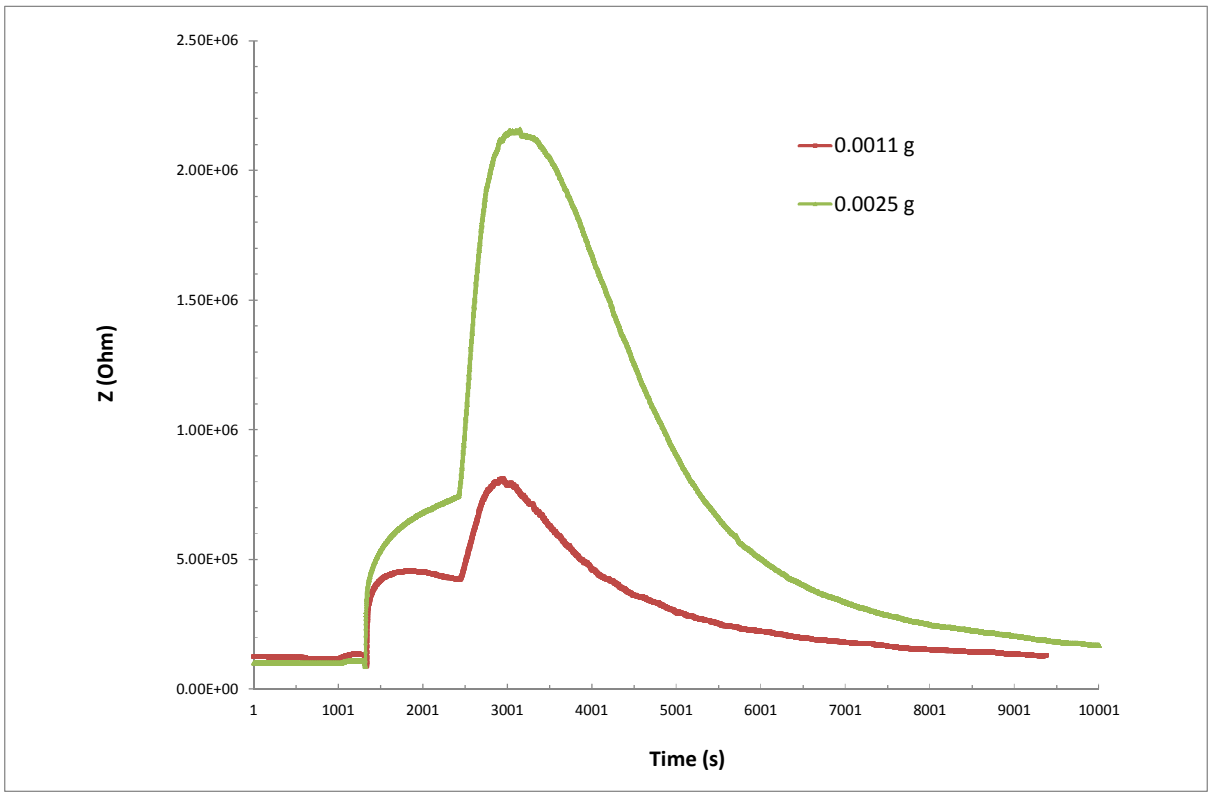

Figure 31. Detection of Phenol using ZnO sensor. Comparison between different amount, 0.0011 g (red line) and 0.0025 g (green line), flow rate 625 mL/min

As previously briefly mentioned, phenol was expected to be a reducing compound. However, it behaves as an oxidizing compound. Consequently, to understand if other kind of reactions can occur similar compounds were investigated: 2,6- di-tert-butyl-p-cresol (DBPC) and 2,6-di-tert-butyl-phenol (DTBP), whose structure is shown in figure 32. The former has a methyl group in the para position while the latter has an hydrogen atom.

Figure 32. Molecules of 2,6-di-tert-butyl-phenol (left) and 2,6- di-tert-butyl-p-cresol (right)

In figure 33 a comparison among the signals of pure phenol, DBPC and DTBP in comparable amounts (16 mg) obtained using commercial-ZnO based sensor set at 250°C. The behaviors of pure phenol and DTPB are equivalent (impedance increase, oxidizing behavior) and opposite to that of DBPC (impedance decrease, reducing behavior).
It can be supposed that a kind of reaction that involves the para position can occur (dimerization, polymerization). Further investigation is thus required.

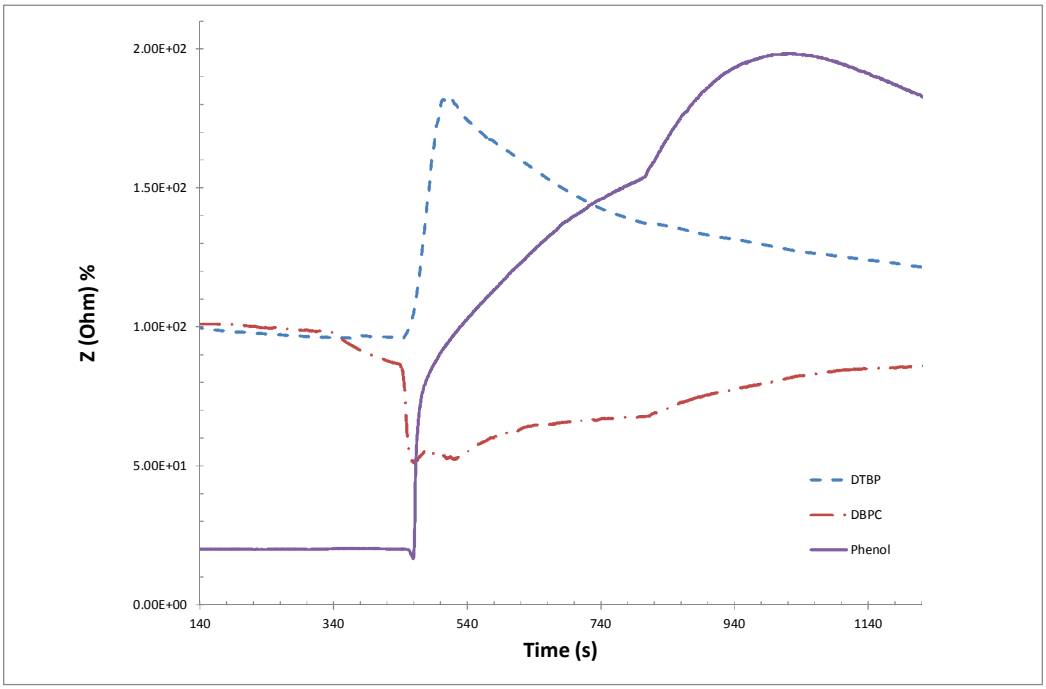

Figure 33. Comparison of ZnO sensor's response (commercial type) exposed tophenol with different level of substitution. Purple solid line is pure phenol, red dotted line is DBPC and blue dotted line is DBP.

The effect of divinylbenzene, a compound that is prone to polymerize easily, was investigated (in order to see if a possible polymerization of phenol could have the same effect). However the responses of both flowerlike and commercial ZnO sensors were low and not trustworthy. The impedance, after a small initial increase, did not varied significantly due to an extensive and visible polymerization of the bifunctional molecule (the flask was heated at 70°C, a temperature sufficiently high to induce autopolimerization). The result of the tests conducted successively with phenol were all negative because of a complete fouling of the sensors by the polymer (see table 4). A decrease in impedance is observed with no correlation with the amount of phenol.

Amount phenol (µg)	Sensor's response (%)
50	10.13
100	11.30
200	10.99

Table 4. Sensor's response of an already used and yellowed flower-like sensor, exposed to phenol (solution deposited on glass slide).

Very often, dry type transformers are used in industrial facilities were a lot of different organic molecules can be freely present in the air and are not connected to any thermal degradation of the epoxy resin. Consequently, the influence of other volatile molecules, to be considered as interferences, was also tested. The results are summarized in figure 34, where the vertical axis is the log of the difference between the initial and the final impedance values. If we exclude phenol, which shows an opposite behavior, all other molecules (methylmethacrylate, phthalic acid, heptanoic acid, butanol) provide a positive response (impedance decrease) and can lead to false positive results.

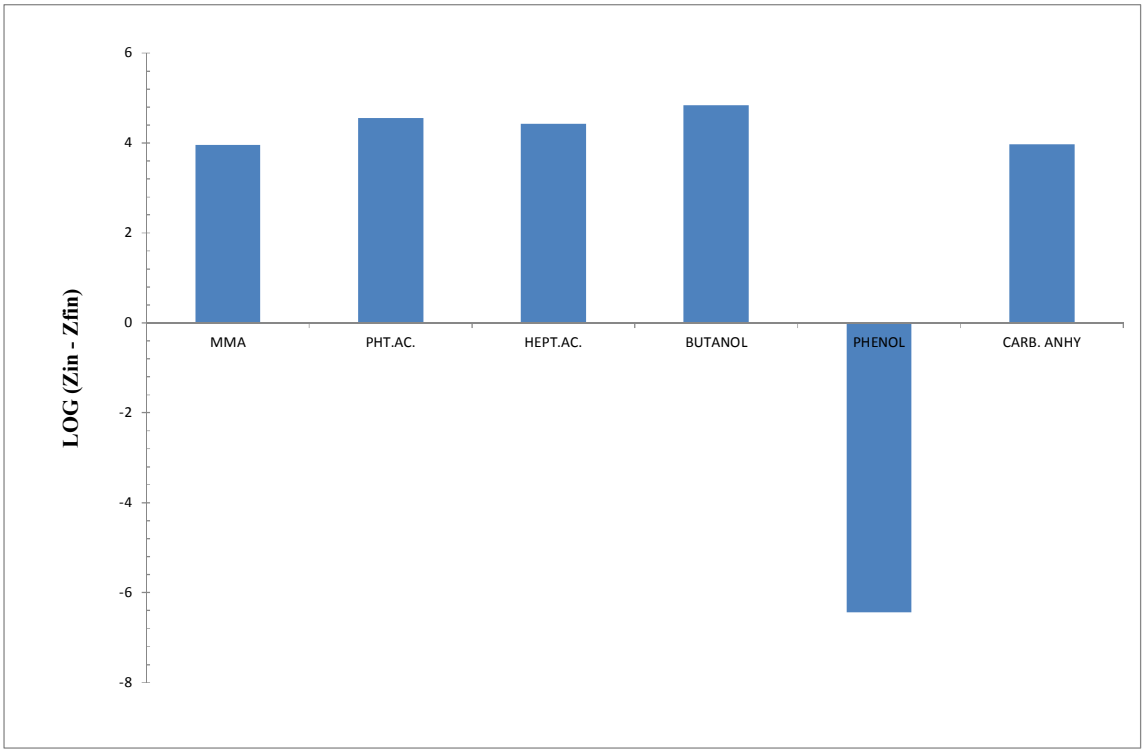

Figure 34. Comparison between sensor's response from water and formaldehyde (37% aqueous solution) obtained with a ZnO sensor commercial

4.6.2.2.3 Epoxy Resin

Finally, a flower-like ZnO sensor was exposed to the vapors coming from a piece of epoxy resin kept at 200°C for more than an hour. The resulting curve is visible in figure 35. The impedance value decreases quickly and remains quite stable, at least as long as the air flow is kept on. However, even in this case the vapors seems to persist inside the flask.

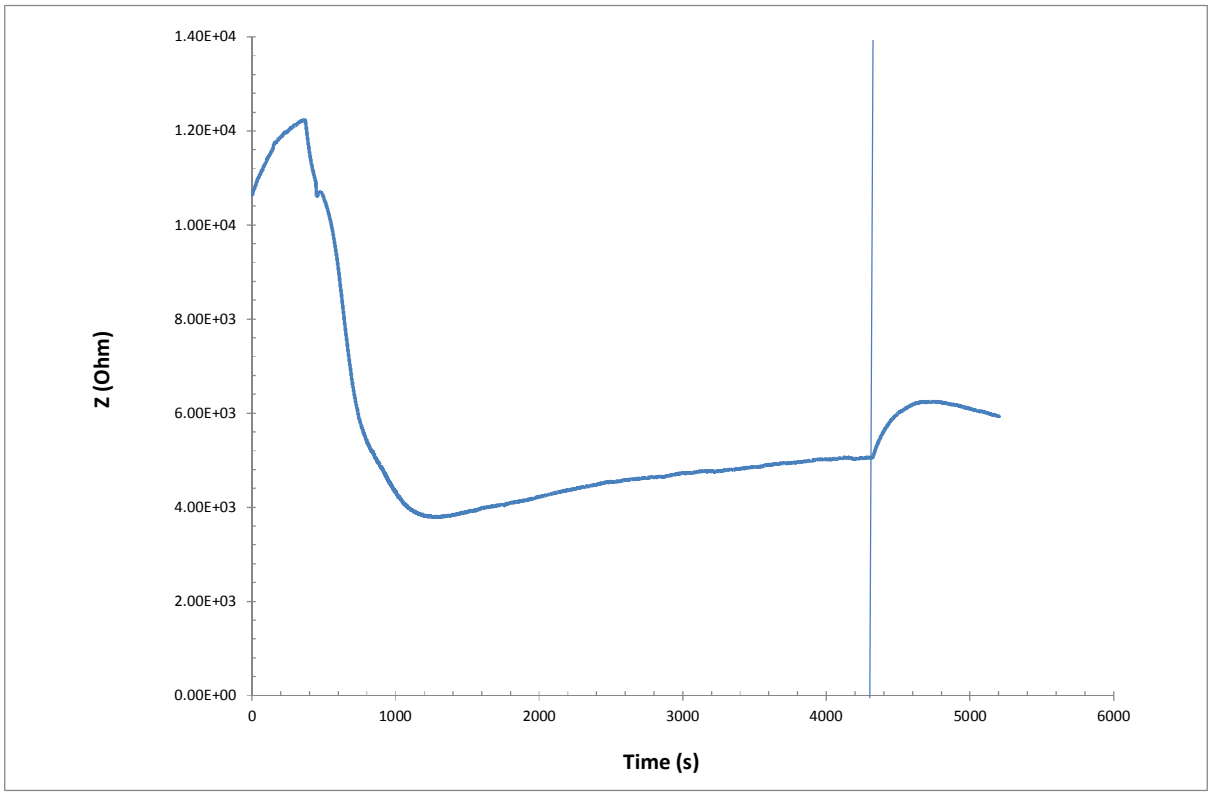

Figure 35. ZnO sensor's response (flower-like ZnO) exposed to the vapors of a piece of resin heated at 200°C.The blue vertical line on the right hand side indicate the time when the pure air flow is restored

4.7 Conclusion

The results obtained with CuO-based sensors were quite unsatisfactory because of an almost insignificant response. On the contrary, in the case of ZnO, the sensors turned out to be highly sensitive, but affected by a very low selectivity. An interesting behavior can be observed with phenol which yields an unexpected and still incomprehensible increasing impedance signal. The presence of phenols is principally investigated in aqueous solution due to their ubiquitous diffusion as pollutants but there is also an interest in their occurrence as an airborne contaminant (industrial exhaust, wood fire, cigarette smoke) [14]. For their detection , different types of techniques are adopted, like optical, electrochemical and electro-biochemical [15]. However the use of a ZnO-based sensor, which shows a response opposite to the expected one, could be an interesting alternative. Unfortunately, the general very low specificity of ZnO is in line with the performance provided by commercial sensors and such a behavior could not be acceptable if the sensors have to be installed in an industrial environment where the possibility of cross contaminations is high and unavoidable.

Before trying to modify the CuO and ZnO-based sensors making the former reactive and the latter more cognate with selected molecules (like anhydrides and phenolic compounds), an integration of the ZnO-based sensor with an industrial-scale monitoring device should be evaluated. Consequently, in the next chapter the development of an on-line and in-field device and its coupling with one of the sensors (ZnO) fabricated so far will be explained.

4.8 References

[1]Interaction of Anhydride and Carboxylic Acid Compounds with Aluminum Oxide Surfaces Studied Using Infrared Reflection Absorption Spectroscopy; J. Van den Brand, O. Blajiev et. al.; Langmuir, 2004, Volume 20, Issue 15, June 2004;

[2]Reactivity of ZnO Surfaces toward Maleic Anhydride; Stefanie Gil Girol, Thomas Strunskus et. al.; J. Phys. Chem. B, 2004, Volume 108, Issue 36, August 2004

[3] Proceedings of the 16° annual meeting of Adhesion Society; Gordon and Breach Publisher, Adhesion International 1993

[4]CuO nanocrystals with controllable shapes grown from solution without any surfactants; Junwu Zhu, Huiping B. et al.; Materials Chemistry and Physics Volume 109, Issue 1, May 2008

[5]The Merk index, 12° edition

[6]Preparation and characterization of copper oxide nanoparticles and determination of enhancement in critical heat flux; M. Kshirsagar, R. Shrivastava, et al.; Thermal Science Volume 1, Issue 1A,, January 2015

[7]Solution combustion synthesis of nanoscale matherials; A. Varma, A. S. Mukasyan, A. S. Rogachev, K. V. Manujyan; Chem. Rev., 2016

[8] Materials via solution combustion synthesis: a step near to controllability; W. Wen, J-M Wu, et.al.; RSC Advances., Volume 4, Issue 102, 2014

[9] Basic Chemical Principles, Chapter 2; J. A. Conkling, C. J. Mocella; CRC Press Taylor and Francis group, , 2011

[10]Structural analysis of CuO nanomaterials prepared by novel microwave assisted method; A. Chinthakuntla, S. Chakra et al.; J. atoms and molecules/ Volume 4, Issue 5, 2014

[11]The influence of the crystalline nature of nano-metal oxides on their antibacterial and toxicity properties; Ilana Perelshtein1, Anat Lipovsky1, et al.; Nano Research, Volume 8, Issue 2, 2015

[12] Synthesis, characterization, and functionalization of ZnO nanoparticles by N-(trimethoxysilylpropyl) ethylenediamine triacetic acid (TMSEDTA): Investigation of the interactions between Phloroglucinol and ZnO@TMSEDTA H. Barraka, T. Saied et al.; Arabian Journal of Chemistry, Volume 7, Issue 6, 2016.

[13] Carleton University; https://www.coursehero.com/file/p4p5vrg/Decomposition-and-Decarboxylation-Maleic-anhydride-undergoes-anaerobic-thermal/; (accessed 27th April 2019)

[14] Solid nanoporous sensor for the detection of phenol ; A. borta , L. Mugherli et al.; European Network on New Sensing Technologies for Air Pollution Control and Environmental Sustainability – EuNetAir

[15] Electrochemical gas biosensors; I. Iliev, A. Kaisheva; Frontiers in Biosensorics, F. W. Scheller, F. Schubert J. Fedrowitz editors Volume 81 1997

5 Field Application

The experiments described in chapter 4 become meaningful if the ZnO sensors can find an application in a real industrial situation, which means if they can be installed on a device dedicated to the monitoring of electrical machines. In the former chapters the targets of the research and the results of the lab experiments were explained and detailed. The main two goals were, on the one hand, to determine the by-products of the thermal degradation of epoxy resins for electrical applications and on the other hand to develop sensors responsive to the possible evolved vapors. Above and beyond said targets there is also the necessity to link thermal events to the behavior of the electrical equipment. Luckily a couple of industrial companies were interested in carrying out in-field studies and put their transformers at disposal. Consequently, two prototypes of a sensor-based electronic device were realized to manage different commercial sensors and to collect and transmit the signal generated accordingly. The devices was named DTD, dry transformer detector. The following properties and parameters were searched:

1. Organic Vapors
2. Ozone
3. Sound
4. Environmental humidity
5. Environmental temperature
6. Transformer temperature
7. Dust (dirt)

Each of the items listed above can be somehow related to possible problems in a dry-type transformer. As a matter of fact, an overheating can promote the release of organic vapors from the resin and an electrical discharge could generate ozone. Furthermore environmental conditions in terms of humidity, temperature and dust can influence the correct working of the machine. Finally, the sound can provide information about the correct tightening of nuts and bolts, vibration and workload. Construction, installation, functioning and results are described in the next sections.

An air sampling device was also fabricated and installed in the rooms of the transformer

5.1 DTD design and construction

Two prototypes have been realized using small single board computers and microcontrollers, like Raspberry and Arduino. The sensor-based device is part of a more complex system, whose logical layout is shown in figure 1. The components named slave are those carrying the sensors and they are connected, through a switch, to a central unit called master, which is linked to the internet via a GSM modem. On a dedicated web page, it is possible to read and download the collected data.

The slave module was made of electronic parts and sensors purchased from the market and assembled in a dedicated box. The characteristics of the sensors are herewith listed:

1. Dust sensor: Amphenol SM-PWM-01C; *minimum dust size 1 µm*
2. Ozone sensor: Spec Sensor 968; *0-5 ppm, 20 ppb resolution*
3. Thermal Sensor: Melexis mlx 90614; *32x24 pixels IR array*
4. VOC sensor: Figaro TGS 2620; *50/50000 ppm*
5. PC microphone: Gyvazla; *20Hz-16KHz, stereo, 16 bits*
6. T/Hum. Sensor: DHT 22, Aosong Electronics; *-30 - +90°C, 5-95% RH*

The master module works as a communication interface between the slaves and the modem and it can also save data locally when the access to the internet is unavailable. Several slave modules can be connectable at the same time.

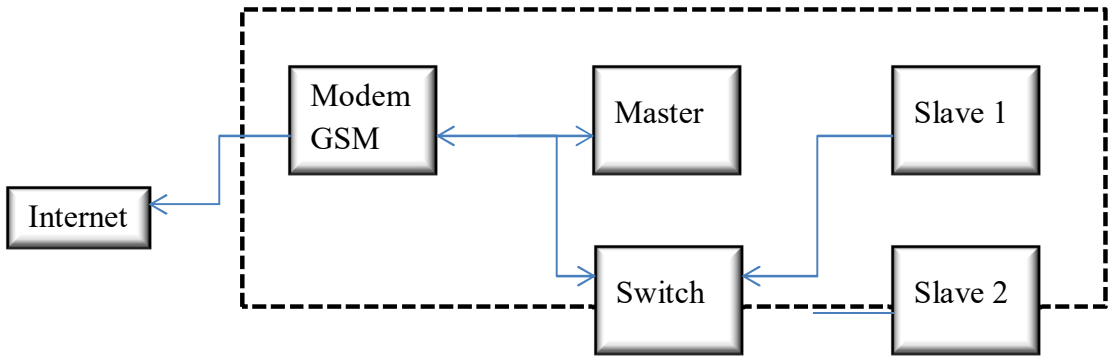

Figure 1. Logical layout of the monitoring system.

5.1.1 Prototype 1

In figure 2, the first prototype of the master (white box) and slave (grey box) modules is visible.

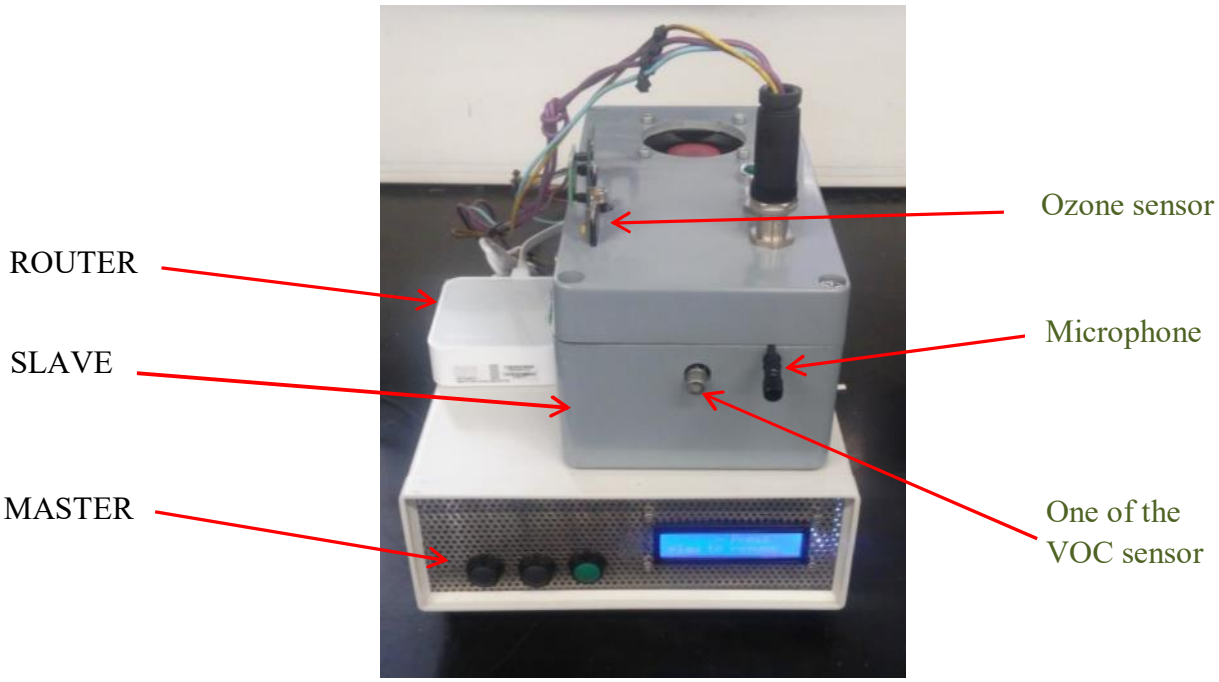

Figure 2. Prototype n° 1. Master, slave and router

In figure 3 a dry-type transformer kept in a big room devoid of forced ventilation and temperature control and the first prototype of the slave module are displayed.
The latter was fastened to the protecting grid in order to ease the maintenance activities without requiring the disconnection of the transformer.

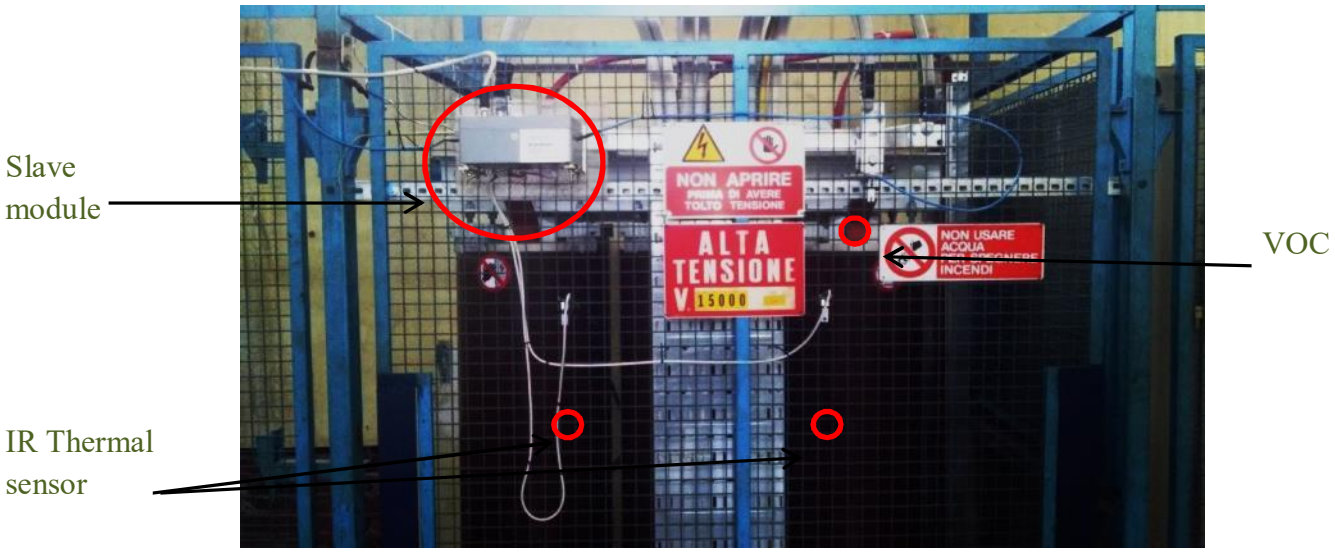

Figure 3. Dry-type transformer and the first prototype of the slave module

In figure 4 the installation of the IR thermal sensors and one of the VOC is highlighted. The latter has been placed as close as possible to one of the transformer phases.

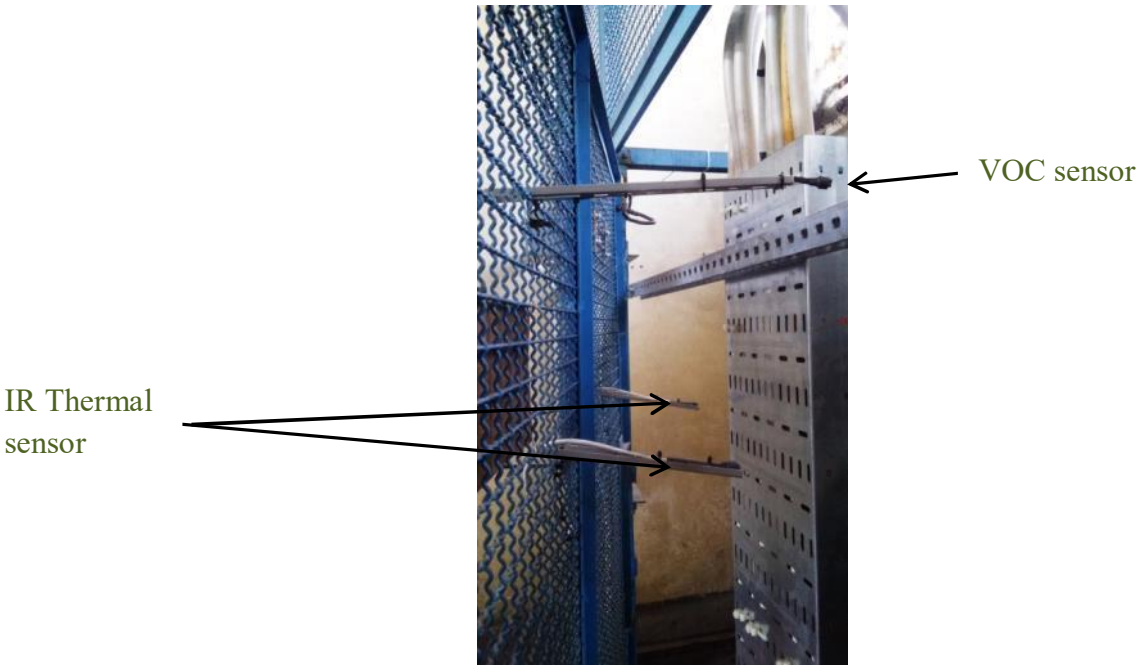

Figure 4. VOC and IR thermal sensor connected to slave

In the next figure (5) an example of the web page used to monitor the values of the sensors connected to the first prototype is shown. The VOC sensor provides a signal in mV.

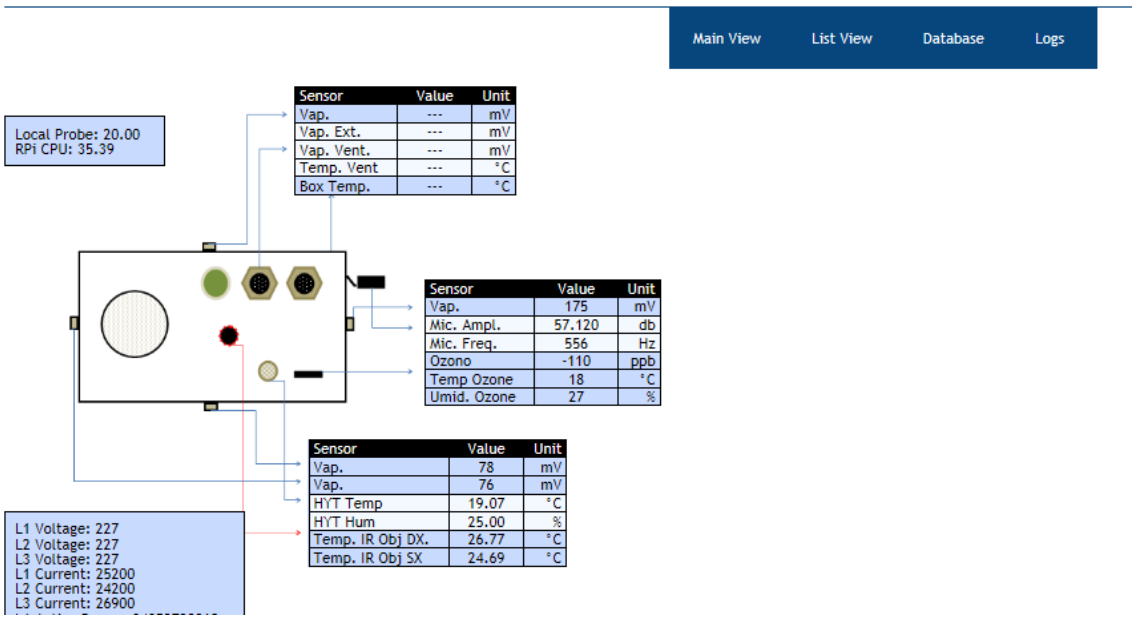

Figure 5. Example of the webpage

5.1.2 Prototype 2

Some problems affected the first prototype, for instance an almost insignificant shielding of the electronic parts from the magnetic field of the transformer (the Slave and Master boxes were made of glass fiber-reinforced plastic), a limited protection from dust and water or a non satisfactory design of the electronic circuit (not fully controllable from remote). These drawbacks and the results obtained from the tests were used to develop a more efficient second prototype. The type of parameters investigated did not change, however the model and number of sensors were partially changed. Furthermore, the number of devices that could be installed in the same facility could be much higher (seven slaves and one master). In figure 6 and 7 the second prototype, master and slave respectively, are presented.

Figure 6. Second prototype of the master unit

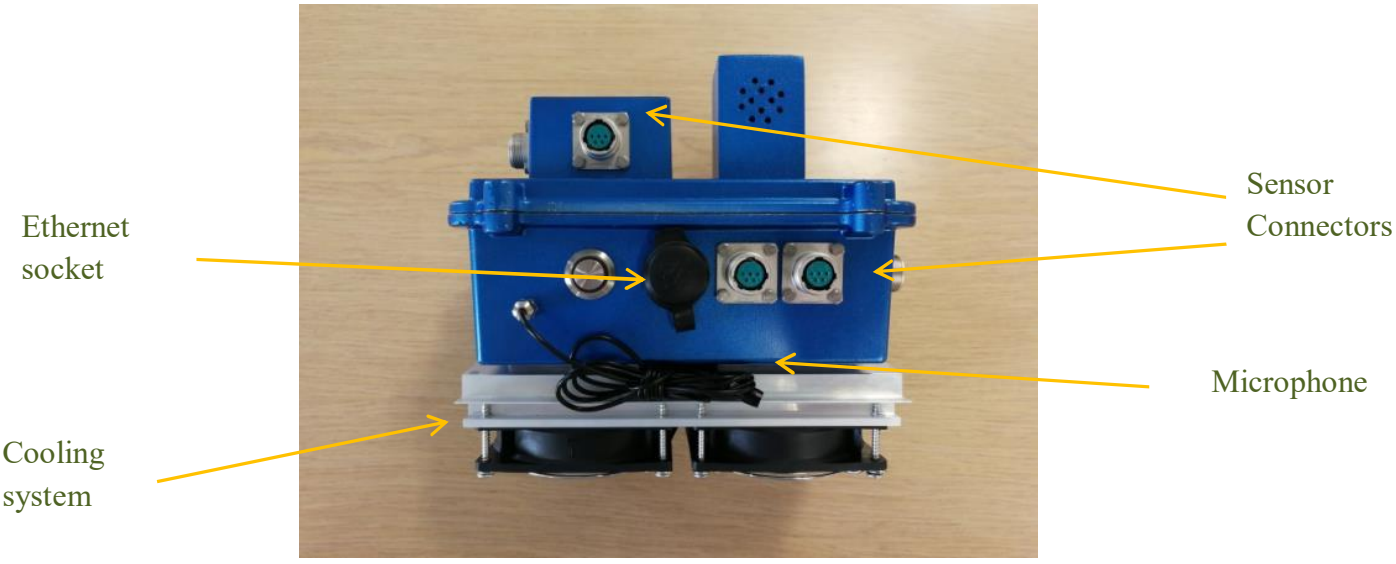

Figure 7. Second prototype of the slave unit

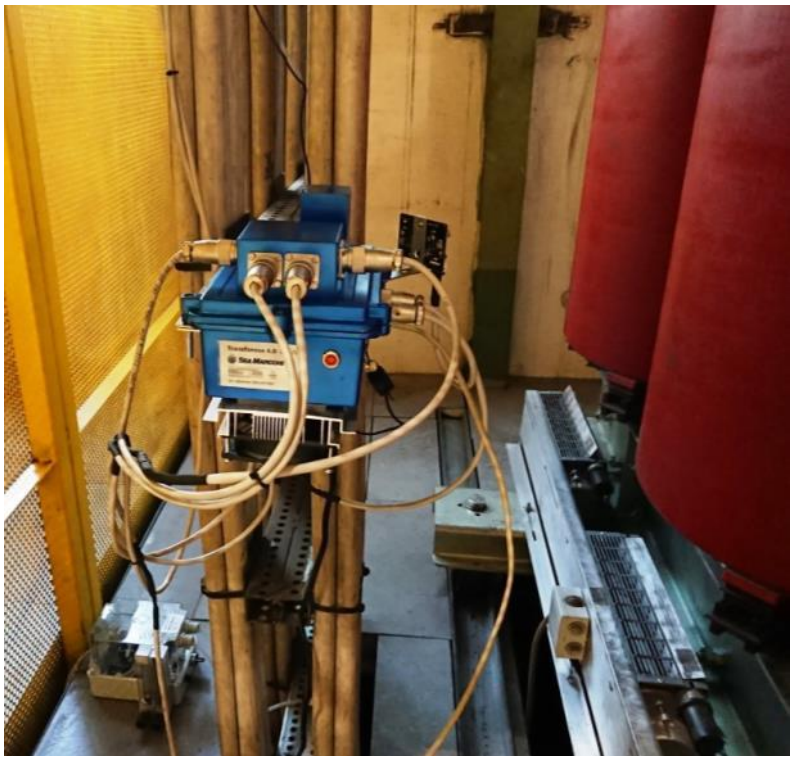

Figure 8. Installation of one of the second prototype (slave module)

The installation of the second prototype (an example is visible in figure 8) was performed on transformers inside an industrial facility (foundry). The monitoring started by the middle of 2018 and is still underway. Each transformer supplies power to different parts of the factory and is consequently stressed by different workloads. The sampling rate of the different properties was set to occur every thirty minutes (it can be remotely changed at any time), with the exclusion of sound and ozone which are measured constantly (every 2 seconds, but only the signals above a certain threshold are transmitted).

5.1.3 Preliminary results

In figure 9 a graph showing the trends of the signals of different sensors is displayed. Samples were taken every 30 minutes (horizontal axis, 42 samples correspond to 21 hours). Ambient temperature and humidity, ozone and VOC has been selected. The intensity of the VOC signal has been reduced (by 1/10) for representation purposes. The ambient temperature and humidity do not vary significantly throughout the day. The VOC sensor signal oscillates within values (500 – 700 mV) that several former trials suggest to be in compliance with an environment slightly polluted by organic vapors. The ozone concentration is the one typical of the season (20-50 ppb) and in line with local monitoring in an industrial environment.

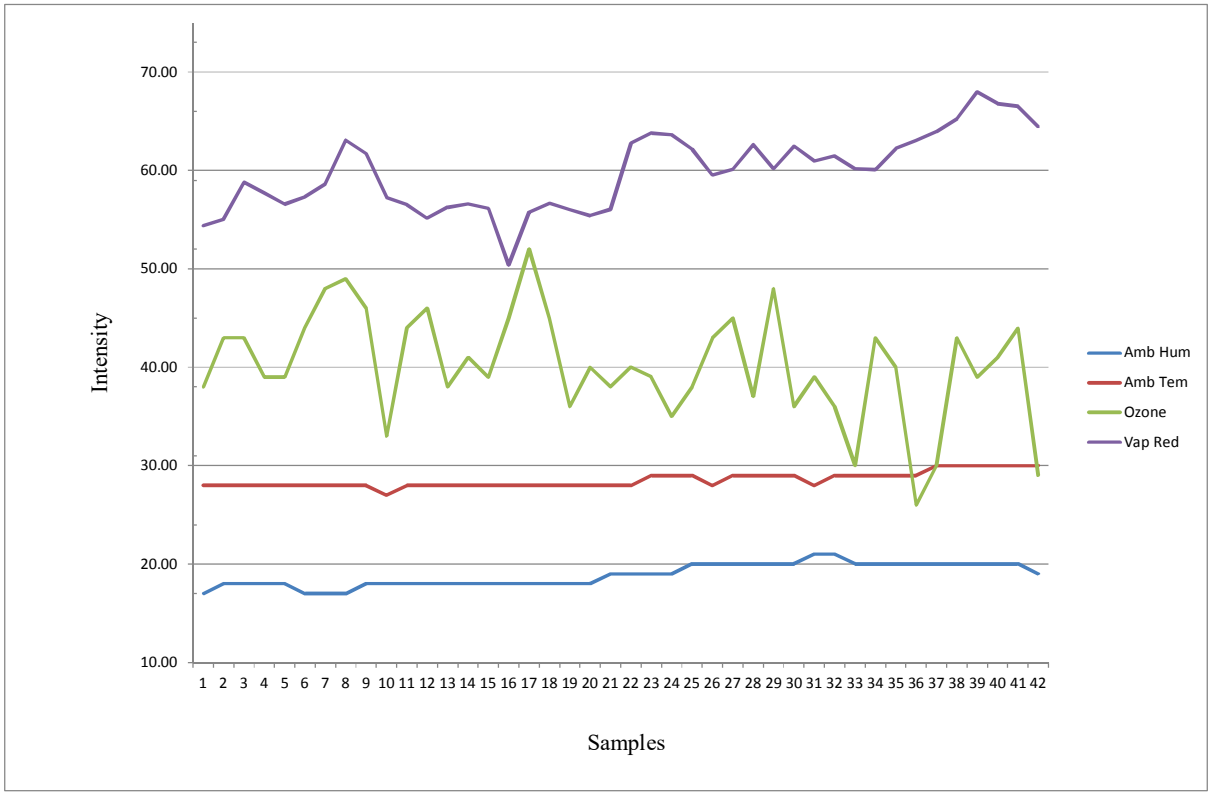

Figure 9. Trend of the sensor's response of four different sensors: relative humidity (%), ambient temperature (°C), ozone (ppb) and vapors(mV), recorded throughout a day of service. The signal given by the VOC sensor has been divided by ten (purple curve, Vap Red).

In figure 10 the comparison between the signals of two VOC sensors installed by two different transformers are shown. Even in this case the sampling rate was set every thirty minutes. It is evident that one of the two sensors (red line) provides a signal that is four-five

times higher than the other (blue line). Even the trend is different, with the higher-signal curve showing a soaring tendency. The reason for this behavior lies in the fact that the sensors are located in an area of the facility where industrial activities producing exhaust gases are performed (in the specific case casting of metals). It comes without saying that such vapors can interfere with the possible compounds that might be released from the transformer.

Figure 10. Comparison between the sensor's response of two VOC sensors installed by two different transformers. The sampling rate is every thirty minutes (42 samples equal 21 hours). The soaring trend of the red curve is the determined by the presence of organic vapors independent of the transformer (interference).

5.2 Air Sampling Unit

A device capable of sampling and trapping the air surrounding an in-service transformer was realized. An example is shown in figure 11. It consists of a membrane sucking pump an air flow regulator and trapping cartridges. The pump is designed to work in continuous thanks to its low energy consumption. This kind of device can provide off-line tests only.

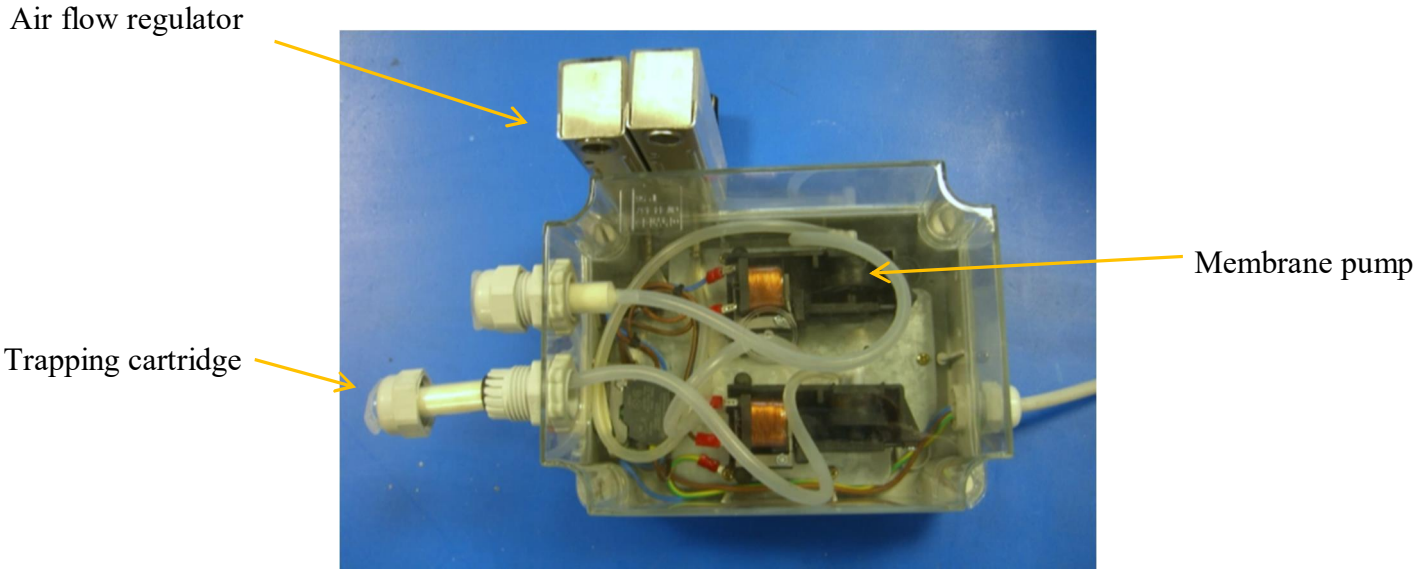

Figure 11. Air sampling device to be placed in the room hosting the transformer

The cartridges were filled with two different adsorbents: Tenax ® and Cyclodecxtrin-based polyurethanes (Synthesized according to patent: use of functionalized nanosponges for the growth, conservation, protection and disinfection of vegetable organisms; Roggero, Tumiatti et al.; WO2013046165 (A1) — 2013-04-04, Pub 2016-04-04). The former is a commercial polyurethane normally used in air sampling tests and the second is another type of polyurethane enhanced by the presence of β- cyclodextrin cavities

Four devices were placed near an equivalent number of transformers and are currently running. One was installed along with the first prototype and the other three with the second. Within the last group, one sampling apparatus was placed in the same room were the transformer relative to figure 9 is working. After a few months, the cartridges were replaced with new ones, brought to the lab, eluted with isopropanol and then analyzed through GC-MS technique. Unfortunately, no particular compounds were, so far, detected. This result seems to be in line with what detected by the sensor (limited variation of purple line – Vap Red in figure 9).

5.3 Coupling of DTD with ZnO sensor

One of the ZnO sensor described in Chapter 4, the flowerlike type, was interfaced with the second prototype of the slave module. To accomplish that, a new sensor connector (Figure

12) was fabricated, cutting two small plates from a copper-clad PCB board, which worked as a clamp for the sensor. The contacts and traces were carved only on one of the plates.

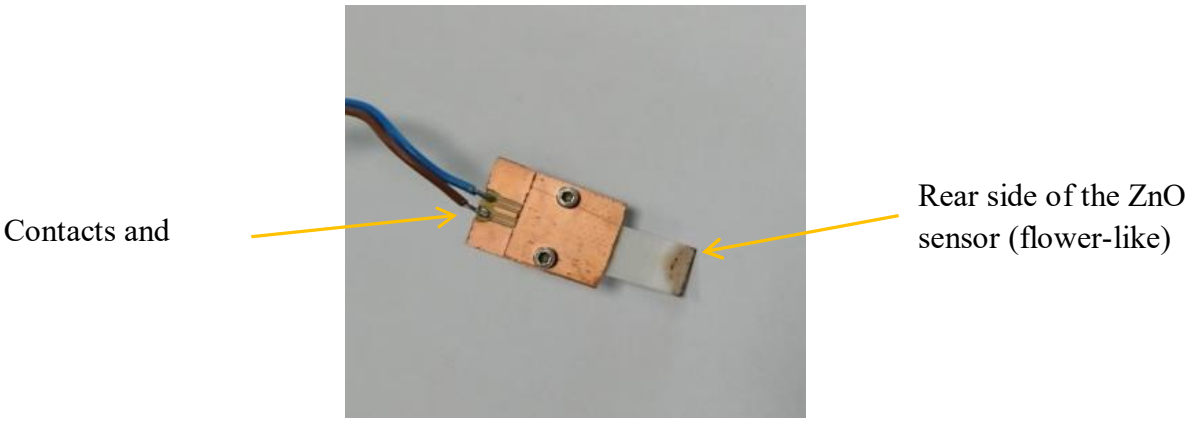

Figure 12. ZnO connector to be used in conjunction with the second prototype of the slave module

Successively a steel block was realized to function as a holder for the sensor, the thermocouple and the heater (cartridge type. 40 W, 12 V, 450°C max). The last one was inserted in a hole bore inside the block (Figure 13).

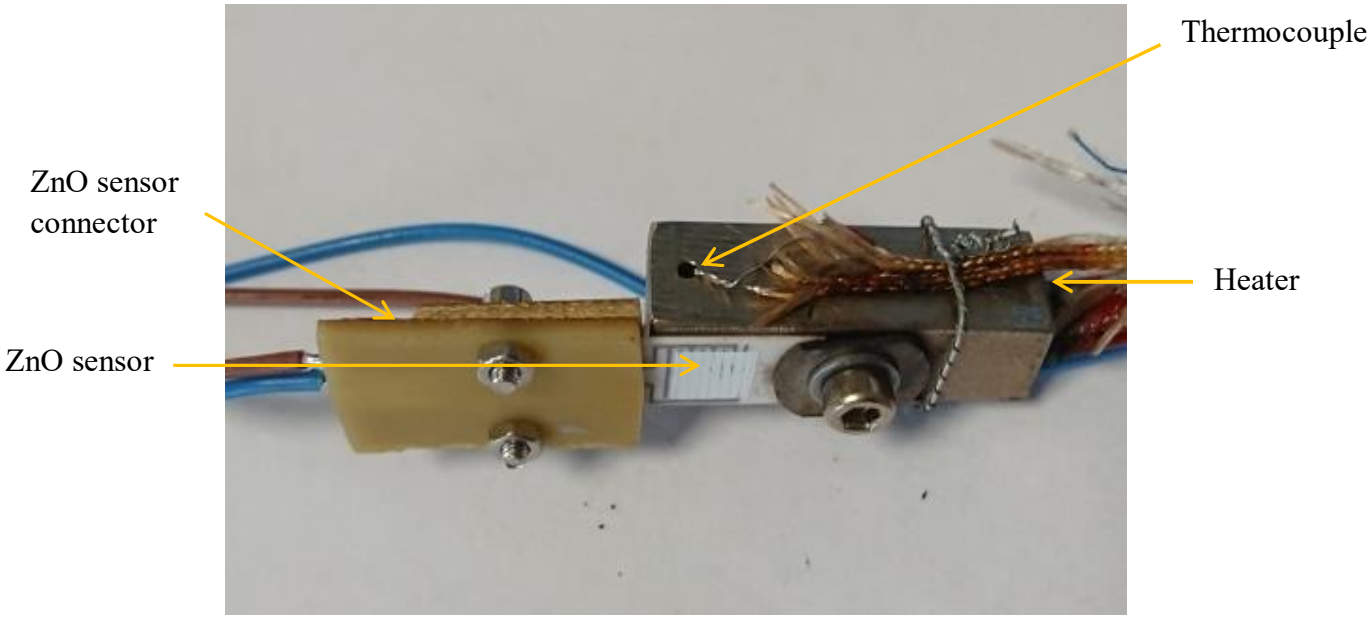

Figure 13. ZnO sensor connector and heater setup

The setup of figure 13 was then connected to one the prototype of the slave module and tested in the lab. As in the case of the experiments described in Chapter 4, a 3-neck 500 ml round bottom flask was used in the experiments (figure 14)

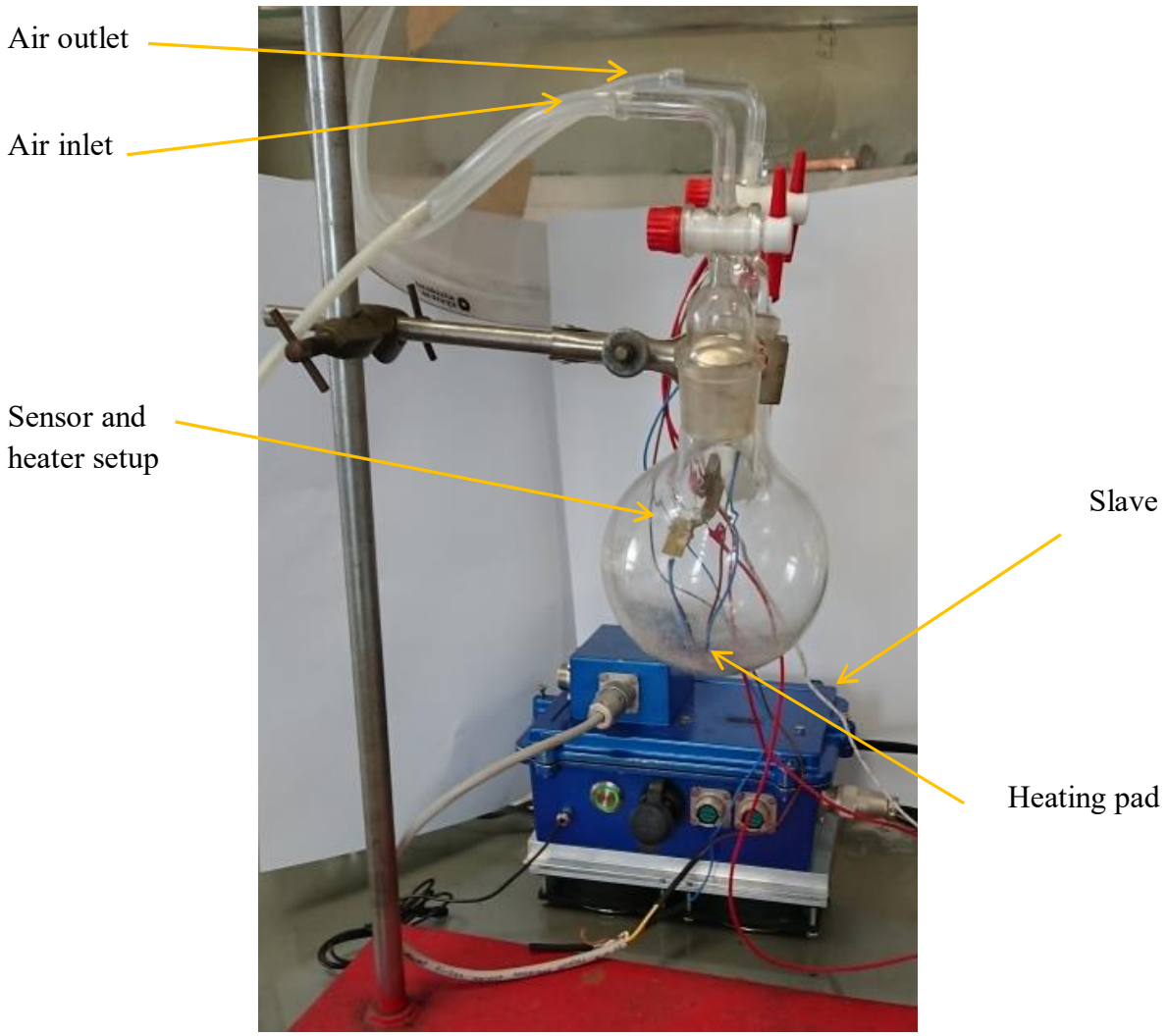

Figure 14. Apparatus to test the ZnO sensor (flower-like), connected to a slave module (second prototype).

The apparatus consisted in 5 main parts: dry air inlet and outlet, slave module, sensor/heater setup and a small heater pad at the bottom of the flask ,on the outside wall. The purpose of the last component was to promote the evaporation of the compounds introduced in the flask in a way that might simulate the release of molecules in a warm place like a dry-type transformer cabinet.

The resistance value generated by the sensor was recorded by the slave module, which controlled also the on/off switching of the heater. The sensor was exposed to some organic compounds. The air flow was kept at 250 mL/min and the heater temperature was set at 250°C. The results obtained are described in the next section

5.4 Preliminary results

The first qualitative tests were performed using some volatile compounds to check the response of the sensor and see if its behavior is equivalent to that observed during the previous tests. Even though the slave module is currently able to measure the mere resistance (R), a decrease in the value was registered in every test. When the air could flow freely through the flask, R oscillated between 30 and 29 kOhm, however, when the air circulation was discontinued the resistance decreased to 24-25 kOhm, due to a smaller heat dissipation. Compared to the dry-air signal measured by the apparatus described in chapter 4 the one quantified here is at least 5 times higher. For instance, when a drop of acetone (~ 17 mg) was introduced into the flask the resistance fell from 25 kOhm to 17 kOhm within a minute (the air was let circulate across the flask). Also Isooctane and isopropanol provided a decrease in the signal.

In figure 15 the curves obtained in duplicate experiments are displayed. Here, an equal amount of carbic anhydride (~ 6 mg) was introduced into the flask (no air). The flask was heated in its bottom part by the small pad, creating an atmosphere of anhydride. When a minimum in the signal was reached the air inlet and outlet were opened to force the compound out. The two curves are very similar in shape and sensor's response, even though the red one is affected by a higher noise. As a matter of fact, in the latter case the temperature of the steel block fluctuated significantly (255 – 245°C) determining a synchronous oscillation in the resistance value. Consequently, in the second experiment, the steel block, provided the part occupied by the sensor, was insulated with a layer of rock wool. The resulting curve, the blue one, appears much more stable.

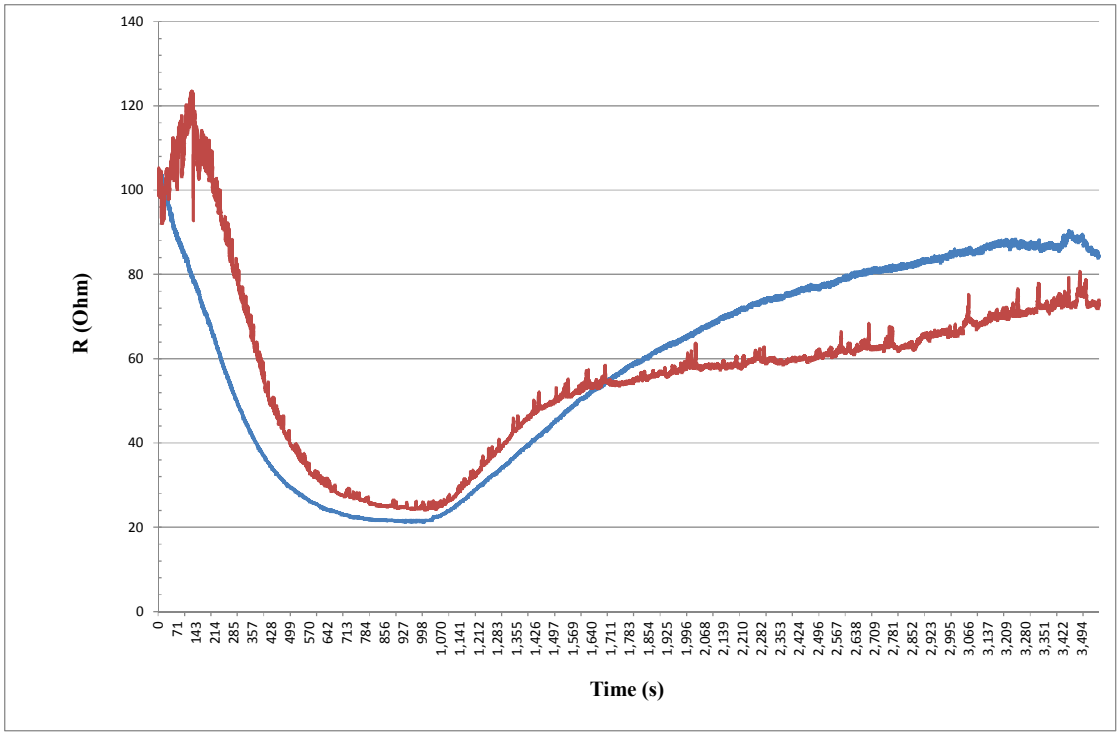

Figure 15. ZnO sensor response (in Ω) after exposure to carbic anhydride. Two tests with the same amount (0.00105 g) were performed.

The results obtained from the in-field tests have demonstrated the feasibility of the on-line monitoring of a dry-type transformer. It is obvious that the detection of organic volatile molecules cannot be separated from the collection of other properties of the machine. The environment where the sensors are placed is also very important, since it could generate organic molecules which may interfere and provide false positive results. It follows that the development and installation of selective sensors becomes really fundamental.

6 Conclusion

Dry-type transformers are electric machines with some advantages, (e.g. low fire risks and no maintenance requirements) with respect to their "brothers" filled with insulating liquids. Obviously, they are also affected by some disadvantages, first and foremost the impossibility of understanding their health conditions. Consequently, the owners of transformers, at least those who cannot tolerate an abrupt and unforeseen outage, are looking for tools that can help to understand the status of the machine and possibly predict if a failure is about to happen. Both electrical and thermal phenomena can occur in a transformer, determining stresses over the materials and especially on polymers, such as epoxies and polyesters. Only the formers are mostly affected. Thus, overheating and electrical discharges can bring about the formation of various organic molecules, which can be detected with the appropriate sensors. Among the possible materials suitable to fabricate a sensor copper and zinc oxides were selected, due to their alleged versatility. The first one didn't provide any useful result (with the exception of its non-reactivity towards the omnipresent moisture), whereas the second one was very reactive against a lot of different molecules, carbic anhydride and phenol included. These compounds were selected to study the degradation behavior, thanks to their possible matchability with the temperature reached by the machine. Furthermore, transformers are often kept in facilities where a lot of interfering molecules can be released during the industrial processes determining a false-positive response. Hence the necessity of providing sensors with a high degree of selectivity is unavoidable. Unfortunately, this aspect could not be investigated yet, but it will be the topic of subsequent studies. However, in parallel with the lab activities, a campaign of pilot scale, in-field activities was also started. For that reason prototypes of a sensor-based devices were built and installed onto transformers to monitor their properties (e.g. chemicals release, sounds, temperature, dust) during functioning. The experiments are still in a preliminary screening phase and have not led to any conclusion yet. It's likely that interpretation of data from an array of sensors by means, for example, of principal component analysis (PCA) will be required to find out correlations and develop a diagnostic tool. Finally, one of the sensors fabricated in the lab was coupled with one of the in-field devices and successfully tested, demonstrating the feasibility of driving the research towards a pilot /industrial scale dimension.